AN ELECTROMAGNETIC ISOTOPE SEPARATOR

C. J. ZILVERSCHOON

PROMOTOR: PROF.DR C.J.BAKKER

AAN IDA

Gaarne maak ik gebruik van de hier geboden gelegenheid, dank te brengen aan allen, die hebben medegewerkt aan de bouw van de separator en het tot stand komen van dit proefschrift.

Hooggeleerde BAKKER, hooggeschatte promotor, ik acht het een groot voorrecht, dat U mij in mijn werkkring in staat hebt gesteld, deze promotie te volbrengen. De hulp en raadgevingen, die ik van U bij de voltooiing van mijn proefschrift mocht ontvangen en Uw voortdurende, actieve belangstelling voor het werk zijn mij tot grote steun geweest.

Hooggeleerde DORGELO, behalve voor Uw waardevolle lessen, ook op niet physisch gebied, ben ik U zeer erkentelijk voor de spontane wijze, waarop U mij in de gelegenheid hebt gesteld, de betrekking te aanvaarden, die uiteindelijk deze promotie mogelijk maakte.

Hooggeleerde HEYN, Uw technische adviezen bij de bouw van de separator zijn van veel nut geweest.

Hoogleraren en Lectoren van de Afdeling der Algemene Wetenschappen en de Afdeling der Technische Natuurkunde van de Technische Hogeschool te Delft, ik ben U zeer dankbaar voor de opleiding, die mij in staat stelde, dit werk te beginnen.

Dat het daarbij ook tot een bevredigend resultaat is gekomen dank ik in de allereerste plaats aan U, Zeergeleerde KISTEMAKER. Onder Uw voortreffelijke leiding kon de opdracht met betrekkelijk weinig krachten in een redelijke tijd worden uitgevoerd. Door Uw uitgebreide kennis en ervaring en Uw levendige fantasie konden ook de vreemdste moeilijkheden worden opgelost. Met Uw aangeboren voortvarendheid en Uw nimmer aflatend enthousiasme hebt U ons team tot een constant hoog tempo geinspireerd. De jaren, welke ik onder Uw leiding heb mogen werken, zal ik mij steeds dankbaar herinneren als een leerzame en genoeglijke tijd.

Aan de STICHTING VOOR FUNDAMENTEEL ONDERZOEK DER MATERIE in wier dienst ik dit onderzoek heb mogen verrichten, gevoel ik mij ten zeerste verplicht.

Beste SCHUTTEN en NABBEN, jullie hebt als electronici, tezamen met verschillende volontairs, een zeer belangrijk aandeel gehad in de bouw en het onderhoud van de separator. Ik heb groot respect voor het vele uitmuntende werk, dat jullie in de loop der jaren hebt afgeleverd.

Beste ROL en COEN DE VRIES, ik ben jullie dank verschuldigd voor de vele daadwerkelijke hulp, die ik van jullie mocht ontvangen. Onze samenwerking in het "bedieningsteam" van de separator is steeds gekenmerkt geweest door een buitengewoon prettige sfeer.

Beste DE VRIES en JANSZ, het prepareren van inlaatmateriaal voor de ionenbron en het vrijmaken en analyseren van de opgevan-

gen isotopen uit de collector zijn primaire onderdelen van het scheidingsproces. De vaak zeer moeilijke chemische problemen, die daarbij rezen, zijn door jullie steeds op voortreffelijke wijze opgelost.

Beste BOERBOOM, met de serieuze en vlotte uitvoering van de massaspectrometrische analyse van gescheiden isotopen heb je mij een grote dienst bewezen.

Ook op de andere wetenschappelijke medewerkers in het Laboratorium, hoewel niet direct betrokken bij de bouw van de separator, heb ik nimmer een vergeefs beroep gedaan wanneer enigerlei hulp gewenst was. Ik ben daarvoor zeer erkentelijk.

Voor de uitwerking en realisering van ontelbare, vaak zeer moeilijke constructies ben ik grote dank verschuldigd aan Meester JANSSEN, die zich met zijn uitgebreide ervaring en grote vindingrijkheid inderdaad onmisbaar heeft gemaakt.

Ook het overige technische personeel van het Laboratorium voor Massaspectrografie heeft, gezien de jeugdige leeftijd der betrokken krachten, vaak opmerkelijke prestaties geleverd.

De uitvoering van zwaar constructiewerk kon aanmerkelijk bespoedigd worden, doordat gebruik kon worden gemaakt van de werkplaatsen van de Centrale Oost van het Gemeentelijk Energiebedrijf, waarin ons Laboratorium gastvrijheid geniet. Terwijl de verstandhouding met alle instanties van dit bedrijf zeer goed te noemen is, past mij wel een bijzonder woord van dank aan de chef en het personeel van de CENTRALE WERKPLAATS, waar het leeuwendeel van het grote constructiewerk werd uitgevoerd. Van onschatbare betekenis zijn hierbij geweest de talrijke adviezen van de heer HOOGVORST met wie alle technische problemen op prettige wijze besproken werden.

Zeer belangrijke hulp mochten wij ontvangen van de Afdelingen GRONDLEIDINGEN en TECHNISCHE CONTROLE van bovengenoemd bedrijf.

Gaarne dank ik ook de N.V. WERKSPOOR, die, belichaamd in de heer THURING, ons vele malen met een welhaast beschamende bereidwilligheid is tegemoetgekomen.

Wat de verwezenlijking van mijn proefschrift betreft, dank ik in de eerste plaats MERTON ROBERTSON voor de serieuze correctie van de Engelse tekst. Helaas moesten na deze correctie nog verschillende wijzigingen worden aangebracht, hetgeen een excuus moge zijn voor nog aanwezige taal- en stijlfouten.

Ik dank voorts Mej. DE VLETTER voor het correcte typen van het manuscript en de heer DUIN voor de verzorging van het tekenwerk.

Tenslotte gaat mijn dank uit naar een ieder, die op enigerlei wijze heeft bijgedragen tot de tot stand koming van dit proefschrift.

CONTENTS

Chapter I

GENERAL CONSIDERATIONS

§ 1. Purpose of isotope separation

Isotopes are elements with the same nuclear charge, but with different atomic weights. Their electron configurations, and therefore their chemical properties, are practically identical. Their nuclear structures, however, and consequently their nuclear properties, are different.

In particular, when an element consisting of various isotopes is used as a target (*e.g.* in a cyclotron) a mixture of radioactive isotopes may be created. Measurements on these mixtures can give complicated results, the interpretation of which is often difficult and sometimes impossible, especially when the radioactive isotope to be studied is created from a stable isotope of low natural concentration.

In those cases it is of great importance that the nuclear physicists have the disposal of a pure stable isotope or at least of a mixture in which that particular isotope has been enriched appreciably.

Other applications of separated isotopes in nuclear physics are a.o.: the use of B^{10} in neutron counters and of U^{235} in reactors.

§ 2. Historical development of the separation of isotopes

It is peculiar that the first separation of isotopes on an appreciable scale was effected before the existence of isotopes had been fully recognised. In fact, the separation was carried out to prove this existence.

It was in 1912 that Thomson [1] analysed canal rays by means of parallel electric and magnetic fields. By placing a photographic plate perpendicular to the direction of the rays he obtained parabolic curves on it which indicated the place where the ions struck the plate. Each parabola corresponded to a particle with a definite ratio e/M, which essentially made his instrument a mass spectrograph.

In analyzing neon, Thomson observed two parabolas corresponding to the atomic weights 20 and 22. His assistant F. W. Aston sus-

pected they dealt with two kinds of neon of a type similar to the isotopes at the end of the periodic table discovered by Soddy [S1] a short time before. Aston tried to separate these neon isotopes. After a rather unsuccessful attempt on the fractional distillation of liquid neon he applied the method of *diffusion*.

The principle of this method is the following: In a mixture of two gases in thermal equilibrium, the molecules of the two components have the same mean kinetic energy. However, the mean velocities of the molecules are then unequal. They are inversely proportional to the square root of their masses.

When such a mixture is allowed to diffuse partially through a porous wall, the light component will emigrate faster than the heavy one, and in the diffusate the ratio will be altered in favour of the light component.

By the separation factor S is meant the quotient of the isotope ratios in the phases after and before the separation process.

In the beginning of the diffusion process $S = \sqrt{\frac{M_1}{M_2}}$, but it diminishes gradually because of the enrichment of the residual gas in the heavier component.

If a fraction f of the gas is allowed to diffuse, the separation factor is given by:

$$S = \frac{f^{\mu}}{1 - (1-f)^{\mu}} \qquad (2 - 1)$$

with

$$\mu = \sqrt{\frac{M_1}{M_2}} \qquad (2 - 2)$$

For the neon isotopes and $f = \frac{1}{2}$, $S = 1.035$.
So the alteration in the isotope ratio or the enrichment is only a few procent.

The formulas mentioned are only valid in the case when the diameter of the pores is small as compared to the mean free path of the gas molecules. Since the gas stream must be ruled by the Knudsen law, the diffusion process is generally carried out at a low pressure, *e.g.* 10 mm Hg. Unless the pores are very small, the separation factor will diminish at higher pressures.

Aston [A1] allowed neon to diffuse through a clay barrier and repeated it several times. At last, he determined the density of the lightest and the heaviest portion. These showed a measurable difference, *viz.* 20.15 and 20.28 respectively. As a result, he obtained neon containing 7.5 and 14 % Ne^{22} (in stead of 10 %, which is the natural abundance).

In 1916 W.D.Harkins [H3] applied the same method on HCl to se-

parate the chlorine isotopes. By 1921 he had diminished the abundance of Cl^{37} (normally 24.6) to 20.8 %.

In 1932 Hertz [H1] introduced the *cascade method* in the diffusion process. A large number of similar separation stages were linked in series in a special way (Fig. 1).

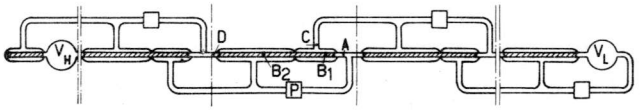

Fig. 1. Cascade method according to Hertz

The gas mixture is supposed to enter the stage at A. Part of it diffuses through the clay pipe B_1 and is pumped away at C. This gas has been enriched in the light component. The rest flows through the tube B_2 and diffuses partly through its wall. The diffusate has about the same composition as the original gas and is therefore pumped back to A. At D gas flows out that has been enriched in the heavier component. The exit D is connected to the entrance A of the next stage and the exit C to the entrance A of the preceding stage. As a result the concentration of the heavy component increases continually from the right to the left in the apparatus. The completion of the circuit at both ends is to be seen in the diagram.

In the beginning of the process, the whole apparatus is filled with the gas mixture and the pumps are started. When the state of equilibrium has been reached (which can last several hours) the gas in V_H has become enriched in the heavy component, the gas in V_L in the lighter one.

With his apparatus, consisting of 24 stages, Hertz was able to alter the isotope ratio of neon from 1 : 9 to 1 : 1.25. Harmsen, Hertz and Schütze [H4] succeeded in making practically pure Ne^{22}. By applying the process on methane they could enrich the isotope C^{13} (normally 1 %) to 10 %.

In the meantime other separation methods had been developed. In Leiden the *fractional distillation* had been investigated.

If this method is to meet with success, it is necessary that the vapour pressures of the isotopes should be different.

Urey, Brickwedde and Murphy [U1] derived the following formula for the vapour pressures of solid H_2 (p_1) and HD (p_2):

$$\ln \frac{p_1}{p_2} = \frac{W_1 - W_2}{RT} + \frac{\Phi_1 - \Phi_2}{R} + \frac{3}{2} \ln \frac{M_1}{M_2} \qquad (2-3)$$

Here W is the zero point energy, Φ is an integral, taken from

Debye's theory on specific heat and depending both on the temperature and the mass of the molecules.

It is acceptable to take equation (2 – 3) as valid for the liquid – gas equilibrium in the immediate vicinity of the triple point. Applying (2 – 3) on liquid H_2 and HD one finds near the triple point temperature the separation factor $S = \frac{p_1}{p_2} = 2.7$ but in the case of neon S is only 1.06.

Keesom, Van Dijk and Haantjes built rectification columns to separate the neon isotopes at a temperature somewhat above the triple point. After some experiments with a column of 19 plates, by which a measurable separation could be achieved [K1], a large column of 85 plates was constructed and neon mixtures with 2 and 58 % Ne^{22} were obtained [K2]. With another column they made hydrogen containing 3 % HD (normally 0.04 %) [K3].

One year previous to this Urey *et al* [U1] had obtained a mixture with 0.4 % HD by simple distillation of liquid hydrogen. In this way they proved spectroscopically the existence of deuterium. Attempts to separate the oxygen isotopes (in water) [L1] and the nitrogen isotopes (in ammonia) [W1] by rectification met with little success.

Concurrently with the Leiden experiments came the first application of *electrolysis* as an isotope separation method. The possibility had been pointed out by Kendall and Crittenden as early as 1923 [K4]. In 1932 Washburn and Urey [W2] found that in the electrolysis of water the escaping hydrogen gas contained less deuterium than the residual water. Only one year later Lewis [L2] prepared concentrated heavy water (33 % D_2O) by this method.

The mechanism of the electrolytic separation has not been explained quantitatively. Some factors can be mentioned that will cause fractionizing. Important is the exchange reaction:

$$H_2O + HD = HDO + H_2 \qquad (2 - 4)$$

for which the equilibrium constant is 3 – 3.5, which is substantially different from unity. The cause of this will be discussed later.

Because hydrogen gas escapes from the cathode, it will be mainly the lighter isotope. However, this cannot be the only process, for experimental values of the separation factor appear to be much larger than 3 (even up to 17 [E1]).

The de-ionizing of hydrogen ions at the cathode is supposed to cause also fractionizing. This is acceptable because of the difference of the energy levels for the electrons in D and H [G1].

The value of the separation factor depends on the condition of the electrode surface, on the current density, on the concentrat-

ion of the electrolyt and on possible contaminations. If certain organic compounds are added, it is possible to "poison" the electrolyt. This poisoning means that the hydrogen gas is retained at the cathode for some time by the organic compounds; the time being long enough to establish equilibrium of the reaction (2 - 4). That is why a separation factor of about 3 is always found in those cases, whereas a normal value in industrial processes is 5 to 6.

Starting with a volume of water V_o in which the concentrations of the lighter and heavier isotopes are L_o and Z_o respectively and then continuing the electrolysis to a final volume V, the concentrations L and Z achieved can be calculated from Rayleigh's formula for ideal distillation:

$$\frac{L_o}{L}\left(\frac{Z}{Z_o}\right)^S = \left(\frac{V_o}{V}\right)^{S-1} \qquad (2 - 5)$$

In this way Harteck [H5] computed that - with a separation factor of 5 - the volume of natural water must be diminished to 10^{-5} of the original volume to obtain 98 % D_2O. When the process has been in progress for some time, the escaping hydrogen gas has a higher concentration of deuterium than the normal one. Therefore, it is collected, burned and electrolysed again.

The electrical energy required to carry through this process is of the order of 100 kWh per gram of 98 % D_2O [G2].

In 1934 attempts were made to use the electrolysis of water for the separation of the oxygen isotopes [G3] [W3], but with little success, due to the fact that the separation factor is near to unity (1.03).

A few years later Holleck [H6] did succeed in partially separating the lithium isotopes by the electrolytical method. He obtained 12.6 % Li^7 (normally 7.8 %).

Hertz introduced an improvement in his cascade diffusion method in 1934 [H2]. In order to obviate the difficulties which are connected to the use of clay pipes (adsorption at and contamination of the very large internal surface) he replaced these pipes by mercury *diffusion pumps* of a special type, which also fractionate.

The separation factor of such a pump was calculated by Barwich [B1], who found:

$$\ln S = C\,(\sqrt{M_1} - \sqrt{M_2}) + \tfrac{1}{2} \ln \frac{M_1}{M_2} \qquad (2 - 6)$$

The constant C depends, among other things, on the pump dimensions.

The separation factor is larger than in the case of diffusion through porous walls. The diffusion rate is also larger, but the

pressure to be used is lower (a few mm Hg). By means of a cascade of 12 pumps Hertz obtained neon with 50 % Ne^{22} with the equilibrium being reached after 45 minutes. To attain this goal with his *first method*, he needed a cascade of 24 stages and a start-up time of 11 hours [H4].

With this *second method* of Hertz, Barwich [B1] constructed an apparatus with 48 pumps with which he prepared nearly pure Ne^{20}, O^{18} (10 %) and A^{36} (10 %). Others applied the method to carbon and nitrogen [H7].

The *electromagnetic separation* had been considered by Aston as early as 1922 [A2]. The first attempts of Morand [M1] met with no success, but in 1934 results were reported both from England and the United States.

The principle is that of the mass spectrometer: An ion beam is made of the material to be separated and these ions, after electric acceleration, are carried through a magnetic field. Here the beam is deflected and this deflection is larger for the lighter ions than for the heavier ones.

When different isotopes are present in the beam, the beam will be split up and the separated isotopes can be collected with an appropriate receiver.

Under ideal circumstances it is possible to separate the isotopes in one stage ($S = \infty$).

On the other hand, the yield is small because the ion currents used are very low. With an ion current of 1 μA the transport is about 1 μ gram atomic weight per 24 hours.

By electromagnetic separation, Smythe, Rumbaugh and West [S2] obtained 1 mg of pure K^{39}. The lithium isotopes could be separated too.

Oliphant, Shire and Crowther [O1] prepared targets containing about 10^{-8} g of pure Li^6 and Li^7 for nuclear physical experiments. Smythe and Hemmendinger [S3] succeeded in separating the potassium and rubidium isotopes and proved that the radioactivity of these elements belongs only to the isotopes K^{40} and Rb^{87}. Walcher [W4] collected 90 μg Rb^{85} and 30 μg Rb^{87}, which he proved to be pure spectroscopically. Yates [Y1] prepared targets of Li^6, Li^7, B^{10}, B^{11} and C^{12} for nuclear physical experiments.

A very important separation method arose in 1936: the *chemical exchange reaction method*. Though, in general; the chemical properties of isotopes are the same, this is not the case with the equilibrium constant of exchange reactions. When these reactions are carried out, with one of the elements having two isotopes L and H present, *e.g.* in this way:

$$LX + AY = AX + LY \qquad (2 - 7\ 1)$$

$$HX + AY = AX + HY \qquad (2 - 7\ h)$$

then the equilibrium constants for (1) and (h):

$$K_1 = \frac{[AX]\,[LY]}{[LX]\,[AY]} \quad \text{and} \quad K_h = \frac{[AX]\,[HY]}{[HX]\,[AY]} \qquad (2 - 8)$$

differ from each other slightly.

The effect is as if the reaction

$$LX + HY = HX + LY \qquad (2 - 9)$$

had an equilibrium constant

$$K = \frac{[HX]\,[LY]}{[LX]\,[HY]} \neq 1 \qquad (2 - 10)$$

K = the separation factor S of the process. Urey and Greiff [U2] calculated S for various exchange reactions by way of the relation:

$$S = K = \frac{Q_{HX}\ Q_{LY}}{Q_{LX}\ Q_{HY}} \qquad (2 - 11)$$

Q being the partition function of the molecules. Since Q depends on the mass of the particles, it is different for isotopes. That is why the equilibrium constant K and the separation factor S are $\neq 1$.

With the electrolysis we mentioned the reaction

$$HD + H_2O = H_2 + HDO \qquad (2 - 4)$$

for which $K \approx 3$.

For reactions between isotopes other than hydrogen, K is in general close to unity.

Therefore, it is necessary to use a large number of stages in series.

Huffman and Urey [H8] built a column over 10 m tall. This column (Fig. 2) consisted of a cylinder that was divided into a large number of chambers, separated from each other by conical walls. A vertical shaft could rotate in the cylinder and cones were fitted on this shaft as well, one in each chamber of the cylinder.

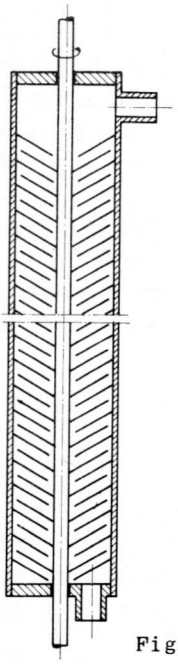

Fig. 2. Principle of Urey's rectification column

The column in question contained 621 pairs of cones. It was used for exchange reactions between a liquid and a vapour which were supplied at the top and the bottom respectively.

In this column Urey, Hoffman, Thode and Fox [U3] carried out the reaction:

$$N^{15}H_3 + (N^{14}H_4)_2\,SO_4 = N^{14}H_3 + (N^{15}H_4)_2\,SO_4 \qquad (2-12)$$

After 10 days they obtained a solution with 2.4 % N^{15} (normal 0.4 %).

With the reaction

$$C^{13}O_2 + KHC^{12}O_3 = C^{12}O_2 + KHC^{13}O_3 \qquad (2-13)$$

the C^{13}-percentage of $KHCO_3$ was changed from 1.1 to 1.36 % [U4].

Thode and Urey [T2] made columns of a somewhat modified construction. They consisted of glass tubes in which the liquid flew down along glass spirals.

By connecting some of these columns in a cascade 70 % N^{15} could be prepared after a start-up time of 30 days.

By means of the reaction

$$Na\,H\,S^{32}\,O_4 + S^{34}\,O_2 = Na\,H\,S^{34}\,O_4 + S^{32}\,O_2 \qquad (2-14)$$

the abundance of S^{34} (normal 4.2 %) could be increased to 6.8 % [T3].

In 1938 Clusius and Dickel [C3] found a means of using *thermal diffusion* for the separation of isotopes. The thermal diffusion effect was discovered theoretically by Enskog [E2] and Chapman [C2] and experimentally by Chapman and Dootson [C1]: When in a mixture of gases with different molecular weights a temperature gradient is maintained, a concentration gradient will occur.

The magnitude of the effect depends on the law that rules the mutual forces of the molecules and it is largest for molecules that behave like elastic spheres. The following approximation formula of the separation factor was deduced for this case by Jones and Furry [J1].

$$S = 1 + 0.9\,\frac{M_1 - M_2}{M_1 + M_2}\,\ln\frac{T_H}{T_C} \qquad (2-15)$$

(T_H being the temperature at the "hot" side and T_C at the "cold" side of the vessel). If one takes T_H = 900 °K and T_C = 300 °K, it follows from (2 – 15) that for the neon isotopes. S = 1.047. Here too a cascade is necessary in which each stage passes on its lighter component to one side and its heavier component to the other.

This state was obtained by Clusius and Dickel [C3] in a remarkably simple way: They placed a tube with a cold wall in a vertical position. Inside this tube a hot wire was stretched. Then in each horizontal section an elementary process, as mentioned, takes place and moreover the gas will rise along the wire and go down along the wall due to the difference in density between hot and cold gas. This state is equivalent to a cascade with each "stage" passing the lighter gas to a higher and the heavier gas to a lower "stage".

The concentration of the light gas will increase at the top of the tube, that of the heavy gas at the bottom. The total separation factor of such a column, depending on its length, can be considerable, *e.g.* 20. With a 36 m column Clusius and Dickel separated the chlorine isotopes in HCl [C4]. They obtained 99.4 % Cl^{37} and 95.5 % Cl^{35}. Joris [T5] succeeded in enriching the carbon isotope C^{13} from 1.1 to 2.1 % in a column 12 m high.

The process is also practicable with liquids. Korsching and Wirtz [K6] altered the abundance of the zinc isotopes in a $ZnSO_4$ solution appreciably.

During and after the Second World War the methods mentioned were further improved. Fine results were obtained by means of thermal diffusion and exchange reactions especially. The enriched isotopes C^{13}, O^{18}, N^{15} and S^{34} used in tracerwork are prepared by these methods in most cases.

Clusius and Becker [C5] constructed a thermal diffusion column of 82 m total height and, when the equilibrium was reached after a few months, they obtained 99 % $N^{14}N^{15}$ with it.

By the exchange reaction HCN + NaCN Urey *et al* [H9] prepared 25 % C^{13}.

J.Koch [K11] constructed an electromagnetic separator by which he made targets for nuclear physical experiments.

Walcher [W5] prepared Tl – targets as well as others with his mass spectrograph.

Bernas and Nier [B2] separated the zinc isotopes with a 60^{o} mass spectrometer.

However, the most spectacular undertaking is the enormous scale on which the problem of separation was tackled for the production of U^{235} for the "atomic bomb". It is known from the Smyth report [S4] that powerful installations, using the diffusion principle, were built. In contrast with Hertz's cascade, which was a closed system, a modification was introduced, in such a way that natural uranium was continuously brought in and separated uranium removed. This cascade consists of several thousands of stages through which the uranium is pumped as UF_6.

The electromagnetic method was also applied and a large number

of so called "calutrons" were built. Outstanding progress was made in this domain.

Formerly very low ion currents (up to some μA) had been used in electromagnetic separators, so that space charge effects could not cause aberrations. But now the ion current was raised, even to about 100 mA and the influence of the space charge was counteracted by means of electrons (See § 4).

In Canada the production of deuterium takes place mainly by means of exchange reactions [G4]. The application of proper catalysts to accelerate the establishment of equilibrium is very important.

In Scandinavia the production of heavy water by electrolysis is still of major importance.

Concerning to electromagnetic separators in Europe, Bergström *et al* [B6] built one in Stockholm. It is a 90^{o} type and the ion currents used are of the order of 10 – 100 μA.

In Harwell a very high intensity separator was constructed, after the principles of the Oak Ridge plant [A3].

In Paris Bernas [B3] has built a 60^{o} type separator. His collector currents amount to 4 mA.

Several other separation methods have not been discussed, but these are only useful in special cases, or equivalent results can be obtained easier.

Some of these methods will be mentioned briefly:

1. *The ultra centrifuge* [S13]

The centrifugal force causes an enrichment of the heavier isotope near the outer wall. In the United States a trial plant for the uranium separation was built on this principle, but large scale application did not follow.

2. *Photochemical separation* [K8]

The photochemical dissociation of molecules *e.g.* $COCl_2$, is carried out with light of a wave length, corresponding to the absorption line of one of the isotopic molecules.

3. *The isotron* [S4]

By means of velocity modulation (as in a klystron oscillator) ion "bunches" are formed, which have different drift velocities for each isotope. The bunches are then selected by an r.f. transverse field.

4. *He-separation* [D1]

Use is made of the super fluid state of He^4. He II is conducted along a surface and the He^3 remains behind.

5. *Ion migration* [K9]

A tube is *e.g.* partly filled with $PbCl_2$ and partly with LiCl, both in liquid state. A potential difference is applied to the tube, which causes the Li-ions to cross the boundary between the two substances and penetrate into the $PbCl_2$. As Li^6 has a greater mobility than Li^7, a concentration gradient of the two isotopes will occur. Brewer and Madorsky [B5] applied a counter current to this method.

§ 3. Choice of the method

When a choice must be made from the separation methods, treated in the preceding section: diffusion, rectification, electrolysis, thermal diffusion, exchange reaction and electromagnetic separation, the following points are of interest:

1. *Universal usefulness for all elements.*
2. *Purity of the product obtained.*
3. *Yield.*
4. *Quantity of substance required to carry out the process (Hold-up).*
5. *Time needed.*
6. *Cost.*

The question as to which of these points are the most important, depends on the purpose of the separation.

When it is producing isotopes for tracer work, a yield as large as possible is wanted, whereas the purity of the isotope is of secondary importance. The method used does not need to be universal, since for different elements different methods may be applied. In this case a continuous process is likely to be used so the quantity of substance in the apparatus or the so called "hold up" can be large. The time of separation and the start-up time for the establishment of production are also of little interest but costs of production are very important.

The situation is completely different, when isotopes are separated for nuclear physical experiments. Then any type of isotope may be ordered on short notice, so the method should be universal. In general the isotopes must be as pure as possible, but very small quantities will suffice. The quantity of substance available to be separated may be very small (*e.g.* when artificial radioactive isotopes are to be separated), so a large hold-up cannot be permitted. When separating these radioactive isotopes, a short process time is of great significance. The cost is no primary factor.

For purposes of comparison, the electromagnetic method of separation can be placed in many respects opposite the other five mentioned. These last are often taken together under the name: "statistical methods", because they are all based on the average behaviour of the reacting particles. For these methods, the separation factor per stage is small, so a large number of stages or a large column is necessary to get a sufficient over all separation factor. This is especially the case with the separation of heavy isotopes, where the separation factor per stage is close to unity. The yield may be substantial, but in most cases the hold-up and the start-up time too.

The methods are far from universal (consider *e.g.* the electrolysis and the exchange reactions), the complete separation of elements, containing more than two isotopes in an appreciable amount, is very hard to realize.

On the other hand the electromagnetic separation can be used for all elements, if appropriate ion sources and receivers are available. With proper focusing, the separation factor can be very large, in which case one has rather pure isotopes in one stage. No matter how many isotopes the element contains, they can all be separated.

The hold-up is small and the separation takes place very quickly. However, the yield is small (of the order of milligrams per day).

The separator to be built was primarily designed as an auxiliary instrument for research in nuclear physics.

From what precedes, it is evident that the most advantageous method for this is the electromagnetic one.

§ 4. Space charge compensation in electromagnetic separators

As long as the ion currents in a mass spectrometer are very small, the paths of the individual ions are determined only by the starting conditions and the electric and magnetic fields externally applied. By properly shaping these fields an ideal focus can be obtained.

When the ion current is increased gradually, the image will begin to broaden at a certain value. For still larger currents this effect is serious and finally will reach the point were the ion beams for different isotopes are so completely mixed that effective separation is no longer possible.

The cause of this aberration is the space charge in the ion beam: the beam diverges due to the mutual electrostatic repulsion of the ions in accordance with Coulombs law.

The magnitude of this divergence can be calculated in a simple way. For a 180°-spectrometer Smith *et al* [S6] find an aberration

$$\Delta s = \frac{8 \pi c^2 e i_i r^2}{M v_i^3} \qquad (5 - 1)$$

where r = the main radius of the ions' trajectories;
i_i = the ion current per cm height of the beam;
M = the mass and v_i the velocity of the ions.

The following example may prove that the divergence is even serious at low currents. In our separator the ion source has an exit slit of 100 × 2 mm^2. A normal accelerating voltage is 25 kV and the main radius 102 cm.

According to formula (5 – 1) an aberration of 2 mm will occur at about 1 μA per cm or 10 μA in total for ions of mass number 100.

The total yield of all isotopes is then about 1 mg per 24 hours.

In order to raise the yield, the ion current must be increased and, if possible, up to the limit established by the ion source. A modern source can have an output of several mA. From formula (5 – 1) it is clear that the focus will be very poor at these currents if no preventative measures are taken.

Robinson pointed out that, when space charge is present, a good focus can be obtained by placing the collector so that the ions travel through an angle $\pi+\gamma$, where γ is given by [R2]

$$\gamma = \frac{4 \pi c^2 e i_i r}{M v_i^3 \alpha} \qquad (5 - 2)$$

α being the radial angle of entrance of the beam.
Taking r = 102 cm, $\alpha = \frac{1}{6}$ radian, ions of mass number 100 and 25 kV accelerating voltage, we find that $\gamma = \frac{\pi}{2}$ for an ion current as low as 0.25 mA/cm. Due to this displacement of the collector, the dispersion of the separator (the distance between the images of two adjacent masses) is reduced by a factor of two. It is obvious that this method is not practicable for large ion currents.

During the last war a simple solution was applied by Lawrence in the so called "calutron" [S6 S4]. It utilizes the fact that the high energy beam of ions will ionize the residual gas in the vacuum chamber. If precautions are taken so that no external electrostatic fields are present, the potential gradient inside the beam is such that the slow ions created diffuse out of the beam, but the electrons are trapped in it. The presence of these electrons reduces the positive space charge.

Whereas electrons generally have little effect in space charge compensations due to their great mobility, this is not the case

in a magnetic field. In the separator this field, B, stands at right angles to the radial electric field E, caused by the residual space charge in the beam. Supposing the electrons to be at rest when they are created, they will describe cycloid-like paths perpendicular to both fields and therefore in the direction of the beam with a drift velocity given by $v_d = \frac{E}{B}$ [Z1].

Assuming an electric field strength in the partly compensated beam of 1 V/cm and a magnetic field of 1000 gauss, $v_d = 10^5$ cm/sec. This is small as compared to the thermal velocity of the electrons, which is of the order of 10^8 cm/sec. For 25 kV accelerating voltage, the ion velocity in the beam is from $1.4 \cdot 10^7$ to $2.2 \cdot 10^8$ cm/sec depending on their mass. As a result the electrons are effective for space charge compensation.

The beam passes through a kind of plasma with potential differences of only a few volts. In this way it is possible to handle ion beams of several mA, in which the space charge is counteracted to a large extent by electrons [B4 L7].

The formation of a space charge compensated beam requires a finite time, which is much longer than the time of flight of the ions in their semicircular orbits.

To make an estimation of this formation time τ, suppose an ion current of density J and velocity v passing through the residual gas in the vacuum chamber. The number of secundary electrons created per unit time is then:

$$\frac{dN_-}{dt} = \frac{J \sigma_i N_o}{e} \qquad (5 - 3)$$

σ_i being the ionization cross section and N_o the number of molecules per cm^3 in the residual gas.

When the beam is completely neutralized, the final situation will be given by:

$$N_- = N_+ = \frac{J}{ev} \qquad (5 - 4)$$

If we neglect the loss of electrons during the formation of the beam, the formation time τ will be:

$$\tau = \frac{N_-}{\frac{dN_-}{dt}} = \frac{1}{N_o \sigma_i v} \qquad (5 - 5)$$

There are not many measured values of σ_i available in our region of mass and energy and these differ appreciably. Taking an average value of $\sigma_i = 10^{-16}$ cm^2 [M3], $N_o = 10^{12}$ (corresponding to a pressure of $3 \cdot 10^{-5}$ mm Hg and $v = 2.10^7$ cm/sec we come to a formation time of the order of $5 \cdot 10^{-4}$ sec.

The following points are of importance:

1. Quick fluctuations in the ion current (with a time constant of the order of the formation time or shorter) can disturb the space charge compensation and "blow up" the beam. A good "very short time-stability" of the ion source output is required.
2. Pressure and the kind of residual gas are of significance.
3. The electrons are most effective in the presence of a magnetic field. So it is advantageous to have the ion orbit from source to collector within the magnetic field.
4. Strong externally applied electric fields in the vacuum chamber will disrupt the compensation by tending to pull away the electrons.

It will be shown that these considerations have an influence upon the choices of both the shape of the field in the separator and of the type of ion source to be used.

§ 5. Aberrations. Choice of the analyzing field

It is necessary that the ion beams of different isotopes strike the collector in different places. It would be ideal, if each separate ion beam cut the collector plane as a mathematical line with these lines being parallel for different isotopes.

In reality the lines broaden to areas, which may have curved boundaries.

Causes of aberrations are:

1. Energy spread of the ions.
2. Finite radial and axial angles of entrance of the beam.
3. Finite width of the slits in ion source and acceleration system.
4. Interaction of ions with the molecules of the residual gas in the vacuum chamber.
5. Divergence of the beam due to space charge.
6. Reflection of ions against the walls of the vacuum chamber.
7. Instability of the accelerating voltage or the electric or magnetic fields.

Methods to eliminate these aberrations, as much as possible, will now be discussed successively.

1. *Energy spread*

We can try to design an ion-optical system in such a way that particles with different energy, but the same mass, are focused on the collector. It is not possible to obtain this so called velocity focusing with a magnetic or an electric field alone. The use of combined magnetic and electric fields is necessary. This is obvious from the following consideration:

Assume a beam of ions in which all particles leave the ion source at one point (0,0,0) and in one direction (α, β, γ). However, there are particles with different mass M and there is a spread in the kinetic energy $1/2\ Mv_o^2 = eV_o$, with which they leave the source. The beam passes through an electromagnetic field (E,B). The fields and accelerating potentials are assumed to be static, so time of flight or bunching methods, as in the isotron [S4], are excluded from discussion.

In a pure magnetic field the equations of motion for an ion are:

$$F_x = M\frac{d^2x}{dt^2} = e\ (B_z\frac{dy}{dt} - B_y\frac{dz}{dt}) \qquad (5-1)$$

Likewise for F_y and F_z.

Putting $s = v_o t$

$$\frac{Mv_o}{e}\cdot\frac{d^2x}{ds^2} = B_z\frac{dy}{ds} - B_y\frac{dz}{ds} \quad \text{etc.} \qquad (5-2)$$

The initial conditions are:

$$\text{For} \qquad s = 0, \quad x = 0, \ \frac{dx}{ds} = \cos\alpha \qquad (5-3)$$

etc.

The orbit $z = f(x,y)$ is found by solving (5 – 2) using (5 – 3) and eliminating s.

Velocity focusing takes place at the point x_1, y_1, z_1, if $z_1 = f(x_1,y_1)$ independently of v_o. By making this condition one can compute the required fieldshape B (x,y,z).

However, equation (5 – 2) contains v_o only in the parameter Mv_o/e. As a result $z_1 = f(x_1,y_1)$ can only be made independent of Mv_o/e, Then velocity focusing will be inherent with mass focusing, which means that there is no mass separation at all.

In a pure electric field the orbit can be calculated similarly from the equations:

$$M\frac{d^2x}{dt^2} = e\,E_x \qquad \text{etc.} \qquad (5-4)$$

or

$$2V_o\frac{d^2x}{ds^2} = E_x \qquad \text{etc.} \qquad (5-5)$$

with starting conditions

$$s = o \quad x = o \quad \frac{dx}{ds} = \cos\alpha \qquad \text{etc.} \qquad (5-6)$$

From (5 – 5) it is clear that the orbits of all particles with

the same initial kinetic energy eV_o are identical. It follows that no mass separation can be achieved at all.

In a combined electric and magnetic field, the equations determining the orbits contain M and v_o in the form of two parameters. The fieldshape can be taken in such a way that $z_1 = f(x_1, y_1)$ is independent of v_o, but not of M. Then mass separation with velocity focusing is achieved.

Velocity focusing is very important in mass spectrographs, where the exact determination of masses is the object. In those instruments a very sharp line is required. In most cases they are "double focusing": their fields are designed in such a way that both velocity focusing and direction focusing (see below) are realized at the collector. Well known mass spectrographs were made by Aston [A1], Bainbridge [B7], Dempster [D2], Bainbridge and Jordan [B8], Mattauch [M2] and Jordan [J2].

Some double focusing mass spectrometers were also made [B9 B10]. However, modern mass spectrometers are used primarily for measuring concentrations. Since an extremely sharp line is not necessary for such measurements, velocity focusing is generally not applied, which allows considerably simpler equipment. However, ion sources which give nearly mono-energetic ion beams, are used [N1 T4].

It was pointed out in § 4 that the ion beam in the separator, after being accelerated, should not be subjected to strong electrostatic fields, because these would pull away electrons which form the compensating space charge. That is the reason why the application of velocity focusing in the separator is not desirable.

As a result, only a small energy spread of the ions from the source can be permitted. The radius of the orbit of an ion in a homogeneous magnetic field is given by [Z1]

$$r = \frac{1}{B}\sqrt{\frac{2MV_i}{e}} \qquad (5-7)$$

(B being the magnetic induction and eV_i the energy of the ions) and so

$$\frac{\Delta r}{r} = \frac{1}{2}\frac{\Delta V_i}{V_i} \qquad (5-8)$$

In a 180^o-instrument the ions pass through a semicircle and the aberration due to the energy spread is

$$\Delta s = 2\,\Delta r = \frac{\Delta V_i}{V_i} \cdot r \qquad (5-9)$$

Taking V_i = 25 kV and r = 102 cm and allowing an aberration of

0.4 mm, the energy spread of the ions must not exceed 10 eV. This demand can be properly realized with certain types of ion sources (see § 8).

2. Angles of entrance of the beam

Suppose we have a monokinetic ion beam, diverging from a point source and entering a magnetic field. Then equations (5 – 2) and (5 – 3) are valid.

As the beam is mono energetic the parameter Mv_o/e is the same for all particles having the same mass. It is possible, in principle, to shape the field in such a way that all such particles are focused at the collector independently of the initial conditions α, β, γ.

For particles with another mass, Mv_o/e will be different and these will describe other orbits.

As a result direction focusing is possible in a pure magnetic field without disturbing the mass selection. Of course, a combination of electric and magnetic fields can also be used for direction focusing.

As mentioned, an electrostatic field cannot be allowed in the separator; therefore direction focusing can only be obtained by properly shaping the magnetic field. This can be done in a number of ways.

We distinguish between radial and axial focusing. When the first fails, the beams of successive isotopes will become partially mixed, resulting in a reduction of the separation factor.

Insufficient axial focusing causes a loss of ions to the upper and lower walls of the vacuum chamber, which results in a reduction of the yield.

The mixing of isotopes must be considered as a more serious drawback than the decrease of the yield. Therefore, the radial focusing is the more important.

In a homogeneous magnetic field radial focusing occurs after 180^o. See fig. 3.

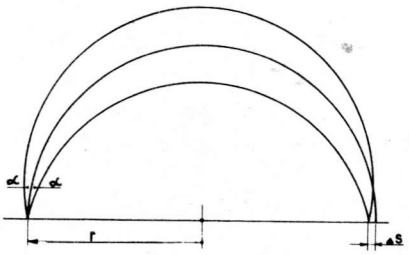

Fig. 3. Radial focusing in homogeneous magnetic field

Classen applied this type of focusing in his determination of e/m for electrons [C6] and Dempster [D3] constructed his mass spectrograph on this principle. Several 180°-spectrometers are known from the literature [T5 T6 B11].

In 1933 Barber [B12] proved that the aforementioned focusing is a special case of a more general principle.

It states: If the central ray of a diverging beam of ions, all having the same momentum, enters and leaves a homogeneous magnetic field at right angles to the boundaries of the field, the ions will be focused in a first order in a point lying on the line connecting the (point-) source with the centre of the central ray in the magnetic field (Fig. 4).

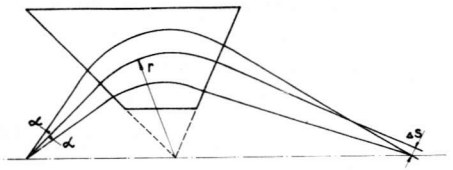

Fig. 4. Focusing in a sector type mass spectrometer

This theory was verified experimentally by Stephens [S7].

Bainbridge and Jordan used a 60° sector field in their mass spectrograph in 1936 [B8]. Nier was the first to utilize the sector field in a mass spectrometer [N2].

At the present most mass spectrometers are designed according to this principle [C7 T7 N1], because the magnetic flux required is less with the sector type than with the 180° type for the same resolution. Smaller and cheaper generators for the excitation of the field can be used and the stabilization is easier to attain. Moreover, the ion source of a sector type is placed in a separate constant magnetic field, which prevents mass discrimination due to the scanning of the main field.

The focusing mentioned is not perfect. It can easily be shown [S7] that the aberration Δs (in fig. 3 and 4) is given by

$$\Delta s = r \alpha^2 \qquad (5 - 10)$$

This means that the focusing is of the first order, the aberration being a quadratic function of the radial angle of entrance α.

An improvement of the focusing is possible. Obviously the outer and inner rays of the beam are deflected excessively with respect to the central ray.

By making the boundaries of the magnetic sector field curved

in stead of straight, the path of the central ray in the magnetic field, and so the deflection, can be somewhat increased.

The problem of how to shape the boundaries so as to get a radial focusing of second order was solved by several authors [H10] [K10] [S8].

In reality the magnetic field has no abrupt limits: there is a certain fringing field. By means of shimming it is possible to get a good focus experimentally. (Shimming is the process of applying small plates of iron locally in a magnetic field in order to shape it to give better focusing properties.)

Another way of causing the outer and inner rays of the beam to focus with the central ray is to shape the magnetic field in such a way that it decreases on both sides of the central ray.

An axially symmetric field shape required for perfect focusing after 180^{o} was first calculated by Bock [B13]. Unfortunately he made a mistake in his calculations by using an approximation, which was not permitted in this case. The correct derivation of the field was published by Beiduk and Konopinski [B14]. Langer and Cook constructed a beta spectrograph based on this field [L3].

When an inhomogeneous magnetic field is applied, axial focusing is also possible. Svartholm and Siegbahn calculated the focusing properties of rotationally symmetric fields [S9].

They showed that radial and axial focusing of the first order occur after angles given by

$$\Phi_r = \pi \left\{ \frac{B(r_o)}{B(r_o) + r_o B'(r_o)} \right\}^{1/2} \qquad (5-11)$$

and

$$\Phi_z = \pi \left\{ \frac{B(r_o)}{-r_o B'(r_o)} \right\}^{1/2} \qquad (5-12)$$

respectively, r_o being the main radius of the field.

For a homogeneous field ($B' = o$) this yields: $\Phi_r = \pi$, $\Phi_z = \infty$.

No axial focusing occurs for any fields with $B'(r_o) \geq 0$. Radial focusing is not possible for fields that fall off faster than the inverse ratio of the radius.

The field $B = B_o \left(\frac{r}{r_o}\right)^{-½}$ is interesting.

There $\Phi_r = \Phi_z = \pi\sqrt{2}$ and both radial and axial focusing occur after 255^{o}.

Svartholm and Siegbahn [S9] were the first to apply this field shape. They used it in a beta spectrograph and the results were satisfactory.

Expanding the field $B = B_o \left(\frac{r}{r_o}\right)^{-½}$ in a power series

$$B = B_o \sum_{n=o}^{\infty} b_n \left(\frac{r - r_o}{r_o}\right)^n$$

we obtain $b_o = 1$ $b_1 = -\frac{1}{2}$ $b_2 = 3/8$.

Svartholm [S10], Shull and Dennison [S11 S12] and Rosenblum [R3] showed that b_1 determines the angles of focusing and b_2 the aberration.

The radial aberration Δs caused by radial and axial angles of extrance α and β is $\frac{4}{3}\beta^2 r_o$ when $b_2 = \frac{1}{8}$, $\frac{2}{3}(\alpha^2 + \beta^2)r_o$ when $b_2 = \frac{1}{4}$ and $\frac{4}{3}\alpha^2 r_o$ when $b_2 = \frac{3}{8}$.

In most cases the slits in ion source and acceleration electrodes are long as compared to their width so that the system can be considered as two dimensional. Then α will have larger values than β and $b_2 = \frac{1}{8}$ is preferable. In that case the radial focusing is of second order in α.

Verster [V2] investigated the focusing properties of rotationally symmetric fields of the general form $B = B_o \sum_{n=o}^{\infty} b_n \left(\frac{r-r_o}{r_o}\right)^n$. He verified the cases mentioned above.

3. Finite width of the slits

An ion beam can be focused into a line on the collector when it emerges from a (real or virtual) line object. This is *e.g.* the case, when a perfectly parallel beam leaves the exit slit of the ion source (object at infinity).

Fig. 3 shows how a line source in a homogeneous magnetic field causes a broad parallel beam of ions after 90^o and a line focus of first order after 180^o. From this it is obvious that a parallel beam from a slit of finite width will be focused to a line after 90^o.

Sector fields can be used similarly. By properly shaping the magnetic field a focusing of higher order can be obtained. The method mentioned, the so called magnetic lens spectrometer, can be used with advantage when a broad and parallel ion beam is extracted from the source.

A useful source for alkali ions is the hot anode type [K7 K12] in which the ion emitting surface and the beam can be broad.

In most other sources, however, which work on the principle of a gaseous discharge, the exit slit must not be made too wide, because a sufficiently high pressure must be maintained in the source and at the same time a good vacuum in the chamber.

The magnetic lens spectrometer was first applied by Smythe, Rumbaugh and West for the separation of the Li and K-isotopes [S2]. They used an ion source with an emitting surface of 30 cm^2.

The separators of Walcher [W4] and Koch [K11] were also of the magnetic lens type. The parallel beam of ions was obtained by

means of an electrostatic lens. This parallelism was limited by the spread in initial velocity of the ions.

In modern sources with high ion output the ions do not leave the slit in a parallel beam nor can they be considered to emerge from a line. Instead, they diverge from an area of finite width. This area is at the smallest cross section of the beam; it may be the exit slit in the source or a slit in some other electrode, but it can also be located just outside the source. This can be the case when the potential distribution in the source is "self focusing" (see § 8).

The broadening of the object line results in a corresponding "aberration" of the image.

4. Interaction with gasmolecules

The total length of ion path in separators can extend to some meters. Therefore the possibility of a collision between an ion and a gasmolecule is appreciable even at a fairly low pressure. The mean free path for fast ions in a residual gas at a pressure of 3.10^{-5} mm Hg is just of the order of the total path length in our separator, a few meters [M2].

When the incident ions and the scattering particles have the same mass, approximately one half of the scattered ions gets only a very slight deviation from their original path; the other half can be considered to be scattered equally at random directions between 0 and $\frac{\pi}{2}$. As for the first half, the maximum value θ_o of the deviation angle is given [M2] by:

$$\theta_o = \frac{\pi}{2\ k\ a} \qquad (5 - 13)$$

where k is the wave number of the wave, corresponding to a particle of the beam, $k = \frac{2\pi Mv}{h}$ and a is the atomic diameter.

Making use of (5 – 7) we can write (5 – 13) as

$$\theta_o = \frac{h}{4\ a\ e\ r\ B} \qquad (5 - 14)$$

In a 180^o instrument, as is our separator, the aberration due to this deflection is a maximum for those collisions which take place at 90^o beyond the ion source and it is [B13]

$$\Delta s = \theta_o r = \frac{h}{4\ a\ e\ B} \qquad (5 - 15)$$

Taking $a = 2.10^{-8}$ cm and substituting the well known values of h and e, we come to

$$\Delta s = \frac{5}{B}\ \text{cm} \qquad (5 - 16)$$

$$B = B_o \sum_{n=o}^{\infty} b_n \left(\frac{r - r_o}{r_o}\right)^n$$

we obtain $b_o = 1$ $b_1 = -\frac{1}{2}$ $b_2 = 3/8$.

Svartholm [S10], Shull and Dennison [S11 S12] and Rosenblum [R3] showed that b_1 determines the angles of focusing and b_2 the aberration.

The radial aberration Δs caused by radial and axial angles of extrance α and β is $\frac{4}{3}\beta^2 r_o$ when $b_2 = \frac{1}{8}$, $\frac{2}{3}(\alpha^2 + \beta^2)r_o$ when $b_2 = \frac{1}{4}$ and $\frac{4}{3}\alpha^2 r_o$ when $b_2 = \frac{3}{8}$.

In most cases the slits in ion source and acceleration electrodes are long as compared to their width so that the system can be considered as two dimensional. Then α will have larger values than β and $b_2 = \frac{1}{8}$ is preferable. In that case the radial focusing is of second order in α.

Verster [V2] investigated the focusing properties of rotationally symmetric fields of the general form $B = B_o \sum_{n=o}^{\infty} b_n \left(\frac{r-r_o}{r_o}\right)^n$. He verified the cases mentioned above.

3. Finite width of the slits

An ion beam can be focused into a line on the collector when it emerges from a (real or virtual) line object. This is *e.g.* the case, when a perfectly parallel beam leaves the exit slit of the ion source (object at infinity).

Fig. 3 shows how a line source in a homogeneous magnetic field causes a broad parallel beam of ions after 90^o and a line focus of first order after 180^o. From this it is obvious that a parallel beam from a slit of finite width will be focused to a line after 90^o.

Sector fields can be used similarly. By properly shaping the magnetic field a focusing of higher order can be obtained. The method mentioned, the so called magnetic lens spectrometer, can be used with advantage when a broad and parallel ion beam is extracted from the source.

A useful source for alkali ions is the hot anode type [K7 K12] in which the ion emitting surface and the beam can be broad.

In most other sources, however, which work on the principle of a gaseous discharge, the exit slit must not be made too wide, because a sufficiently high pressure must be maintained in the source and at the same time a good vacuum in the chamber.

The magnetic lens spectrometer was first applied by Smythe, Rumbaugh and West for the separation of the Li and K-isotopes [S2]. They used an ion source with an emitting surface of 30 cm^2.

The separators of Walcher [W4] and Koch [K11] were also of the magnetic lens type. The parallel beam of ions was obtained by

means of an electrostatic lens. This parallelism was limited by the spread in initial velocity of the ions.

In modern sources with high ion output the ions do not leave the slit in a parallel beam nor can they be considered to emerge from a line. Instead, they diverge from an area of finite width. This area is at the smallest cross section of the beam; it may be the exit slit in the source or a slit in some other electrode, but it can also be located just outside the source. This can be the case when the potential distribution in the source is "self focusing" (see § 8).

The broadening of the object line results in a corresponding "aberration" of the image.

4. Interaction with gasmolecules

The total length of ion path in separators can extend to some meters. Therefore the possibility of a collision between an ion and a gasmolecule is appreciable even at a fairly low pressure. The mean free path for fast ions in a residual gas at a pressure of 3.10^{-5} mm Hg is just of the order of the total path length in our separator, a few meters [M2].

When the incident ions and the scattering particles have the same mass, approximately one half of the scattered ions gets only a very slight deviation from their original path; the other half can be considered to be scattered equally at random directions between 0 and $\frac{\pi}{2}$. As for the first half, the maximum value θ_o of the deviation angle is given [M2] by:

$$\theta_o = \frac{\pi}{2\ k\ a} \qquad (5 - 13)$$

where k is the wave number of the wave, corresponding to a particle of the beam, $k = \frac{2\pi Mv}{h}$ and a is the atomic diameter.

Making use of (5 – 7) we can write (5 – 13) as

$$\theta_o = \frac{h}{4\ a\ e\ r\ B} \qquad (5 - 14)$$

In a 180^o instrument, as is our separator, the aberration due to this deflection is a maximum for those collisions which take place at 90^o beyond the ion source and it is [B13]

$$\Delta s = \theta_o r = \frac{h}{4\ a\ e\ B} \qquad (5 - 15)$$

Taking $a = 2.10^{-8}$ cm and substituting the well known values of h and e, we come to

$$\Delta s = \frac{5}{B}\ \text{cm} \qquad (5 - 16)$$

and even at rather low field strengths of a few hundred gausz, this aberration is of no importance.

At these very small angles of deviation, the energy loss of the ions is negligible, as it is proportional to θ^2.

In order to get an impression of the effect of the ions scattered at random directions we shall consider the case of a 180^o homogeneous field spectrometer in the median plane of which an ion beam of very small cross section is passing.

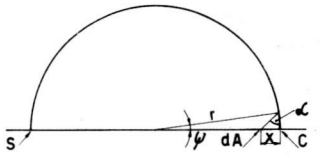

Fig. 5. Scattering of ions in 180^o instrument

S is the ion source, C the image at the collector. The height of the collector is 2 h. The number of ions emitted from the source per unit of time is N_o. We shall derive the number of scattered ions dN_x striking the small area dA = 2 h dx at a distance x from the image.

When the mean free path for this type of scattering is λ, the number of ions scattered in the small traject r d ψ is

$$d\,N = \frac{Nr}{\lambda}\, d\,\psi \qquad (5 - 17)$$

and

$$N = N_o\, e^{\frac{-(\pi-\psi)\,r}{\lambda}} \qquad (5 - 18)$$

The angular distribution of the scattered ions is given by

$$dN\ (\alpha, \beta) = \frac{Nr}{2\pi\lambda} d\psi\ d\alpha\ \cos\ \beta\ d\beta \qquad (5 - 19)$$

where α is the radial and β the axial angle of deflection.

When 2 h $\ll \pi R$, most of the scattered ions will be lost to the upper and lower walls of the vacuum chamber and only those ions scattered at very small values of ψ will make an appreciable contribution to dN_x.

Since an exact treatment is only possible by the use of numerical calculation we shall suffice with an approximate solution which enables an estimation of dN_x within a factor of two.

We shall assume that for $\psi > 2h/r$, all the scattered ions are lost tot the upper and lower walls of the vacuum chamber and for $\psi < 2h/r$ all the scattered ions reach the collector.

Since 2h/r is a small angle, the trajectories of the scattered

ions will be assumed to be straight lines, which involves that the energy loss due to the scattering, has no influence on the paths.

Then

$$\alpha = \tan^{-1} \frac{x}{r\psi} \qquad (5 - 20)$$

$$d\alpha = \frac{r\,\psi}{r^2\psi^2 + x^2}\,dx \qquad (5 - 21)$$

and

$$dN_x \approx dx \int_0^{\frac{2h}{r}} \frac{N_o\, e^{\frac{-\pi r}{\lambda}}}{\pi\,\lambda} \frac{r\,\psi}{r^2\psi^2 + x^2}\, r\, d\psi \qquad (5 - 22)$$

with the solution

$$dN_x \approx \frac{N_o\, e^{\frac{-\pi r}{\lambda}}}{2\,\pi\,\lambda} \ln \left\{1 + \left(\frac{2h}{x}\right)^2\right\} dx \qquad (5 - 23)$$

If we substitute r = 102 cm, λ = 600 cm, h = 6 cm, which may be normal values for our separator at operating conditions, it follows from (5 – 23) that even in the immediate vicinity of the image, the intensity of scattered ions per mm width at the collector is less than 0.1 % of the total beam intensity of the image. At a distance of 1 cm from the image, it is below 0.01 %. For normal separations this contamination is not serious but when very rare isotopes are to be separated, their purity can be spoiled appreciably. Moreover, the values mentioned will be increased by approximately a factor of M_i/M_m when the mass M_i of the incident particles is greater than the mass M_m of the scattering particles. This may be of importance, when heavy isotopes are being separated.

Serious is also the loss of ions which, according to (5 – 18) will amount to about 40 % under the conditions mentioned.

The most common type of interaction is the elastic collision, but inelastic collisions, the most important of which is the charge exchange, can also make a great contribution. The cross section of this process is relatively large, when the residual gas in the vacuum chamber is of the same kind as the ions. In that case there is a state of resonance which is characterized by a large value of the cross section. Not many data are available and these differ appreciably for various gases and ion velocities. Keene [K17] gives a value of 8.10^{-16} cm^2 for 15 keV He^+ ions in He gas. At a pressure of 4.10^{-5} mm Hg this corresponds to a free path for ion exchange of λ_e = 9 m.

From all this it is clear that a good vacuum in the separator is of great significance.

5. Space charge

The effect of space charge on the focusing and the possibility of space charge compensation were discussed in § 4.

6. Reflection

After reflection against a wall of the vacuum chamber, ions can enter the collector slit of another isotope and cause contamination. This inconvenience can be reduced by properly fitted baffles. Nevertheless, rather serious contamination of rare isotopes can be expected.

7. Instability of fields

Very stable magnetic and electric fields are required. Consider *e.g.* a homogeneous field spectrometer. The radius of the ion path is given by:

$$r = \frac{1}{B}\sqrt{\frac{2MV_i}{e}} \qquad (5-7)$$

The variations in the radius, due to variation of mass, magnetic field and accelerating voltage respectively, are

$$\frac{\Delta r}{r} = \frac{1}{2}\frac{\Delta M}{M} \qquad (5-24)$$

$$\frac{\Delta r}{r} = -\frac{\Delta B}{B} \qquad (5-25)$$

and

$$\frac{\Delta r}{r} = \frac{1}{2}\frac{\Delta V_i}{V_i} \qquad (5-26)$$

When the heaviest isotopes with *e.g.* $M = 235$ and $\Delta M = 1$ are separated, the distance, at the collector, between the two images is $\frac{1}{235}\,r$ according to (5 – 24). If we allow the images to shift over 10 % of this distance because of field and voltage changes, it is required that $\frac{\Delta V_i}{V_i} < \frac{1}{2350}$ and $\frac{\Delta B}{B} < \frac{1}{4700}$. So the stability must be at least 1 : 2500 for V_i and 1 : 5000 for B (§§ 22 and 25).

Choice of the magnetic field

The considerations of § 4 with respect to space charge compensation play an important part in the choice of the type of analyzing field to be used. The beam must not be subjected to strong electrostatic fields after having passed the acceleration system and it will be advantageous to have the ion orbits from source to collector within the magnetic field.

As the exit slit of the ion source is quite narrow, the magnetic lens is of no advantage here. Instead, it has the disadvantage of confining the ions to a narrow parallel beam, thus increasing space charge effects.

In order to have maximum ion output, the angle of entrance of the beam must be allowed to be as large as possible.

As a result a homogeneous field cannot be used. *E.g.* in a 180^{o} instrument with r = 100 cm and allowing $\alpha = 1/6$, the aberration $\Delta s = \alpha^2 r = 28$ mm, which limits the separating power to 36 (see § 6).

A second order radial focusing is necessary. Both the fields of Beiduk and Konopinski and of Svartholm and Siegbahn satisfy our conditions.

The last field is more favourable in some respects.

In the first place the dispersion D (*i.e.* the distance between the images of two isotopes at the collector) is for Svartholm $2 \frac{\Delta M}{M} r_o$ while for Konopinski it is $\frac{\Delta M}{M} r_o$. For the same dispersion, the main radius of Svartholm's field can be taken half as large as Konopinski's, but the magnetic field must extend over $\pi \sqrt{2}$ in stead of π radians. The total flux is about 0.7 of that of Konopinski's. As a result the magnet and its generator and stabilizer are somewhat smaller.

Secondly, the focusing properties of Svartholm's field differ from those of Konopinski's field. The first one has a first order axial focusing, the second has only a weak axial focusing for positive radial angles of entrance $\alpha > 0$. The effect of Svartholm's axial focusing is not favourable in the case of a long ion exit slit. Ions starting their path outside the median plane, with a velocity component directed towards this plane, *e.g.* caused by the weak axial focusing of the acceleration system, will be overfocused, which increases the possibility of loss to the upper and lower walls of the vacuum chamber.

The radial aberration caused by the axial angle of entrance is larger for Konopinski ($5{,}4\ \beta^2 r_o$) than for Svartholm ($\frac{4}{3}\ \beta^2 r_o$ when $b_2 = \frac{1}{8}$).

On the other hand, however, the technical realization of Konopinski's field is easier than is that of Svartholm's field. This does not refer to obtaining the correct field shape since that is only a matter of machining the pole pieces. But is does necessitate the construction of a 255^{o} magnet which is more difficult than is that of a semicircular one.

Moreover, the relative position of the ion source (at high voltage level) and the receiver (at earth level), both voluminous installations, is considerably more favourable for Konopinski's field.

5. Space charge

The effect of space charge on the focusing and the possibility of space charge compensation were discussed in § 4.

6. Reflection

After reflection against a wall of the vacuum chamber, ions can enter the collector slit of another isotope and cause contamination. This inconvenience can be reduced by properly fitted baffles. Nevertheless, rather serious contamination of rare isotopes can be expected.

7. Instability of fields

Very stable magnetic and electric fields are required. Consider *e.g.* a homogeneous field spectrometer. The radius of the ion path is given by:

$$r = \frac{1}{B}\sqrt{\frac{2MV_i}{e}} \qquad (5-7)$$

The variations in the radius, due to variation of mass, magnetic field and accelerating voltage respectively, are

$$\frac{\Delta r}{r} = \frac{1}{2}\frac{\Delta M}{M} \qquad (5-24)$$

$$\frac{\Delta r}{r} = -\frac{\Delta B}{B} \qquad (5-25)$$

and

$$\frac{\Delta r}{r} = \frac{1}{2}\frac{\Delta V_i}{V_i} \qquad (5-26)$$

When the heaviest isotopes with *e.g.* M = 235 and $\Delta M = 1$ are separated, the distance, at the collector, between the two images is $\frac{1}{235}$ r according to (5 – 24). If we allow the images to shift over 10 % of this distance because of field and voltage changes, it is required that $\frac{\Delta V_i}{V_i} < \frac{1}{2350}$ and $\frac{\Delta B}{B} < \frac{1}{4700}$. So the stability must be at least 1 : 2500 for V_i and 1 : 5000 for B (§§ 22 and 25).

Choice of the magnetic field

The considerations of § 4 with respect to space charge compensation play an important part in the choice of the type of analyzing field to be used. The beam must not be subjected to strong electrostatic fields after having passed the acceleration system and it will be advantageous to have the ion orbits from source to collector within the magnetic field.

As the exit slit of the ion source is quite narrow, the magnetic lens is of no advantage here. Instead, it has the disadvantage of confining the ions to a narrow parallel beam, thus increasing space charge effects.

In order to have maximum ion output, the angle of entrance of the beam must be allowed to be as large as possible.

As a result a homogeneous field cannot be used. *E.g.* in a 180^{o} instrument with r = 100 cm and allowing $\alpha = 1/6$, the aberration $\Delta s = \alpha^2 r = 28$ mm, which limits the separating power to 36 (see § 6).

A second order radial focusing is necessary. Both the fields of Beiduk and Konopinski and of Svartholm and Siegbahn satisfy our conditions.

The last field is more favourable in some respects.

In the first place the dispersion D (*i.e.* the distance between the images of two isotopes at the collector) is for Svartholm $2 \frac{\Delta M}{M} r_o$ while for Konopinski it is $\frac{\Delta M}{M} r_o$. For the same dispersion, the main radius of Svartholm's field can be taken half as large as Konopinski's, but the magnetic field must extend over $\pi\sqrt{2}$ in stead of π radians. The total flux is about 0.7 of that of Konopinski's. As a result the magnet and its generator and stabilizer are somewhat smaller.

Secondly, the focusing properties of Svartholm's field differ from those of Konopinski's field. The first one has a first order axial focusing, the second has only a weak axial focusing for positive radial angles of entrance $\alpha > 0$. The effect of Svartholm's axial focusing is not favourable in the case of a long ion exit slit. Ions starting their path outside the median plane, with a velocity component directed towards this plane, *e.g.* caused by the weak axial focusing of the acceleration system, will be overfocused, which increases the possibility of loss to the upper and lower walls of the vacuum chamber.

The radial aberration caused by the axial angle of entrance is larger for Konopinski ($5{,}4\ \beta^2 r_o$) than for Svartholm ($\frac{4}{3}\ \beta^2 r_o$ when $b_2 = \frac{1}{8}$).

On the other hand, however, the technical realization of Konopinski's field is easier than is that of Svartholm's field. This does not refer to obtaining the correct field shape since that is only a matter of machining the pole pieces. But is does necessitate the construction of a 255^{o} magnet which is more difficult than is that of a semicircular one.

Moreover, the relative position of the ion source (at high voltage level) and the receiver (at earth level), both voluminous installations, is considerably more favourable for Konopinski's field.

Conclusions that could be drawn from indications and details that trickled out, led to the conviction that the successful electromagnetic separation of uranium in the United States had been carried out in separators of the 180^{o} type. This was also an important factor in our considerations which led to the decision to apply the field of Beiduk and Konopinski in our separator.

§ 6. Image formation in Konopinski's field

Beiduk and Konopinski [B14] determined the shape required for a magnetic field to give perfect focusing beyond 180^{o}. It is:

$$B_z(r,o) = B_o\left(1 - \tfrac{3}{4}\delta^2 + \tfrac{7}{8}\delta^3 - \tfrac{9}{16}\delta^4 + \tfrac{51}{320}\delta^5 \ldots\right) \qquad (6-1)$$

Here $B_z(r,o)$ is the magnetic field in the median plane of symmetry ($z = o$) and δ is given by

$$\delta = \frac{r - r_o}{r_o} \qquad (6-2)$$

where r_o is the main radius of the field.

The focusing is perfect only for ions from a point source and whose orbits lie in the median plane. Actually the source will have finite dimensions and the ions may be emitted at an axial angle β. This was also taken into account by Beiduk and Konopinski. They evaluated the orbits of ions under various initial conditions and found the following parametric expressions for the orbit:

$$\varphi = \frac{\pi}{2} - \omega_o t + \delta_1 \sin\omega_o t + \alpha(1 - \cos\omega_o t) \qquad (6-3)$$

$$\begin{aligned}\zeta = {} & \zeta_1 + \beta\omega_o t - 3\alpha\beta - \tfrac{3}{2}\delta_1\zeta_1 + \tfrac{3}{2}(\beta\delta_1 - \alpha\zeta_1)\omega_o t + \\ & + \tfrac{3}{2}(\alpha\zeta_1 - 2\beta\delta_1 + \alpha\beta\omega_o t)\sin\omega_o t + \\ & + \{3\alpha\beta + \tfrac{3}{2}\delta_1(\zeta_1 + \beta\omega_o t)\}\cos\omega_o t\end{aligned} \qquad (6-4)$$

$$\begin{aligned}\delta = {} & \delta_1\cos\omega_o t + \alpha\sin\omega_o t + \beta^2 + \tfrac{5}{8}(\alpha^2 + \delta_1^2) - \tfrac{3}{4}(\zeta_1 + \beta\omega_o t)^2 + \\ & + \tfrac{3}{2}(\alpha\delta_1 + \beta\zeta_1)\sin\omega_o t + (\tfrac{3}{4}\zeta_1^2 - \tfrac{1}{4}\delta_1^2 - \alpha^2 - \beta^2)\cos\omega_o t + \\ & + \tfrac{3}{8}\{(\alpha^2 - \delta_1^2)\cos 2\omega_o t - 2\alpha\delta_1\sin 2\omega_o t\}\end{aligned} \qquad (6-5)$$

Here α = the radial and β = the axial angle of entrance,

$$\omega_o = \frac{e\,B_o}{M} \qquad (6-6)$$

$$\zeta = \frac{z}{r_o} \qquad (6-7)$$

φ is the angle coordinate as shown in fig. 6. δ_1, ζ_1 is the starting point of the ion at the source.

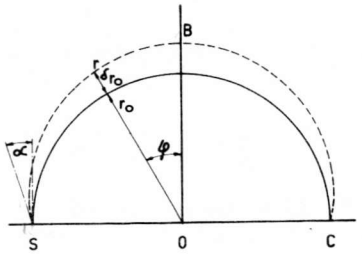

Fig. 6. Ion paths in Konopinski's field

From the relations (6 – 3), (6 – 4), (6 – 5) δ and ζ can be determined for any value of φ.

A diaphragm or baffle to limit the beam dimensions is placed at $\varphi = o$, where the cross section of the beam is a maximum.

At this baffle ($\varphi = o$):

$$\zeta_o = \zeta_1(1 - 0.85\ \alpha - 1.5\ \delta_1) + \frac{\beta\pi}{2}(1 + 0.23\ \alpha + 0.23\ \delta_1) \qquad (6-8)$$

$$\delta_o = \alpha\ (1 + 0.5\ \delta_1 + 0.25\ \alpha) - 0.85\ \beta^2 - 0.75\ \zeta_1(\zeta_1 + 1.14\ \beta) \qquad (6-9)$$

And at the collector ($\varphi = -\frac{\pi}{2}$):

$$\zeta_2 = \zeta_1 + \beta\pi - 3\ \zeta_1\ (\delta_1 + 0.5\ \pi\alpha) - 4\ \alpha\beta \qquad (6-10)$$

$$\delta_2 = -\delta_1 + 0.5\ \delta_1^2 - 5.41\ \beta^2 - 1.5\ \zeta_1^2 - 4.71\ \beta\zeta_1 \qquad (6-11)$$

In order to study the image, we shall make further approximations based on the restrictions:

$$|\delta_1| \leq 0.001 \qquad (6-12)$$

$$|\zeta_1| \leq 0.05 \qquad (6-13)$$

$$-0.19 < \alpha < 0.11 \qquad (6-14)$$

(See § 20)

$$|\beta| \leq 0.03 \qquad (6-15)$$

which are valid in our separator. We simplify the equations (6 – 12) – (6 – 15) to

$$\zeta_o = \zeta_1 - 0.85\ \alpha\zeta_1 + 0.5\ \beta\pi + 0.12\ \pi\alpha\beta \qquad (6-16)$$

$$\delta_o = \alpha - 0.85\ \beta^2 - 0.75\ \zeta_1^2 - 0.86\ \beta\zeta_1 \qquad (6-17)$$

$$\zeta_2 = \zeta_1 + \beta\pi - 1.5\ \pi\alpha\zeta_1 - 4\ \alpha\beta \qquad (6-18)$$

$$\delta_2 = -\delta_1 - 5.41\ \beta^2 - 1.5\ \zeta_1^2 - 4.71\ \beta\zeta_1 \qquad (6-19)$$

It is obvious from these that the only result of a small variation of δ_1 is a similar displacement in δ_2. Therefore, the image of a long and narrow rectangular object can be found by determining the image of a straight line and then adding the width of the object.

We shall now consider the object line $\delta_1 = 0$. The image of this line is curved, due to the inhomogeneity of the field. For an object emitting a parallel ion beam, the shape of the image can be determined by eliminating ζ_1 from (6 – 18) and (6 – 19). This yields

$$(1 - 4.7\ \alpha)^2\ \delta_2 = -1.5\ \zeta_2^2 + (5.1\ \beta + 10.2\ \alpha\beta)\ \zeta_2 - 5.4\ \beta^2 - 55\ \alpha^2\beta^2 \qquad (6-20)$$

This is a parabola with its axis in the δ direction and with a parameter $-\frac{1}{3}\ (1 - 4.7\ \alpha)^2$. In reality the beam is not parallel but various values of α and β will occur. However, they will be limited by the baffle placed at $\varphi = 0$.

Each emitting point of the object line will project an image of the outline of the baffle opening upon the collector. The area enclosed by such an image is actually the image of the emitting point. Its shape is found by eliminating α and β from the equations (6 – 16) – (6 – 19). The result is:

$$\delta_2 = -1.51\ \zeta_o^2 - 0.61\ \zeta_1^2 + \delta_o\zeta_1^2 + 0.80\ \zeta_o\zeta_1 - 3.8\ \delta_o\zeta_o\zeta_1 + 0.09\ \zeta_1\zeta_2 - 0.27\ \zeta_o\zeta_2 \qquad (6-21)$$

$$\zeta_2 = 2\ \zeta_o - \zeta_1 - 2.5\ \delta_o\zeta_o \qquad (6-22)$$

Suppose a rectangular baffle opening limited by vertical lines $\delta_o = a$ and horizontal lines $\zeta_o = b$. From (6 – 21) and (6 – 22) it follows that these lines are projected as

$$(2 - 2.5\ a)^2\ \delta_2 = (-\ 2.04 + 0.7\ a)\ \zeta_2^2 + (-\ 1.58 - 9.8\ a)\ \zeta_1\zeta_2 +$$

$$+ (-\ 2.34 + 0.5\ a)\ \zeta_1^2 \qquad (6 - 23)$$

and

$$\delta_2 = (1.60\ \zeta_1 - 0.27\ b - 0.40\ \zeta_1^2/b)\ \zeta_2 - 1.51\ b^2 +$$

$$- 2.22\ b\zeta_1 + 1.71\ \zeta_1^2 - 0.40\ \zeta_1^3/b \qquad (6 - 24)$$

being parabolas and straight lines respectively.

Fig. 7 shows the image of the points $\zeta_1 = 0$, $\zeta_1 = + 0.02$ and $\zeta_1 = + 0.05$, defined by the baffle: $a_1 = + 0.11$, $a_2 = - 0.19$, $b_1 = + 0.06$, $b_2 = - 0.06$.

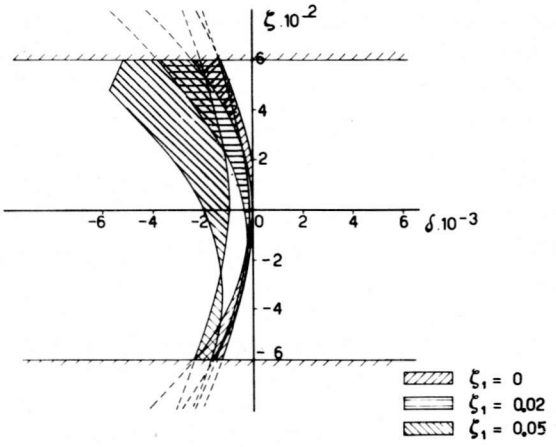

Fig. 7. Images of three points, defined by a rectangular baffle.

In the figure the limits $\zeta_2 = \pm 0.06$ of the collector slit are indicated. As $\zeta = 0$ is a plane of symmetry, the images of points with negative ζ_1 are just the reverse of those with positive ζ_1. The image of the line $\delta_1 = 0$ will be the area covered by the image of all its points from $\zeta_1 = - 0.05$ to $\zeta_1 = + 0.05$. From the part of fig. 7 above the line $\zeta_2 = 0$ it can be seen that this area is limited:

a. above and below by the boundaries of the collector slit.
b. on the right side by the projections of the baffle-line $\delta_o = - 0.19$ from $\zeta_1 = 0$.
c. on the left side by the projection of the baffle-lines $\delta_o = + 0.11$ and $\zeta_o = \pm 0.06$ from $\zeta_1 = \pm 0.05$.

The fact that the image is curved is of little importance. The curvature is not great (note the different scales on the δ and the ζ axis in fig. 7) and it is possible to make a curved

$$|\beta| \leq 0.03 \qquad (6-15)$$

which are valid in our separator. We simplify the equations (6 – 12) – (6 – 15) to

$$\zeta_o = \zeta_1 - 0.85\ \alpha\zeta_1 + 0.5\ \beta\pi + 0.12\ \pi\alpha\beta \qquad (6-16)$$

$$\delta_o = \alpha - 0.85\ \beta^2 - 0.75\ \zeta_1^2 - 0.86\ \beta\zeta_1 \qquad (6-17)$$

$$\zeta_2 = \zeta_1 + \beta\pi - 1.5\ \pi\alpha\zeta_1 - 4\ \alpha\beta \qquad (6-18)$$

$$\delta_2 = -\delta_1 - 5.41\ \beta^2 - 1.5\ \zeta_1^2 - 4.71\ \beta\zeta_1 \qquad (6-19)$$

It is obvious from these that the only result of a small variation of δ_1 is a similar displacement in δ_2. Therefore, the image of a long and narrow rectangular object can be found by determining the image of a straight line and then adding the width of the object.

We shall now consider the object line $\delta_1 = 0$. The image of this line is curved, due to the inhomogeneity of the field. For an object emitting a parallel ion beam, the shape of the image can be determined by eliminating ζ_1 from (6 – 18) and (6 – 19). This yields

$$(1 - 4.7\ \alpha)^2\ \delta_2 = -1.5\ \zeta_2^2 + (5.1\ \beta + 10.2\ \alpha\beta)\ \zeta_2 - 5.4\ \beta^2 - 55\ \alpha^2\beta^2 \qquad (6-20)$$

This is a parabola with its axis in the δ direction and with a parameter $-\frac{1}{3}\ (1 - 4.7\ \alpha)^2$. In reality the beam is not parallel but various values of α and β will occur. However, they will be limited by the baffle placed at $\varphi = 0$.

Each emitting point of the object line will project an image of the outline of the baffle opening upon the collector. The area enclosed by such an image is actually the image of the emitting point. Its shape is found by eliminating α and β from the equations (6 – 16) – (6 – 19). The result is:

$$\delta_2 = -1.51\ \zeta_o^2 - 0.61\ \zeta_1^2 + \delta_o\zeta_1^2 + 0.80\ \zeta_o\zeta_1 - 3.8\ \delta_o\zeta_o\zeta_1 + 0.09\ \zeta_1\zeta_2 - 0.27\ \zeta_o\zeta_2 \qquad (6-21)$$

$$\zeta_2 = 2\ \zeta_o - \zeta_1 - 2.5\ \delta_o\zeta_o \qquad (6-22)$$

Suppose a rectangular baffle opening limited by vertical lines $\delta_o = a$ and horizontal lines $\zeta_o = b$. From (6 – 21) and (6 – 22) it follows that these lines are projected as

$$(2 - 2.5\ a)^2\ \delta_2 = (-\ 2.04 + 0.7\ a)\ \zeta_2^2 + (-\ 1.58 - 9.8\ a)\ \zeta_1\zeta_2 +$$

$$+ (-\ 2.34 + 0.5\ a)\ \zeta_1^2 \qquad (6 - 23)$$

and

$$\delta_2 = (1.60\ \zeta_1 - 0.27\ b - 0.40\ \zeta_1^2/b)\ \zeta_2 - 1.51\ b^2 +$$

$$- 2.22\ b\zeta_1 + 1.71\ \zeta_1^2 - 0.40\ \zeta_1^3/b \qquad (6 - 24)$$

being parabolas and straight lines respectively.

Fig. 7 shows the image of the points $\zeta_1 = 0$, $\zeta_1 = + 0.02$ and $\zeta_1 = + 0.05$, defined by the baffle: $a_1 = + 0.11$, $a_2 = - 0.19$, $b_1 = + 0.06$, $b_2 = - 0.06$.

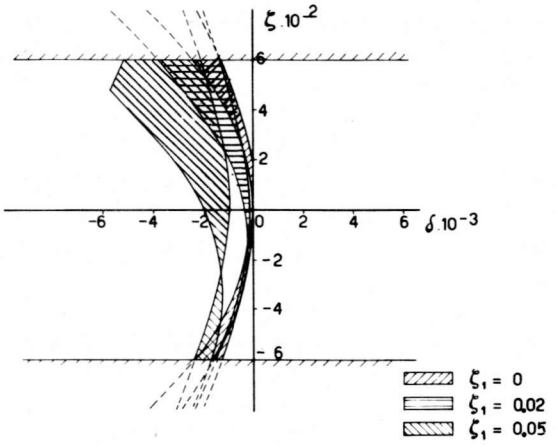

Fig. 7. Images of three points, defined by a rectangular baffle.

In the figure the limits $\zeta_2 = \pm 0.06$ of the collector slit are indicated. As $\zeta = 0$ is a plane of symmetry, the images of points with negative ζ_1 are just the reverse of those with positive ζ_1. The image of the line $\delta_1 = 0$ will be the area covered by the image of all its points from $\zeta_1 = - 0.05$ to $\zeta_1 = + 0.05$. From the part of fig. 7 above the line $\zeta_2 = 0$ it can be seen that this area is limited:

a. above and below by the boundaries of the collector slit.
b. on the right side by the projections of the baffle-line $\delta_o = - 0.19$ from $\zeta_1 = 0$.
c. on the left side by the projection of the baffle-lines $\delta_o = + 0.11$ and $\zeta_o = \pm 0.06$ from $\zeta_1 = \pm 0.05$.

The fact that the image is curved is of little importance. The curvature is not great (note the different scales on the δ and the ζ axis in fig. 7) and it is possible to make a curved

collector slit that will conform to the image. More serious is the width of the aberration which has a maximum of 0.005 in our case. Adding the width of the exit slit in the ion source (0.002) and neglecting all other sources of aberrations, we have a total line width of 0.007.

A decrease of this width can be achieved by cutting off the protruding edge on the very left of the image. This is possible by shaping the baffle in such a way that ions with large positive α and large $|\beta|$ are intercepted (see § 20). In this way the line width is reduced to 0.006.

This corresponds to a separating power of 167 (see below).

A further decrease (which will be necessary for the separation of very heavy isotopes) is possible by curving the exit slit of the ion source slightly in such a way that the images of points with increasing $|\zeta_1|$ shift to the right or by reducing the height of the exit slit of the source.

An important question is, where the images for ions with various masses will be situated; in other words, which will be the shape of the focal plane on the collector side.

To calculate this, we shall make an approximation based on Svartholm's relation for the angle of first order radial focusing [9]:

$$\Phi_r = \pi \left\{ \frac{B(r_o)}{B(r_o) + r_o B'(r_o)} \right\}^{1/2} \qquad (5-11)$$

The main trajectory of the ion beam for which $M = \frac{e B_o^2 r_o^2}{2V}$ follows the principal circle of the field: $B' = 0$ and $\Phi_r = \pi$. For beams with $M \neq \frac{e B_o^2 r_o^2}{2V}$, however, that trajectory is not symmetric with respect to the field. Along the path, δ increases from 0 to δ_2. For Konopinski's field, $B' = -\frac{3}{2}\frac{\delta}{r_o}$. Substituting the average value $B' = -\frac{3}{4}\frac{\delta_2}{r_o}$ in (5 – 11) we come to

$$\Phi_r \approx \pi \left(1 + \tfrac{3}{8}\delta_2\right) \qquad (6-25)$$

From (6 – 25) it follows that the focal plane makes an angle $\tan^{-1}(\frac{3}{8}\pi)$ ($\approx 50^\circ$) with the radius vector at the collector.

We have not succeeded in calculating the aberration for $M \neq \frac{e B_o^2 r_o^2}{2V}$, but the experimental results are satisfactory.

Next we shall discuss the separating power of the instrument.

There is an essential difference between the resolving power R.P. of a mass spectrometer and the separating power S.P. of an isotope separator.

The purpose of a mass spectrometer is to measure intensities. For accurate results it is required that the peaks of different masses be completely separated, which means that the collector current goes to zero between adjacent peaks. The purpose of an isotope separator is to prepare a pure target of a certain isotope.

First it may be noted that the relations (5 – 24) – (5 – 26) are valid in a first approximation for Konopinski's field as well as for a homogeneous field, since $\left(\frac{\partial B}{\partial r}\right)_{r=r_o} = 0$.

Consequently, the dispersion D is given by

$$D = 2 \Delta r = \frac{\Delta M}{M} r_o \qquad (6 - 26)$$

Consider now the images, at the collector, of a series of isotopes with mass M, $M + \Delta M$, $M + 2\Delta M$, etc. The width of the images is s and their relative distance is D ($= \frac{\Delta M r_o}{M}$) (Fig. 8). The width of the collectorslit is w. s, D and w are measured in radial direction.

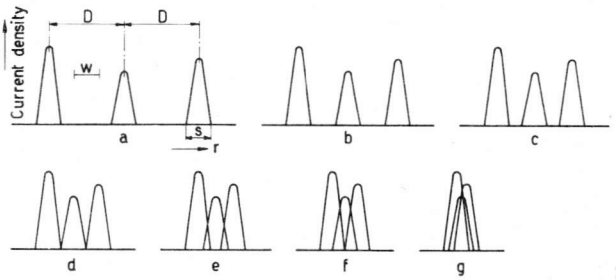

Fig. 8. Relative positions of the images at the collector

We must distinguish between the following cases:

a. $D > s + w$

In the mass spectrometer the peaks are resolved. In the separator a pure target of each isotope is obtained. For a maximum yield we can take w = s in the separator.

b. $D = s + w$

In the mass spectrometer the peaks are then just resolved. We have reached its resolving power:

$$R.P. = \left(\frac{M}{\Delta M}\right)_{max} = \frac{r_o}{s + w} \qquad (6 - 27)$$

c. $s + w > D > s$

In the mass spectrometer the peaks are no longer resolved. In the separator the targets are still pure.

d. $D = s$

In the separator we can obtain a pure target with w = s but we have reached its "efficient separating power":

$$\text{S.P.} = \left(\frac{M}{\Delta M}\right)_{max} = \frac{r_o}{s} \qquad (6 - 28)$$

d. $s > D > \frac{s}{2}$

It is still possible to obtain a pure target by making $w < (2D-s)$. Of course the yield will be seriously curtailed by doing this.

f. $D = \frac{s}{2}$

To obtain a pure target, we must take w = o. We have thus reached the separating power for zero yield:

$$(\text{S.P.})_o = \left(\frac{M}{\Delta M}\right)_{max} = \frac{2r_o}{s} \qquad (6 - 29)$$

g. $D < \frac{s}{2}$

Complete separation of all the isotopes is no longer possible.

In case (g) the targets of the lightest and the heaviest isotope of the series can still be obtained in a pure state by using a collectorslit with w = D and shifting its position over a distance $\pm \frac{s - D}{2}$. Actually the boundaries of the peaks are not so abrupt as in fig. 8. Due to the scattering of ions on gas molecules and reflections the peaks will have "wings" of low intensity. The width s of the image is defined such that at its boundaries the intensity is *e.g.* 5% of the maximum intensity, which means that a certain amount of contamination is accepted.

From now on, when speaking of the separating power, we mean the "efficient separating power" (6 – 28).

§ 7. Acceleration of the ions

Various configurations of the acceleration system were investigated by us. The experiments were carried out by means of models on the resistor network (§ 14) as well as in the actual separator.

The most satisfactory system, finally applied, is shown in fig. 9.

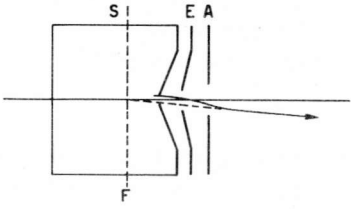

Fig. 9. Acceleration system of the separator

The ion source S and the extraction electrode E are V-shaped in such a way that they form an electrostatic lens according to Pierce [P1]. This lens counteracts the divergence of the beam, during the acceleration, due to the space charge. When a space charge limited current is extracted from the source it produces a parallel beam, but when a smaller current is extracted overfocusing occurs as shown in fig. 9. The ion source is at the accelerating voltage of maximum + 30 kV. The extraction electrode is not earthed, but at an adjustable negative potential of maximum – 10 kV. It is shielded from the beam by the earthed electrode A.

This system has the following advantages over the acceleration by a single electrode:

1. The negative electrode forms an electron mirror for the electrons from the beam. So they cannot reach the ion source and are forced back to the beam. As a result their space charge compensating action is increased.
2. Since the electrons cannot reach the ion source, the load of the high voltage supply and high tension breakdowns are greatly reduced.
3. The location of the focal plane F (fig. 9) from which the ions seem to emerge depends, among other things, upon the potential of the central electrode. Focusing can be adjusted by means of that potential, keeping the net accelerating voltage constant and thus keeping the ion beam on the collectorslit.
4. The lens causes a weak axial focusing of the beam, thus reducing the loss of ions to top and bottom of the vacuum chamber.

§ 8. Type of ion source to be used

Ion sources have been developed in a great variety of types. A recent survey of this subject was given by Thomas [T8].

The source for our separator must meet the following requirements:

a. The ion output must be high.
b. The operating pressure must be low.
c. The consumption of energy must not be too high.
d. The energy spread of the ions extracted from the source must be small.
e. It must be universally applicable to various kinds of ions.
f. One type of ions, preferable atomic, must predominate.
g. Rapid fluctuations in the ion output cannot be permitted.

We shall now discuss these requirements in more detail.

a. Large output

Three main points of importance for the output of an ion source are:

1. The presence of a large number of ions per unit volume in the discharge.
2. The transport of ions in the discharge to the exit slit.
3. The extraction of ions from the exit slit.

In order to obtain a high ion density, even at a low gas pressure, the ionizing electrons must be used as advantageously as possible.

In the first place this can be achieved by taking the energy of the electrons such that the probability of ionization is a maximum [E3]. Further, by reducing the loss of electrons to the walls of the source (proper shaping of the source and application of an axial magnetic field). And finally by increasing the effective path length of the electrons by using oscillating electrons.

The transport of ions to the exit slit is largely determined by the potential distribution in the source. Consequently, it depends on the discharge conditions. In the case of moderate discharges, the penetration of the electric field from the extraction electrode causes a potential distribution as shown in fig. 10. Because of the focusing of ions on the exit slit, this distribution is called self focusing.

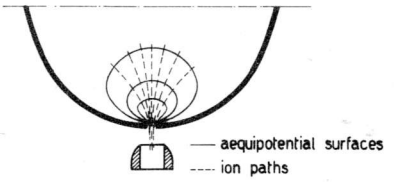

Fig. 10. Self focusing potential distribution in ion source

Concerning the extraction of ions, we must distinguish between two situations. In the first case, all ions focused on the slit may be extracted. But on the other hand it is possible that so

many ions are supplied that a further increase of the output is prevented by the space charge. In that case, the so called space charge limited current is extracted [K15]. The value of this current can be calculated for simple electrode configurations [L4]. For a very large plane emitter placed a distance d from a plane electrode at potential V_i, it is:

$$J_i = \frac{\sqrt{2}}{9\,\pi\,c}\sqrt{\frac{e}{M}}\,V^{3/2}\,d^{-2}\ \text{e.m.e.}/_{\text{cm}^2} \qquad (8-1)$$

if we suppose that the particles are emitted with zero initial velocity.

For other electrode configurations a geometry factor must be added to (8 – 1), but in any case a maximum current exists for each configuration and potential distribution.

This maximum current can be increased by emitting the particles with finite initial velocity. However, the gain will be small if the initial energy is small in comparison to eV_i and this will practically always be the case.

It may be remarked that, if a space charge limited current is extracted, this current cannot be increased by measures in the source: ion production and transport are then sufficient.

b. Low operating pressure

A low operating pressure is important because it means a low gas consumption. Moreover it allows the use of a large exit slit and yet enables the maintenance of a good vacuum in the chamber. A high ion density at low pressures can be obtained by making the path of the ionizing electrons as long as possible. This can be achieved by causing the electrons to oscillate (h.f. sources or magnetic oscillation sources).

c. Low energy consumption

Since the practice is to earth the acceleration chamber, the ion source will be at a high positive potential. The energy needed must be supplied at that high level, which necessitates the use of an insulating transformer rated for the proper power output. Therefore it is necessary to keep this power requirement as low as possible.

d. Small energy spread

The ions in the beam, after extraction from the source, will not all possess exactly the same energy since they were created at different places in the source and consequently at different potentials. It is obvious that the homogeneity of the beam will be better as the potential differences in the source become smal-

ler. Therefore, it is favourable when the ions are created in a plasma where the potential differences are only a few volts.

Energy spread will also occur when ions transfer energy by collisions with gas molecules incurred on their way to the exit slit. However, these collisions have little probability at pressures below which the path in the source is small as compared to the mean free path ($< 4.10^{-3}$mm Hg).

e. Universal application

Some types of ion source can only be used for particular elements. *E.g.* the hot anode source of Kunsman [K7], which is applicable to the alkali ions alone. A very successful modification of this type was developed by Koch [K12].

In general, however, an ion source is a gaseous discharge in which all sorts of ions can be created, if the substance to be ionized is supplied as a gas.

Because many elements have gaseous compounds only at an increased temperature, the source must be constructed in such a way that it can withstand high temperatures. Moreover, it must resist chemical reaction with various substances, even at high temperatures.

f. Atomic ions

Suppose that nitrogen gas is admitted into the ion source. Then N^+ as well as N_2^+ ions will be created. We can choose accelerating voltage and magnetic field strength such that the ions of one of these types reach the collector, but the other ones will be lost from the separation process.

In the case of more complicated molecules, various types of ions occur. If one of these types predominates strongly over all the others, the loss of ions of another mass will not be too serious. Separation of atomic ions is easiest because the separation of heavier masses requires a greater separating power of the instrument.

Several investigations have been carried out on the formation of atomic and molecular hydrogen ions [S5] [N4]. This work was stimulated by the development of proton accelerating devices because the sources of these accelerators must have a large atomic ion output.

From these experiments it turned out that the following factors favour the production of molecular hydrogen ions: low pressure, low electron energy, small current density, small source dimensions and metal walls of the source at a rather low temperature.

The influence of pressure, temperature, electron energy and

current on the atom-molecule ratio for a particular ion source can easily be investigated in the separator.

g. No fluctuations

In § 4 it was emphasized that a short but finite time is needed for the formation of a space charge compensated ion beam. If the ion current from the source fluctuates with a period of the same order as or shorter than one formation time (10^{-4} – 10^{-3} sec), the space charge compensation will be reduced. Therefore a very steady ion current is required.

Concerning the demands *a*, *b* and *d* we require for the source of our separator:

a. Ion output of several mA. With a total collector current of 1 mA an isotope of mass number 100 with a 10% abundance is collected at the rate of 10 mg per day of 24 hours.
b. Operating pressure a few times 10^{-3} mm Hg. With an ion exit slit of 2 cm^2 area and the pumping system used, the pressure in the vacuum chamber will be about a factor of 100 to 50 less than in the source, when gas is admitted to the source.
c. Energy spread less than 10 eV. With an accelerating voltage of 25 kV and a main radius of 1020 mm this will cause an aberration of 0.4 mm.

These conditions and that of universal application are satisfied by the arc source, the h. f. sources and the magnetic oscillation source with filament. The discharge mechanisms of these sources will now be described:

1. Arc source (fig. 11a) [F1 B15]

Electrons from a filament are accelerated through one or two hundred volts and ionize the gasmolecules with which they collide. The anode is a cylinder. In this way the ions are created in a space that is approximately electrical field free and the energy spread will be small. If an axial magnetic field is ap-

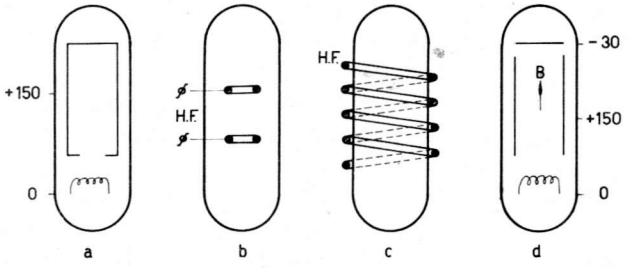

Fig. 11. Discharge mechanism of some ion sources

plied, the electrons are prevented from going directly to the cylinder wall.

2. H.F. sources

The ionizing electrons get their energy from a high frequency field. This field can be applied:

a. by a system of internal or external electrodes (fig. 11b: electrical h.f. discharge [A4]).
b. by a coil around the discharge tube, which induces ring currents in the plasma (fig. 11c: magnetic h.f. discharge [T9]).

The advantage of h.f. sources is the fact that the discharge is maintained by secundary electrons alone: no filament is needed.

3. Magnetic oscillation source with filament (fig. 11d [F2 A5 H11])

Electrons from a filament are accelerated by an anode cylinder. Because of the axial magnetic field, they cannot reach this cylinder. Nor can they reach the reflector plate at the top of the cylinder, which is maintained at a negative potential and so forms an electron mirror. The electrons are therefore forced to oscillate up and down between the filament and the reflector plate. How they finally reach the anode cylinder is not as yet fully understood. The radius of the helical trajectory of an electron depends on its velocity component in the radial direction and it is given by

$$r = \frac{1}{B}\sqrt{\frac{2mV}{e}} \qquad (8 - 2)$$

in which V is the voltage, corresponding to the radial velocity.

If V = 150 Volt and B = 2000 Gausz it follows from (8 – 2) that r = 0.2 mm.

When the electron loses energy by ionizing gas molecules, the radius will decrease. As a result, it is extremely difficult for the electrons, especially for the secundaries, to reach the cylindrical wall. From this consideration it follows that the anode current should be very small in the presence of a strong magnetic field. And indeed this is the case at very low pressures. But when the pressure is gradually increased, the discharge suddenly jumps into another state, the "super state" [V1].

The transition to this state is characterized by a great increase of the anode current (to several amps). Moreover, strong h.f. oscillations, of the noise type, are observed in the discharge. "Hash" is the name employed for these oscillations [B15]. It is supposed that the hash plays an important part in the transport of electrons to the anode: a strong electric h.f. field can enlarge the radius of the electron trajectories to a value which enables them to reach the anode cylinder.

The ion output of these sources in the super state is enormous. Even at very low pressures it can amount to several hundreds of milliamps if the ions are extracted in axial direction [S14]. Axial extraction is always considered to be the best, because the ion current in the discharge is directed axially. This applies to the arc source as well as to the magnetic oscillation source. Unfortunately, the direction of the beam in the separator is perpendicular to the magnetic field. Consequently, a radial extraction of the ions is necessary.

The supply of ions to the exit slit is then provided by diffusion and the penetration of the extracting field.

This reduces the ion output by about a factor of 10.

The magnetic oscillation source with axial extraction is known as the Finkelstein source [F2], that with radial extraction as the Heil source [H11] or Von Ardenne source [A5].

When we were compelled to choose from among the three types of source afore mentioned, the h.f. source seemed advantageous because no filament is needed for its operation. Nevertheless we did not choose it, as we feared that the h.f. oscillations might cause h.f. fluctuations in the output and disturb the space charge compensation. Moreover, the other types mentioned have a larger ion output.

Without doubt the Heil source has the largest output, but the oscillations generated in the discharge may cause a fluctuating beam and will increase the energy spread of the ions.

From fig. 11 it is clear that a Heil source can be converted to an arc source by simply connecting the reflector plate to the anode cylinder. This is the reason that we decided to construct a Heil source for our separator and try to utilize its high ion output. When it turned out that the application of this source was not possible, it was switched to the arc type (§ 32).

§ 9. Charge materials for the ion source

Since the mechanism of the ion source is essentially a gaseous discharge, the isotopes to be separated must be supplied to the source in the form of a gas.

There are a few gaseous elements, like Cl_2, but most of the elements are solids. In some cases it is possible to use a gaseous compound of a solid element. *E.g.* CO_2 or CO – gas might be used as charge materials for carbon. For these gases the pressure in the source can be controlled by means of an adjustable leak.

Many elements have suitable compounds in the form of liquids.

When the vapour pressure of such a liquid is sufficiently high at room temperature (at least several cm Hg) it can be applied similarly with an adjustable leak. In this way CS_2 can be used as well as several chlorides, such as $SiCl_4$ and BCl_3. Sometimes (*e.g.* with $SnCl_4$) it will be necessary to increase the vapour pressure by placing the container in a thermostated furnace at an elevated temperature. By placing the adjustable leak also in the furnace we can handle liquids which have a vapour pressure of about 1 mm Hg at room temperature.

For several elements, no suitable gaseous or liquid compounds can be found. In those cases the solid element or compound is put into a cruicible which is situated close to the ion source inside the vacuum chamber. The connection to the source is very short and no adjustable leak is used; the pressure is controlled by regulating the temperature.

With a maximum obtainable temperature of 800° C almost any one of the remaining elements can be supplied in this way (see § 34).

Of the methods mentioned, the charge of gaseous material is not the most preferable. For most separations, the total amount of charge is of the order of 1 to 100 grams, which is a rather large volume amount for gases, unless very high pressures are used. Moreover, a pressure stabilizing device is necessary to assure a constant gas flow to the source.

For still another reason it is advantageous to make use of charge materials which have a low vapour pressure at room temperature. This is obvious from the following consideration:

Suppose that gas is admitted to the source, the pressure in the ion source is p_s, in the vacuum chamber p_v. The ion density for one type of ions in the source depends on the pressure: $\rho(p_s)$. The extracted current of these ions from the source i_s is proportional to this density, as long as the ion current is not space charge limited (§ 8). Consequently

$$i_s = k_1 \, \rho(p_s) \, , \qquad (9 - 1)$$

k_1 depending on the source dimensions and the configuration and tensions of the acceleration system.

For ideal focusing the collector current can be given by

$$i_c = i_s \, . \, e^{-l/\lambda} \qquad (9 - 2)$$

where l = the total path length of the ions from source to collector and λ = the total mean free path for scattering and charge exchange.

Neglecting the residual gas pressure when no gas is admitted to the source, we have the relation:

$$p_v = \frac{C}{S} p_s \qquad (9 - 3)$$

C being the "gas-conductance" of the ion exit slit and S the pumping speed in the vacuum chamber.

If we suppose $\rho = k_2 p_s$ (which is approximately true in the low pressure region [F1]), we come to:

$$i_c = \frac{k_1 k_2 S}{C} p_v \, e^{-1/\lambda} \qquad (9 - 4)$$

Since λ is inversely proportional to p_v, i_c will be a maximum for that value p_{v_o} of p_v, where $\lambda = 1$ and

$$i_{c_o} = \frac{0.37 \; k_1 k_2 S \; p_{v_o}}{C} \qquad (9 - 5)$$

From (9 – 5) it is clear that there is an optimum source pressure $p_{s_o} = \frac{S}{C} \cdot p_{v_o}$ above which an increase of pressure will cause a decrease of collector current.

When, however, a solid charge material is applied, the pressure in the greater part of the vacuum chamber will not be influenced by the source pressure: most of the inlet material will condense on the walls in the immediate vicinity of the source.

At a source pressure p_{s_o} the collector current will be almost three times as high as in the case of a gas and with p_s it may still be increased. In practice, we shall not increase the pressure in the source too much, because the rather high pressure in the acceleration region will give rise to breakdowns and energy spread of ions.

For the collection of the isotopes it is also of great importance that the charge material has a very low vapour pressure (§ 10).

Further points of interest are the chemical activity of the charge materials and the abundance of atomic ions in the extracted ion beam. These properties must be considered for each particular element. It is clear that an element has advantages over a compound as a charge material. Not only because fewer types of ions will be created, but also because no volatile components are formed. The latter will *e.g.* be the case with chlorides, where chlorine gas is formed. This causes a loss of ions in the vacuum chamber in a way similar to that suffered with gaseous charge materials, though the residual pressure will be smaller.

§ 10. Collection of the separated isotopes

In principle, the separated isotopes are collected by placing a metal surface at 180° beyond the ion source. With a proper focusing, the ions of different masses will strike this surface at different places and thus may be collected separately.

In general, it is not possible to use a simple plate, placed perpendicular to the ion beam, since this can result in an extremely high loss of material.

This is due to the fact that for many elements a large fraction of the ions (which can easily amount to over 50%) will be reflected and leave the surface again either as ions or as atoms. Moreover, material once deposited on the surface will be struck by the beam and thus be removed, eventually together with mother material of the collector plate (sputtering).

In order to reduce these difficulties we make use of collector chambers as shown in fig. 12.

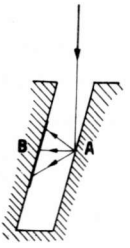

Fig. 12. Cross section of collector chambers

The beam strikes the chamber wall A and after reflection or sputtering the material is collected at the wall B where it is safe from being hit by the primary beam.

Still there is an appreciable loss which can amount to over 30%.

Of course, the distance between the chambers must be chosen such, that each isotope is collected in its particular chamber.

Attention must be paid also to the loss, due to evaporation of the collected isotope out of the collector chamber. Suppose:

M = the mass number of the isotope,

p = its vapour pressure in mm Hg,

A = the area of the collectorslit in cm^2,

T = the temperature of the collector,

α = the evaporation coefficient = 1.

Then the loss of material by evaporation is given to a first approximation by [D4]

$$Q_1 = 5.8.10^{-2}\ A\ p.\ (TM)^{-1/2}\ g.\ at/sec \qquad (10-1)$$

Be i_c = the total collector current in mA.
a = the abundance in % of the isotope to be collected.
Then the supply to the collector by the ion beam is, according to Faraday's law:

$$Q_s = 1.04.10^{-10}\ a\ i_c\ g\ at/sec \qquad (10-2)$$

If we require the loss to be less than 1% of the supply, the demand is:

$$p < \frac{1.8.10^{-11}\ a\ i_c \sqrt{T\ M}}{A}\ mm\ Hg \qquad (10-3)$$

Substituting the rather moderate values: a = 1 %, i_c = 1 mA, T = 300 ^{o}K, M = 40, A = 20 cm^2 we come to

$$p < 10^{-10}\ mm\ Hg \qquad (10-4)$$

giving the order of magnitude of the admissible vapour pressure.

The great majority of the solid elements satisfy the condition (10 – 4) at room temperature. There are, however, a few elements, especially the gaseous ones like O_2, Cl_2 etc. which have a too large vapour pressure. These elements must be bound chemically to a compound of low vapour pressure by providing the collector with a material, which reacts with the entering ions. *E.*g. sulphur may be bound to copper. It is of importance that *many* elements are bound to the collector material either chemically or as an alloy. In those cases the vapour pressure of this compound or alloy must be taken into account in (10 – 3).

There remain the inert gases. Up to now it seems that the only possible way to collect them is to make use of the effect that high energy ions can penetrate into the first few hundred atomic layers of a metal surface. By this method Koch [K13] collected several samples of noble gases. A drawback is that only very small amounts of gases (about 2 μg at/cm^2) can be collected until the surface becomes saturated. It is, therefore, necessary to have the disposal of a large surface area. A possible way is to use a film of a narrow metal sheet, which is gradually unrolled along the collector.

An important problem is the possible contamination of the targets by other isotopes of the same element, especially when an isotope of very low natural abundance is collected. Besides by overlapping of the images due to various aberrations (§ 5), contamination can occur by condensing of the residual gas in the

vacuum chamber on the collector surface. This effect is negligible as long as the condition (10 – 4) is satisfied not only for the vapour pressure of the element, but also for the vapour pressure of the compound, in the form of which the element is admitted to the ion source. If this is not the case, properly fitted baffles, cooled to a low temperature must trap the vapour before it can reach the collector. In this way the condensation of material on the collector surface can be obviated. When the collected isotopes are to be bound chemically in the collector, care must be taken that the target material reacts with the ions, but does not react with the residual gas.

The possibilities of chemical exchange of the collected isotope with the residual gas and with gas adsorpted at the collector must be considered for each particular case.

Chapter II

DESIGN OF THE SEPARATOR AND PRELIMINARY WORK

§ 11. Principal dimensions and shape of the magnet

From the formula for the separating power

$$SP = \left(\frac{M}{\Delta M}\right)_{max} = \frac{r_o}{s} \qquad (6 - 28)$$

it is clear that a large value of r_o is advantageous for the separation of heavy isotopes.

However, r_o is limited primarily by a pure financial reason. Moreover, the yield will be seriously diminished when the total path length πr_o, of the ions, becomes longer than the mean free path for elastic collisions and charge exchange. Since this free path is of the order of a few meters for normal operation pressures of 3 to 4.10^{-5} mm Hg, the main radius of our separator was chosen as 1 meter. The exact value of r_o, as defined by the profile of the pole pieces, is 102 cm. Consequently, when a separating power of 238 is required, the width of the image must be restricted to 4.2 mm. When lighter isotopes are to be separated, a wider image can be permitted in order to increase the yield.

The application of a high accelerating voltage reduces the effects of space charge and energy spread of the ions and, consequently, improves the focusing on the collector. On the other hand, it increases the possibilities of electrical breakdowns at the source and sputtering effects of the ions striking the collector. We chose V_i = 30 kV (maximum). Usually, the separator is operated at about 20 kV.

The magnetic field required can be calculated from:

$$B = \frac{1}{r_o}\sqrt{\frac{2MV_i}{e}} \qquad (5 - 7)$$

Taking M = 238 atomic units and V_i = 30 kV, we find B = 3780 gausz, which is still a relatively weak field.

For lighter elements, B must be correspondingly smaller. For hydrogen (mass number 1) a field of only 250 gausz would be required.

Another fundamental feature of the separator is the height of the gap between the pole faces. With it, the height of the ion

beam and, consequently, the yield will increase. It was compromised at 20 cm.

For a total radial exit angle of 18^{o} and with the field shape used, the maximum width of the ion beam is 30 cm. Therefore, we designed half ring shaped pole pieces with a width of 50 cm. Though some space is lost in the construction of the vacuum chamber, there is enough left for a beam of 30 cm.

When we designed the shape of the yoke, our basic premise was that the vacuum chamber should be accessible from all sides. Especially the ends of the ion path, where the source and the receiver will be situated, must be within easy reach. We came to the shape shown in fig. 13.

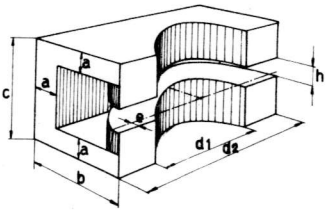

Fig. 13. Shape of the magnet

A very large value of the stray field is inherent with this shape but, since no strong field is required, this drawback is not serious.

The principal dimensions are: d_1 = 150 cm, d_2 = 250 cm, h = 20 cm, a = 30 cm, b = 200 cm, c = 150 cm. b and c were determined such that sufficient room remained for the excitation coil which is wound around the back of the yoke.

The ion path, which extends over 180^{o}, must lie completely within the magnetic field. In view of the space required for the ion source and the receiver, the pole faces were extended over somewhat more than 180^{o}. The distance e = 10 cm.

The area of the pole faces is $1.67.10^{4}$ cm^{2} and with a magnetic field of 3780 gausz, the main flux will be $6.3.10^{7}$ maxwell. A rough calculation, based on measurements on a model of another type [K14] showed that a stray field of more than 80% could be expected. According to a measurement on our resistor network, this value was even 100%.

If we suppose, for security, a stray field of 115%, the maximum flux in the back of the yoke will be $1.3.10^{7}$ maxwell and the maximum induction 17.200 gausz. This is an allowable value for the type of steel used.

§ 12. Design of the excitation coil

The number of ampere turns required follows from the relation:

$$\oint H_l \, dl = 4 \pi N I \qquad (12 - 1)$$

For convenience, we divide a line of force into three parts:

a. in the gap l_g = 20 cm B = 3780 gausz μ = 1.
b. in part of the yoke l_y = 180 cm B = 17.200 gausz μ = 200 [1].
c. in the rest of the yoke l_r = 300 cm B = 13.000 gausz μ = 800 [1].

Then, according to (12 – 1) we need $7.6.10^4$ ampere turns for a field of 3780 gausz in the gap.

Our choice of the excitation current was based on the fact that the coil had to be cooled in some manner. Very effective cooling can be achieved by forcing water through a hollow conductor. Since the cross section of such a conductor cannot be too small, this system suggests the combination: large current, few turns. To make it possible to use a normal D.C. generator, we chose a current of 100 Amps, so 760 turns were needed.

As for the size of the tube, we could make our choice from between some few normal types, which were available. The type most suited for our purpose had an outer diameter of 9 mm and an inner one of 5 mm, so the thickness of its wall was 2 mm and the area of the copper cross section 44 mm^2.

Estimating the average length of one turn at 6.5 m, we came to a total length of about 5000 m. Calculations for a pure copper coil showed that its resistance would be 2 Ω. So we made use of a 22 kW D.C. generator (maximum output 220 V, 100 Amp). Unfortunately, it turned out that the copper of the tubing was not as pure as we had desired. Its resistivity was $2.5.10^{-6}$ Ω cm instead of $1.7.10^{-6}$ Ω cm, which is the value for electrolytical copper. Consequently, the resistance of the coil was 3 Ω instead of 2 Ω and 300 V was required to obtain 100 Amps through the coil. This was achieved by means of an additional power supply, 90 V, 100 Amps, consisting of a six phase transformer with selenium rectifying cells (§ 22).

In order to prevent the formation of boiler scale we permit the temperature of the cooling water to increase by only a small amount.

For a raise of 20° C, the amount of water required to carry off 30 kW, is 360 cm^3/sec. It is impossible to force this water through the total length of the coil, since this would require an extremely high pressure.

1) Data obtained from a magnetic analysis of the steel by Dr. J.J.Went, Eindhoven.

Therefore, it was necessary to divide the tube into a number of sections, which are placed in parallel in the cooling circuit. Since the coil would be wound in layers, it was convenient to make each layer a branch in the parallel system.

We designed a coil which was wound in 16 layers with each layer consisting of about 50 turns. The average length of the tubing in one layer is 315 m. and the amount of cooling water is 22.5 cm^3/sec. This means a current velocity v = 115 cm/sec.

With an inner diameter of the tubing d = 0.5 cm and taking the viscosity $\nu = 10^{-2}$ cm^2/sec., we find for Reynolds's number:

$$Re = \frac{vd}{\nu} = 5700 \qquad (12 - 2)$$

Consequently, the current will be turbulent and this is favourable for good heat transfer. The pressure required follows from Blasius' formula:

$$\Delta p = \frac{0.066\ \rho\ v^{7/4}\ l\ \nu^{1/4}}{r^{5/4}} \qquad (12 - 3)$$

where ρ is the density, v the velocity and ν the viscosity of the cooling water, l is the length and r the inner radius of the tube. Substituting our values, we come to $\Delta p = 15$ atm, which is a normal operating pressure for a force pump.

§ 13. The model

The magnetic field in the separator must meet two requirements:

1. in the median plane between the two pole faces, it must have only a z-component which is dependent on the radius in a way calculated by Beiduk and Konopinski [B14] (§ 6).
2. it must be axially symmetric.

The first condition can be satisfied by using specially shaped pole pieces, the second by shimming.

Both the profile of the pole pieces and the shimming pattern were determined experimentally.

To do this a reduced model of the magnet (scale 1 : 5) was constructed. A maximum field of about 2800 gausz could be obtained in the gap by means of a coil of 1200 turns and an excitation current of 8 Amps.

The magnetic field was measured by means of a rotating fluxmeter. A small coil (area 0.2 cm^2) was rotated in the field by a synchronous motor at a rate of 3000 r.p.m. The a.c. voltage generated in the coil was transmitted via sliprings and copper gauze brushes and measured by an accurate meter (rectifying cell-moving coil system).

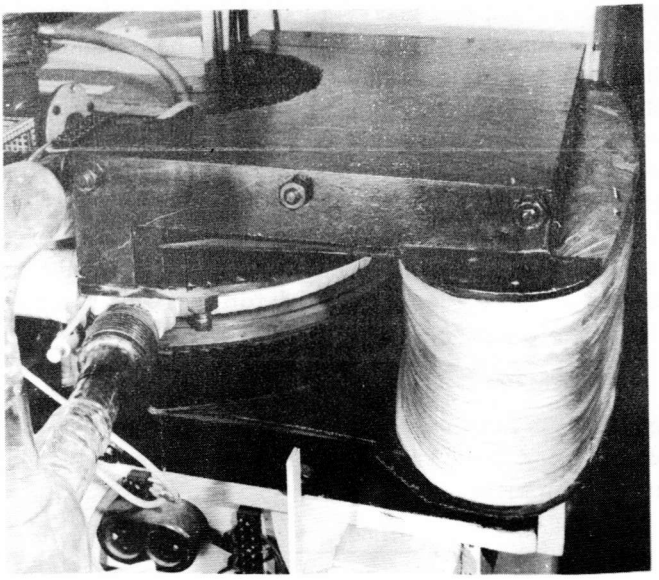

Fig. 14. Model of the magnet (now used for a mass spectrometer)

The flux meter was placed on a movable platform so that the location of the coil could be determined in any position. An accuracy of 0.2% was obtained with this method.

We started the experiments by measuring the influence of grooves and ridges on the shape of the magnetic field. In the gap of the magnet we placed a grooved piece of iron and then the field above and in the vicinity of this groove was measured in a plane, which approximately bisected the remaining gap. In a similar way we measured the field in the vicinity of ridges and combinations of ridges and grooves. Fig. 15 shows the influence of grooves of various widths.

From the afore mentioned measurements we learned how we could obtain the required field shape by profiling the pole pieces.

Before doing this we shimmed our magnetic field until it had become axially symmetric. For this purpose two plane pole pieces were placed in the gap and kept parallel and properly spaced by means of brass bolts and nuts. The thickness of these pole pieces was the same as that of the profiled ones to be used.

The magnetic field in the median plane was measured as a function of r for various values of φ. Fig. 16 shows the result for $\varphi = 0$ and $\varphi \approx 90^{\circ}$ respectively with the last case being measured 1 cm within the front edge of the pole pieces.

By bringing thin sheets of steel between the pole pieces and the yoke, in those places where the field was too weak, we gradu-

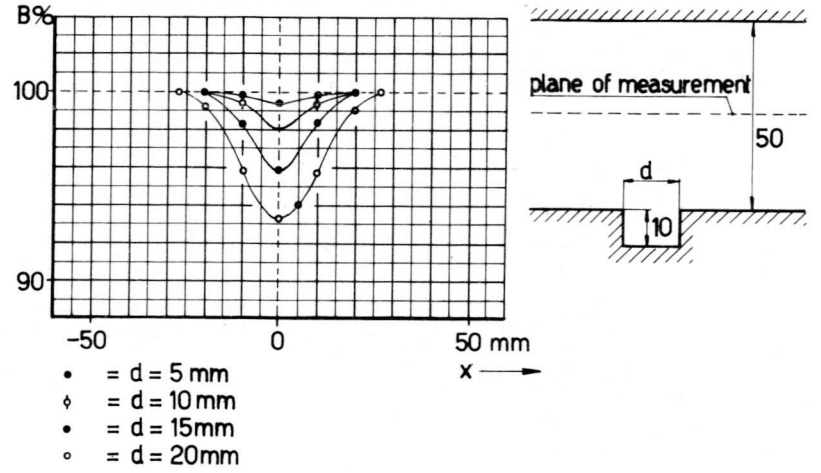

Fig. 15. Influence of grooves in the pole pieces on the shape of the magnetic field

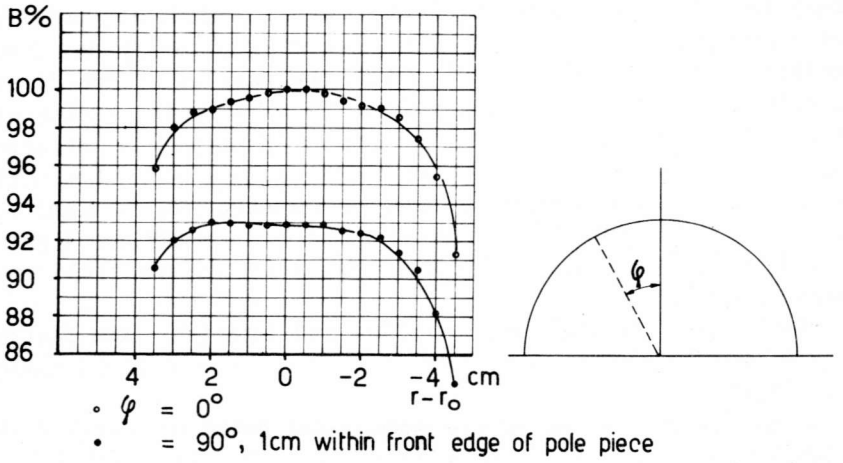

Fig. 16. Shape of the magnetic field before the shimming process

ally succeeded in making the field more homogeneous. We finally obtained the result shown in fig. 17.

When judging the result of fig. 17 we must take into account that the ion beam covers the total available width of the pole piece only at $\varphi = 0$. For all other values of φ, the width of the ion beam is smaller and so is the range where a correct field shape is required.

After this shimming process, the pole pieces were profiled in

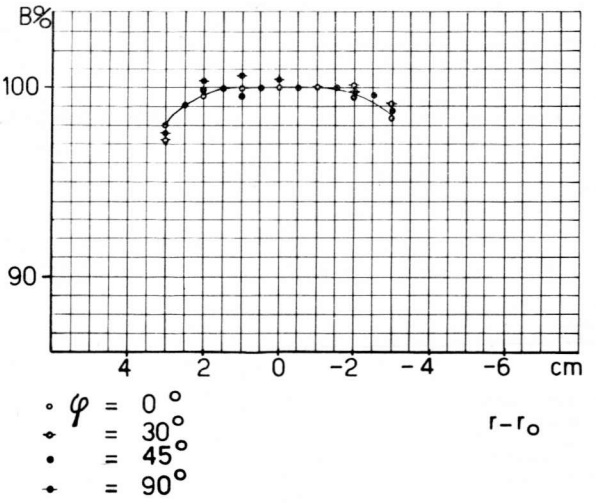

Fig. 17. Shape of the magnetic field after the shimming process

order to obtain Konopinski's field shape. A preliminary profile was designed which was based on the one used by Langer and Cook in their beta spectrograph [L3] and on the results of our first experiments with grooves and ridges. We constructed a pair of pole pieces with this profile and the field shape was measured with our flux meter. Since this configuration showed slight deviations from the theoretical one, we investigated, by means of thin sheets of steel, how the profile had to be modified. A pair of pole pieces of this new profile was made and the field was measured again.

After some very small supplementary modifications, the fourth pair of pole pieces was approved. Fig. 18 shows the field shape thus obtained.

A good approximation of the theoretical shape is achieved at those places where it is necessary (for φ = o over the total width of the beam, here represented by 6 cm).

Next, the influence of the fieldstrength was studied by determining the shape of the field for various excitation currents. No appreciable difference was observed, but this could be expected since we were far from the magnetic saturation of the pole pieces. By measurements at $\varphi = 90^{o}$ and $\varphi = -90^{o}$ the symmetry with respect to φ = o was checked.

The last thing we investigated was the extent to which it would be permissible to bring ferromagnetic material in the vicinity of the magnet without seriously disturbing the magnetic

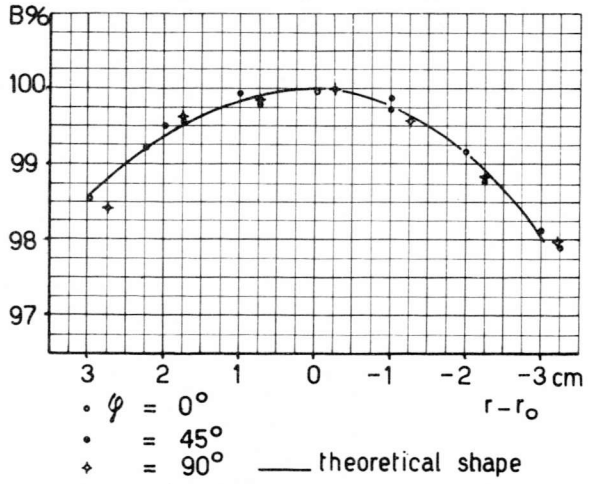

Fig. 18. Shape of the magnetic field finally obtained in the model

field shape. This was of importance in regard to the connection of the vacuum chamber to the steel oil diffusion pump. (After our measurements, we designed a 60 cm long connection of non-magnetic stainless steel.)

The flux meter used by us was suitable for our purpose. The accuracy of 2‰ was ample since this value corresponded to about 0.1 mm thickness of steel, which is a reasonable machining tolerance. A disadvantage was the necessity of cleaning the brushes after every series of ten or twelve measurements.

The field of the big magnet could be measured by another method since the available space was much larger. In this method (§ 23) the drawback of the brushes did not exist and, moreover, the accuracy was much better, *viz.* 0.5‰.

Both the profile of the pole pieces and the shimming pattern determined were used in the big magnet of the separator. Slight deviations might be expected and did occur because the separator and the model do not completely conform: in the separator the semi-circular boundaries of the pole pieces are approximated by polygons.

After the measurements of the field were completed the model became available for other purposes. It was well suitable to form the magnet of a 180° mass spectrometer and as such it is now in use in our laboratory. The isotope analyses mentioned in § 33 were carried out with it.

§ 14. The resistor network

The tracing of ion paths in the separator is of major importance, *e.g.* to facilitate the design of the electrostatic lens to attain optimal focusing conditions.

For this purpose we constructed a resistor network according to De Packh [P2] and Liebmann [L5].

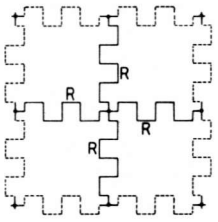

Fig. 19. Arrangement of resistors in a quadratic network

It can easily be shown [P2] that a quadratic network of resistors of equal value (Fig. 19) is ruled by the two dimensional Laplace equation:

$$\frac{\partial^2 V}{\partial x^2} + \frac{\partial^2 V}{\partial y^2} = 0 \qquad (14 - 1)$$

If we assume the width of the slits in the electrode system small as compared to their height, the situation in the separator is two dimensional and the quadratic network is applicable to our case.

Our network [Z2] consists of 3940 resistors, of 3300 Ω each, mounted on a plate of pertinax in a rectangular arrangement of 56 columns and 36 rows.

When hung on the wall this device occupies very little space. For the measurement of an electric field the electrodes, represented by copper wires, are plotted upon the network on an enlarged scale. These "electrodes" are placed at potentials proportional to those used in the actual lens system and the potential distribution is then measured from point to point at the junctions of the resistors.

For this purpose a stabilized supply of four independently adjustable potentials and an electronic voltmeter (impedance 1 MΩ) are available.

Equation (14 – 1) is not exactly correct for the network. The error due to the finite mesh dimension is given in a first approximation by [P2]:

$$e = \frac{a^4}{48}\left(\frac{\partial^4 V}{\partial x^4} + \frac{\partial^4 V}{\partial y^4}\right) \qquad (14 - 2)$$

in which a = the width of the meshes. This error is negligible in most practical cases, when the electrodes are plotted upon the network on a sufficiently enlarged scale. The over all accuracy of the measurements is within 2%.

The boundaries of the electrodes must be approximated by straight lines. Because of the large number of junctions available, this is practicable without difficulties.

The influence of the finite dimensions of the network is diminished by making the resistors at the boundaries 2200 Ω instead of 3300 Ω.

In principle, it is also possible to take account of space charge effects by supplying currents to the network [L5]; however, this implies a complicated device if the space charge is not confined to a few points but distributed over a certain area. Furthermore, we do not know the magnitude of the space charge in the electrostatic lens. Therefore, we determine the ion paths for very low currents (neglecting space charge) and later correct, qualitatively, for the space charge.

After the measurements of the electric field we plot the ion trajectories by applying Snell's law:

$$\frac{\sin \varphi_1}{\sin \varphi_2} = \frac{n_2}{n_1} \qquad (14 - 3)$$

which is valid for electrostatic fields if the refractive index n is taken to be proportional to the square root of the potential V [Z1].

When the influence of the magnetic field is taken into account this method is not applicable. In that case we calculate the ion paths step by step [R4].

Chapter III

CONSTRUCTION OF THE SEPARATOR

§ 15. The yoke

In order to obtain a magnetic field of the shape required, the pole faces had to be profiled in a special way.

To facilitate machining, the pole pieces were designed as separate parts, each 50 mm thick. Consequently, the gap in the yoke was 30 cm.

One method of construction would have been to cast the yoke in a few blocks and to bolt these blocks together, but it turned out that the cost of this would have been twice as high as that of a yoke composed of steel plates. Therefore, we decided to construct the yoke from 3/4" parallel steel plates placed vertically and bolted together (Fig. 20).

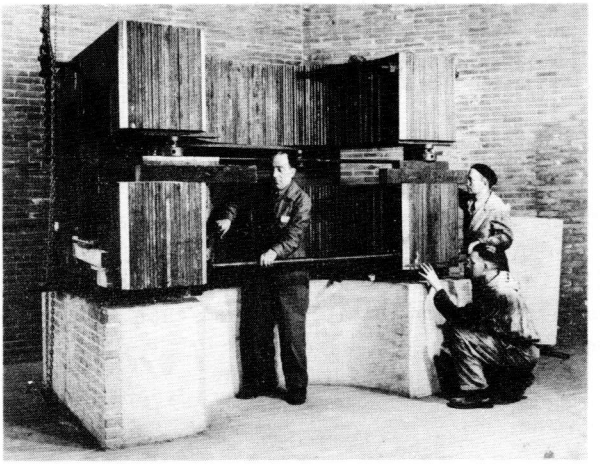

Fig. 20. Mounting of the yoke

The plates were supplied by Koninklijke Hoogovens, IJmuiden. A low carbon type of commercial steel containing 0.10 to 0.15% C was chosen.

The plates were cut into the shape required by acetylene torch. They were then flattened, the surfaces on the lower side and in the gap were dressed and the holes drilled.

The machining, as well as the mounting, was done by Werkspoor Ltd, Amsterdam.

In our Laboratory, which is situated in the former engine room of the East Power Station of the Municipal Electrical Works, Amsterdam, there was a foundation which had supported a 50 tons A.C. generator. Since the total weight of the separator was estimated at about 40 tons, this foundation could be used.

A suitable column of reinforced concrete was erected on it and four pieces of rail were carefully mounted on the column in a horizontal position. On these rails the yoke was placed by "stringing" the plates one after another, on the large bolts. Then the height of the gap was adjusted to precisely 300 mm by means of jacks and steel bars. By hammering, all plates were brought to the correct level.

By turning the nuts on the large bolts the "wings" of the magnet were brought into the correct position and the mounting was completed.

The irregularities in the gap between the individual plates amounted to a maximum of 0.2 mm which is a tolerable value.

The semicircular boundaries of the gap are approximated by the step pattern of the plates. The influence of this approximation on the shape of the magnetic field between the pole pieces is negligible.

§ 16. The excitation coil

a. Preparatory work on the yoke

The total weight of the coil is about 2 tons. To support this coil we mounted an oaken beam of 200 × 200 mm^2 on the inner side of the back of the yoke and 30 mm oaken boards at the same level on the outer sides and rear. The beam was bolted to the yoke and the boards were supported by angle irons of 180 × 180 × 15 mm.

The boards at the sides were made semicircular with a radius of 350 mm so as to conform to the planned dimensions of the coil. On these boards we placed semi-cylindrical oaken filler pieces (radius 150 mm) around which the turns of the first layer could be bent smoothly. The height of these pieces is 680 mm. The board on the rear side and the angle iron beam on which it is mounted were provided with a number of holes (30 mm diameter) through which the ends of the layers could enter the coil.

The upper side of the coil was formed in a similar way but of lighter material. On the inner side of the back an oaken board of 200 × 20 mm^2 was bolted to the yoke. Semicircular boards were screwed onto the filler pieces and four supports at the back side carry a 200 mm wide locking board. This board was furnished, like the lower one, with holes to pass the ends of the individual

layers. All steel and wooden parts, which might come into contact with the windings were covered with two sheets of 0.6 mm leatheroid.

b. Insulation of the copper tubing

The copper tubing which we procured came in pieces of about 25 m that we ourselves had to insulate.

We chose varnished cambric tape, 20 mm wide and 0.15 mm thick, as an insulating material. This is a normal commercial product, the material is very durable and its electric strength is 10 kV. We decided to wind this tape in such a way that each successive turn would overlap half the previous one so that the tubing would be covered with two layers of tape. In this way a safety factor against damage and imperfections was obtained. It was easily calculated from the diameter of the tube and the width of the tape that a winding angle of 20° would be necessary for this procedure and that a total length of 15000 m of tape would be required to insulate 5000 m of tubing. Since it was not feasible to do this insulating by hand we constructed an insulating machine, a sketch of which is shown in Fig. 21.

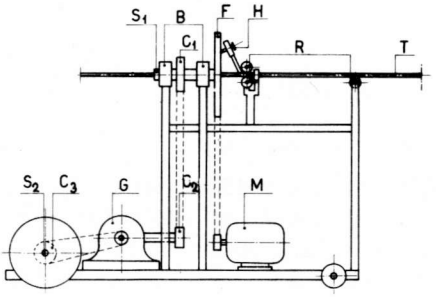

Fig. 21. Sketch of insulating machine

The motor M drives the heavy fly-wheel F, which is mounted on a hollow shaft S_1, which rotates in the ball bearings B. On this shaft a sprocket C_1 is fixed, which via a chain to C_2, is linked to the gear case G. By means of a sprocket C_3, the shaft S_2 is driven. The machine is constructed on a small cart, the front wheels of which are mounted on S_2. When the motor runs the fly-wheel rotates and the cart also moves. The tape holder H, on which a roll of varnished cambric tape can be placed, is attached to F. The set of rollers R guide the tubing.

The insulating was done in the following way:
A 25 m piece of copper tubing T was pushed through S_1 and was stretched taut to its full length by means of tackles. At the beginning of each section the tape was attached to the tube with

cellulose lacquer and the motor was started. As the cart moved along the tube this tube was insulated uniformly and snugly. At the end the tape was attached again but aside from these two places, no glue or lacquer was used. The tape was wound very tightly around the tube because it was held taut by means of an adjustable tension on the tape holder H.

The connection between S_2 and F, which determines the winding angle, consisted of a chain, sprockets and worm gears and consequently could not slip. Since the machine was rather heavy and a very level floor was used, the driving wheels did not slip either.

The insulating of one piece of 25 m tubing took about half an hour and the entire task was completed in 2½ weeks.

On both ends of each piece we left half a meter uninsulated, because of the welding which still had to be done.

c. Welding of the tubes

Each layer of the coil was made up, by welding together, of 12 pieces of 25 m of tubing. These welds must be water tight even at a pressure of 17 atmospheres and they had to be strong enough to withstand the stresses to which they were exposed during the winding of the coil. They must not restrict the passage of the cooling water. Their electrical transition resistance must be very small. They could not be noticeably thicker than the tube itself in order to eliminate difficulties in the winding process and to obviate irregularities in the coil.

The welds were made in the following way: An ending of one of the two tubes to be welded was beveled on the outside (slope 1 : 10) and the other reamed to the same slope on the inside. By means of a clamp they were pulled together and then silver soldered.

A number of trial welds, made in this way, were tested for us by Werkspoor Ltd. In each case the weld proved to be stronger than the copper tube which had a tensile strength of 18 kg/mm^2.

All the actual welds of the tubing were tested:

1. for strength, by subjecting them to a pull of 200 kg, by means of a clamp and a lever.
2. for leakage, by introducing a pressure of 30 atm. nitrogen gas and keeping the joints under water for half an hour.
3. for obstructions, by measuring the time required to force a liter of water at a pressure of 2 atm. through the 300 m tubing of a layer.

The joints were then insulated by hand.

The welds were made and tested at a rate of one layer per day.

d. Winding of the coil

One complete layer of tubing was hung above the magnet on a revolving carrier. The end of the tube was put through the first hole in the lower supporting beam and one turn was wound, being fed down by a man who stood on the magnet and turned the carrier. By means of a wooden clamp, a French tackle and some weights, the turn was pulled tight with a force of 100 kg. With wooden hammers and rubber covered pieces of wood the turn was beaten to conformity. Though the copper was soft when we received the tubing, it had become rather inflexible from the working, especially in the vicinity of the welds. Nevertheless, we succeeded in making uniform layers by the aforementioned process.

In order to keep the turns from springing back after the clamp was loosened, we had to hold them in position. This was done in the first place by tying each turn to the preceding one with cambric tape in twelve places. Furthermore, at the rear of the magnet, a large number of rubber covered boards were driven between the wall and the winding. On the inner side of the yoke this procedure was not possible and this was where bulging of the coil had to be avoided because of the limited space. Therefore, a heavy channel iron beam was temporarily fastened in the gap of the yoke leaving sufficient space for the tubing to pass during the winding process. Six heavy jack screws, by which wooden blocks could be pressed firmly against the winding, were mounted in this beam. Fig. 22 displays the winding of the coil is progress.

On the very left we see the tackle, with clamp, stretching the turns. The tape by which the turns were tied together and the

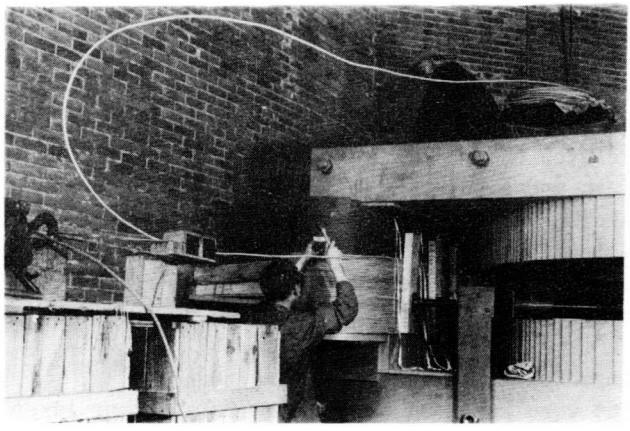

Fig. 22. Winding of the coil

jacks pressing the winding on the inside, as well as some of the boards, doing the same on the back, are visible.

Approximately fifty turns were wound to a layer and then the end of the tube was temporarily tied up.

Before starting each layer a sheet of 0.6 mm leatheroid was put on. Moreover, thermocouples were placed between each two successive layers with a view toward temperature measurements in conjunction with safeguarding the coil (§ 30).

The 16th layer was not complete since the available tubing sufficed for only 35 turns and as a result the total number of turns is 785.

e. Finishing of the coil

After the last turn had been wound the ends of the layers were put through the holes of the upper locking board. A last sheet of leatheroid was applied. Then the coil was closed by a sheet of 1 mm copper which was fastened to the boards and beams of the coil by wood screws. The thermocouple leads were passed through one of the semicircular locking boards.

The copper jacket was not applied merely for an aesthetic reason. In the first place it protects the coil from mechanical damage. Moreover, it prevents small objects (*e.g.* iron filings) from getting into the coil, where they might give rise to short-circuits. For this reason all existing openings were calked with oakum. This also diminishes the air exchange between the inside and the outside of the coil and at the same time entrance of vapours which might cause condensation on the winding.

Finally, the copper jacket acts as a short circuit winding and protects the coil from the very high induction voltage which would occur if, by some accident, the excitation circuit were to be cut suddenly (§ 30). In order to keep the electrical resistance of the jacket as low as possible, we were careful to make good contacts between the separate parts from which it was constructed. This was done by soldering the plates together and by shunting, by means of heavy copper wire, the bolts that tightened the jacket.

To prevent the coil from bulging through the soft copper jacket (*e.g.* due to the Lorentz force) the jacket was supported by six vertical stainless steel strips. On the rear of the magnet, these strips were bolted into the yoke; on the inner side, they were pressed against the coil by means of screw-jacks, with their base against the semicircular protrusions of the yoke.

f. Cooling and electrical connection of the coil

The layers of the coil had to be connected in series electri-

cally, but in parallel for the cooling system. This gave rise to a complication: if, for instance, we should simply connect the tube endings at the low pressure side to a common exit pipe, the system would be short-circuited. Therefore, the connections between the tubes and the exit pipe must be electrically non-conducting, (*e.g.* pieces of rubber tube). However, that would not be sufficient: the cooling water has an appreciable conductivity due to the salts dissolved in it so that a current of about one amp maximum would flow to earth. The loss of this current would be of no importance, but since the conductivity of the water is not constant the leakage currents would vary. Since the total excitation current supplied by the d.c. generator is stabilized 1 : 10,000 (§ 22) this stabilization is no longer valid for the magnetic field, if variable leak currents occur.

In order to avoid this disturbance of the stabilization, we made the connections as shown in fig. 23.

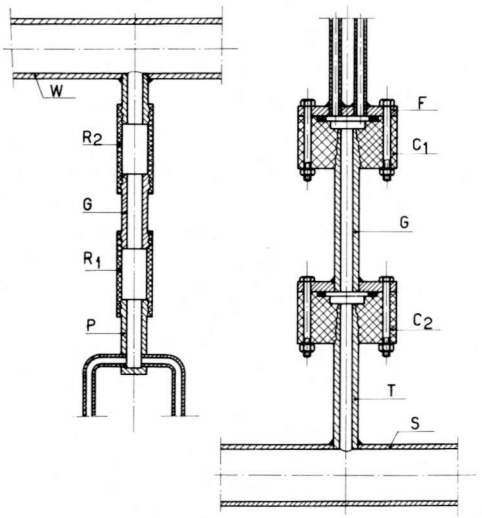

Fig. 23. Connection of the layers of the coil
Left: Low pressure side
Right: High pressure side

The layers of the coil were wound in alternate directions, so two successive layers had to be connected on the top (low pressure side of the cooling) or on the bottom (high pressure side). In this way electrical connections between top and bottom of the coil, were avoided.

On the low pressure side (fig. 23 left) the electrical connection of two successive layers is formed by the pipe P, into which

the ends of the tubing of the layers are silver soldered. By means of the rubber tube R_1, P is connected to the copper "shield" pipe G. A second tube R_2 leads to the exit pipe W.

The shield pipe is brought to the same potential as P. Consequently, no leakage current will flow from P to G or W, although there is a current from G to W.

The potential for G and therefore the leakage current is taken from a resistor, 50 Ω, 2500 Watts, with fifteen taps. This resistor is connected to the D.C. generator in parallel with the excitation coil but outside the stabilized circuit (fig. 30).

Rubber tubes cannot be used on the supply side of the cooling due to the high pressure. The material celleron (or novotext) which is a very strong and waterproof insulation, proved to be suited to our purpose. The construction is shown in fig. 23 (right side).

The shield pipe G is screwed into the upper block of celleron C_1 with the threaded part being tapered. In a similar way the lower block C_2 is connected to the copper tube T, which in turn is silver soldered to the supply pipe S. The electrical connection between the two successive layers is formed by the flange F. The seal between flanges and celleron blocks is provided by rubber rings and bolts. This seal as well as that of the "shield" pipe proved to be perfectly tight.

The supply side is connected to a Sihi force pump and furnished with a manometer; a water meter is inserted in the exit pipe. During operation, a pressure of 17 atm is maintained and 1500 liters of water flow through the coil per hour.

Since it would be dangerous to touch the connections, we mounted screening caps above and below the back side of the coil.

In order to facilitate inspections, these caps are made from clear perspex.

§ 17. Pole pieces and vacuum chamber

In order to utilize fully the gap in the magnetic circuit, the vacuum chamber was designed in such a way that the pole pieces themselves form the upper and lower walls. Since ready accessibility to the chamber is required, the vacuum seal had to be made by means of gaskets. However, this is not practicable with curved walls. Therefore, it was necessary to shape the pole pieces in a special way: the semicircular boundaries were approximated by straight sections for which we chose, in principle, the sides of an equilateral sixteen sided polygon. In order to have both the ion source and the collector completely within the magnetic field

the pole pieces were extended enough beyond 180^{o} to include them (10 cm on each side, as was the yoke). With the field shape required in view the pole pieces were profiled in a manner which had previously been determined by means of the model (§ 13). The deviation of the field shape due to the polygonal approximation will be dealt with in § 23.

The pole pieces were constructed by Werkspoor Ltd. The mounting was carried out in the following way: first a set of shimming plates, the shape of which had been determined with the model, § 13, was placed in the gap of the yoke. Small brass blocks of 25 mm diameter and 15 mm height were put in holes of this set, in such a way that each angular point of the pole piece would be supported and the lower pole piece was then placed on the blocks. Four jacks were set on this pole piece and the upper pole piece as well as the second set of shimming plates were placed on them. This pole piece was then jacked up until we could insert twenty brass supporting blocks which keep the pole pieces the correct distance apart. After the jacks were removed, we wedged small brass blocks between the upper pole piece and the yoke. Like the lower ones these blocks were 15 mm high. When all this had been done, we observed that all supporting blocks were immovable. However, we still "anchored" them by means of small brass blocks, held in place by the profile of the pole pieces.

The supporting blocks were placed at the twenty "corners" of the pole pieces. They each have a cross section of 25 cm^2 and they were carefully machined to have exactly the same height. This ensures that the pole pieces will be parallel. Due to the atmospheric pressure and the magnetic field the pole pieces are pushed toward each other by a force of 25 tons (maximum). Under these circumstances the deformation of the rods is of the order of 0.01 mm, which will not cause any difficulty.

The available height in the chamber is 170 mm, since 15 mm shimming space was left on each side between the pole pieces and the yoke. Of this space a maximum of 11 mm had already been used for the "basic shimming pattern" ascertained by the model, so additional shimming was still possible on a modest scale.

The vacuum sealing of the chamber is done in a manner similar to that used on the Amsterdam 30 MeV synchrocyclotron. The pole pieces are provided on all outer sides with a continuous groove, 15 mm wide and 7 mm deep, as well as with a large number of tapped holes. In the grooves, of both pole pieces, we put an endless (cold vulcanized) rubber gasket of 10×10 mm^2 cross section. Brass plates are bolted upon successive sides of the chamber (Fig. 25; the left plate has been removed in the front view so that the rubber gaskets R become visible.

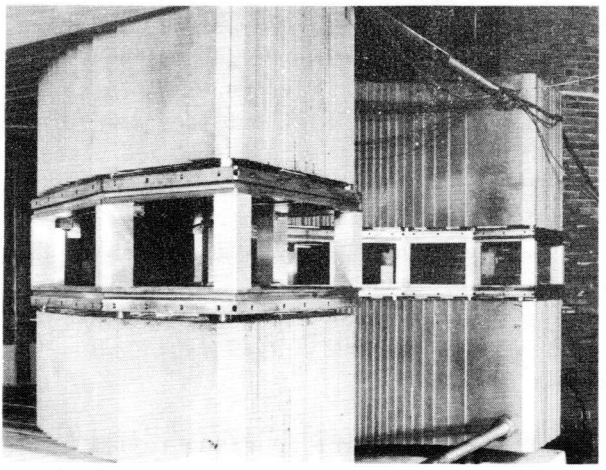

Fig. 24. Vacuum chamber under construction

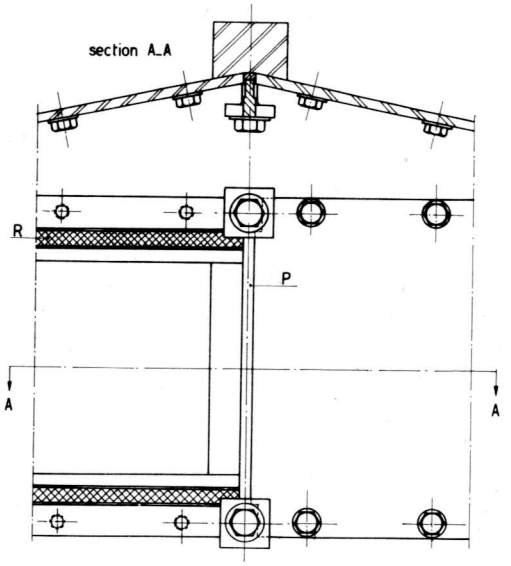

Fig. 25. Seal of the vacuum chamber at one of the interior angles of the pole pieces

In order to obtain a seal between two adjacent plates, these are beveled in such a way that a groove of rectangular cross section, 10 mm wide, is formed between them. Rubber gaskets, 10 mm thick are placed in these grooves and pressed between the plates, the horizontal rubber gaskets, and the brass supporting blocks by means of stainless steel pressing pieces P.

The front plates are actually flanges and carry the ion source and the receiver installation. They are 15 mm thick, as are all other plates which must be weakened in some way, *e.g.* by openings for electrodes or observation windows. The plates that serve only for vacuum sealing are 8 mm thick but they are reinforced by 35 × 12 mm^2 brass strips. In place of the outside plate, on the left, at $\varphi = 67^{\circ}30'$ the flange of the connection to the oil diffusion pump is bolted to the vacuum chamber. This flange is made from 15 mm stainless steel and the sealing is done in the same way as for the other side plates.

§ 18. The ion source

A sketch of the ion source is given in fig. 26 (p. 75). The house, 1, of the source is made from a block of graphite. This house is supported by two stainless steel tubes 2 and 3, which, by means of the flanges 4 – 5 and 6 – 7, are connected to the porcelain insulators 8, through which the tubes enter the vacuum chamber.

The insulators are mounted on a base plate 9 by means of the pressing plate 10; the sealing is effected by rubber gaskets. The filament 11 (2 mm tungsten) is supported by two coaxial copper tubes 12 – 13, which also serve the current supply (180 Amps max.).

The connections of the filament consist of a conical beryllium copper holder 14 with incisions and a stainless steel nut 15, which combination obviates troubles caused by thermal dilatation,

The filament supporting tubes are mounted on the flanges 16 – 17 which are sealed by rubber gaskets and insulated by way of pertinax.

The tubes 2, 3, 12 and 13 are, for the greater part, double walled (not indicated in the figure) and water cooled by means of a closed circulation system with force pump and radiator. The connecting flanges are also cooled by this system. In this way it is possible to have the rubber gaskets at a low temperature, although the house of the source may be at 700° C during operation. Through the lower supporting tube passes the tube 18 carrying the ceramic furnace 19 which, by means of a platinum filament, can be heated to 700° C. Its temperature is indicated by a thermocouple.

(Experiments on the Heil source were carried out by replacing the furnace by a graphite reflector electrode, carried by tube 18 and brought to a negative potential with respect to the cathode.)

The front plate 20 into which the exit slit of the source is

machined, is removable so that different shapes and sizes of slits can easily be applied.

Moreover, it enables an easy cleaning of the source, which cleaning is further facilitated by the application of the separate graphite lining 21.

On the side of the furnace this lining is provided with holes to admit the vapour and on the filament side with a collimating slot through which the primary electrons enter the discharge room.

The molybdenum reflector plate 22, at filament potential, prevents the electrons from going directly to the top of the anode house.

Measures had to be taken to obviate the deposition of metal vapours on insulators. As for the source, this was accomplished by keeping all the insulating material far from the source itself (*viz.* at the connection flanges).

The porcelain high tension insulators are protected by a system of caps and rings 23 shaped like a labyrinth and acting as baffles.

A serious problem is formed by high tension discharges and breakdowns which may easily occur in the vicinity of the source.

We had to face no less than four different types of discharges, *viz:*

1. Cold (Townsend) discharges.
2. Discharges due to field emission.
3. P.I.G. discharges.
4. Trochoidal discharges.

Since the pressure inside the vacuum chamber is quite low, we are on the left side of the Paschen minimum. Consequently, the first type of discharge can be obviated by enclosing the ion source in an earthed screening cap at a small distance from the source and applying also small distances between the electrodes, thus confining the electrostatic field to a limited region.

Field emission can arise at electric field strengths of a few hundred kV per cm. Therefore, the spacing must not be taken too small; 3 mm being a reasonable value. Furthermore, sharp edges and points are avoided and the surface of the electrodes and caps are highly polished.

P.I.G. discharges may also occur, since in the vicinity of the source the shape of the electric and magnetic fields are quite similar to those in the P.I.G. manometer: the pole pieces being negative with respect to the ion source and a component of the electric field being parallel to the magnetic field.

Obviously these discharges can also be suppressed by the earthed screening caps around the source.

Trochoidal discharges can occur wherever the electric field E stands at right angles to the magnetic field B; in that case the electrons tend to move in a trochoidal trajectory perpendicular to both fields. Electrons with zero initial velocity describe a cycloidal path and the radius of the rolling circle is given by [Z1]

$$\rho = \frac{mE}{eB^2} \qquad (18 - 1)$$

When the distance between the ion source and the screening caps is larger than 2ρ, electrons will pass unhampered between them and reach the porcelain insulators where they cause instabilities and give rise to breakdowns.

We can intercept the electrons by making the distance d between source and cap

$$d < 2\rho \qquad (18 - 2)$$

Now, since $E = V/d$ and making use of (18 – 1) and the relation for the principle circle of the separator

$$r = \frac{1}{B}\sqrt{\frac{2MV}{e}} \qquad (5 - 7)$$

we come to the demand:

$$d < r\sqrt{\frac{m}{M}} \qquad (18 - 3)$$

Substituting $r = 1020$ mm and taking the most unfavourable case (uranium – separation) we find $d < 1.5$ mm.

Because this is an impracticably small distance, we have solved the problem in an other way. We have maintained a distance of 3 mm, but we use an undulating cap and protrusions on the source as shown in the front view of the source. In this way an electric field component in the direction of the magnetic field is introduced which pulls away the electrons to the house of the source [R5]. The configuration mentioned is only applied on one side of the source (24) since all electrons emerging from the beam, go that way.

The cap on the other side (25) is a plain one.

When solid charge materials are used, it is of importance that the house of the source is at a higher temperature than the furnace, in order to avoid sublimation in the source. When the source is at 700° C it is easily calculated from Stefan Boltzmann's equation, that the radiation loss can amount up to 2000 Watts.

The total power input of the source may sometimes be of that order, but can also be considerably less.

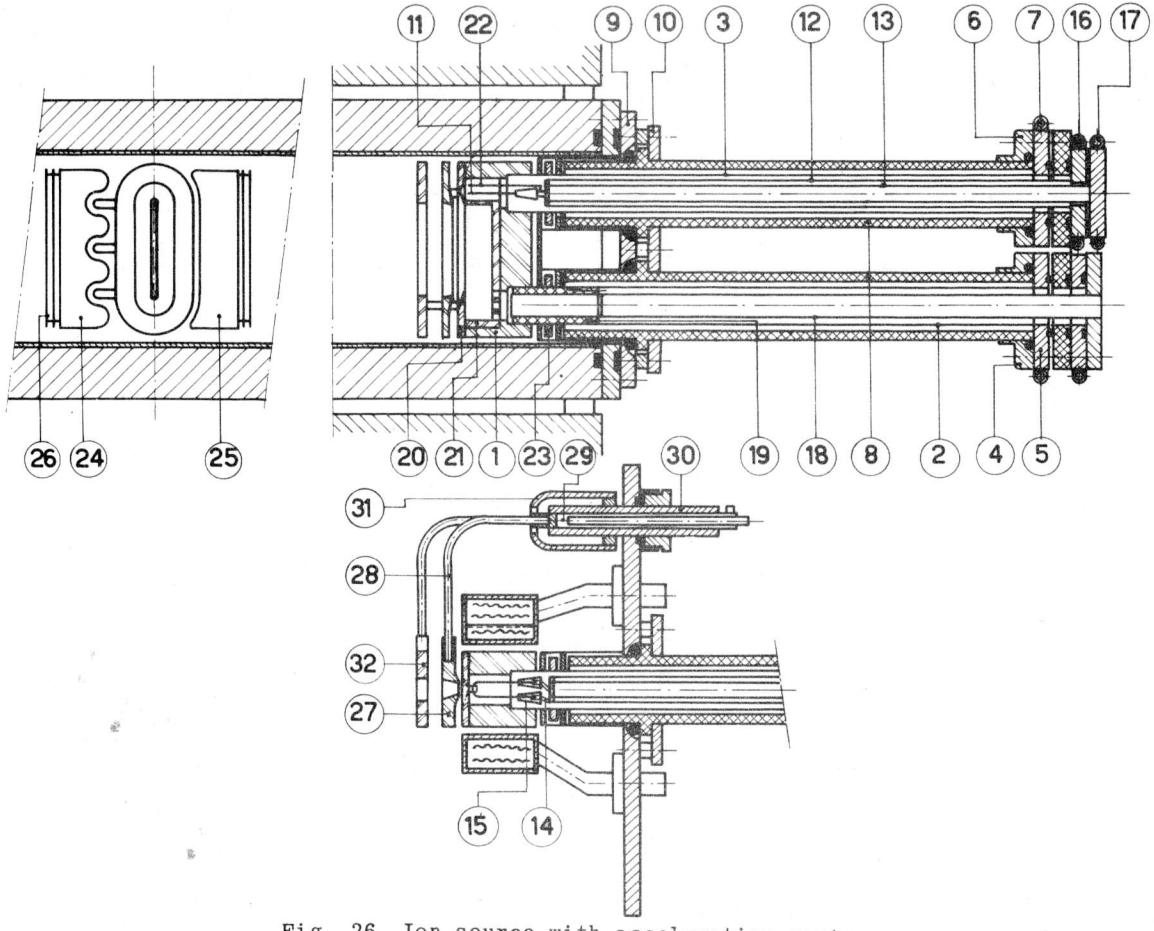

Fig. 26. Ion source with acceleration system

In order to have the temperature of the source independent of the arc voltage and current, it is convenient to make use of a separate heating device. This is accomplished by providing the caps 24 and 25 with an electric heater element. The caps are designed as stainless steel boxes and have a maximum heating input of 1000 Watts each. The radiation shields 26 are fitted to reduce the loss of heat on the "wrong side". In this way the source can be brought to the desired temperature.

§ 19. The acceleration system

Fig. 26 also shows the construction of the acceleration system. The lens electrode 27 is a graphite plate, machined in such a way that it forms a Pierce lens with the front plate of the ion source (§ 7).

It is supported by a stainless steel tube 28, which in turn is screwed into the water cooled copper holder 29.

This holder is luted in the pyrex insulator 30 through which it enters the vacuum chamber. The insulator is vacuum sealed by means of a rubber O-ring which enables an adjustment of the distance between source and electrode. A cap 31 protects the insulator from metal deposition.

The earthed electrode 32 is also a plate of graphite; it is supported in a similar way as the lens electrode. Various slit dimensions and electrode distances were tried. A possible set of data is *e.g.*: Ion exit slit 2 × 100 mm, slit in lens electrode 10 × 110 mm, slit in earthed electrode 15 × 110 mm; distance between source and lens electrode 10 mm, between lens and earthed electrode 15 mm.

The electrodes are heated by radiation and ion bombardement and, because of the low heat transfer through the stainless steel supports they can reach a temperature of several hundreds of degrees centigrade. This is advantageous, since it reduces the amount of inletmaterial depositing on them.

The electrode connections are, together with the ion source, mounted on a foundation plate, which is water cooled by a copper tube soldered on it (not indicated in the figure).

§ 20. Baffles

By baffles all such devices are meant which are designed to intercept unwanted ions or other particles in their original

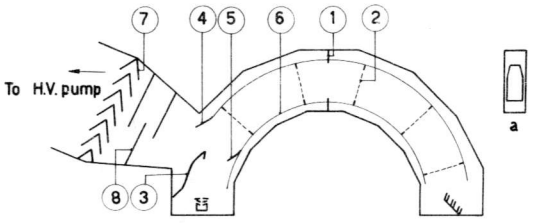

Fig. 27. Location of various baffles

paths. The location of various baffles, applied in our separator, is shown in fig. 27.

The principal ion baffle 1 defines the shape of the ion beam at 90^{o} beyond the ion source. The shape of the baffle opening, shown in view **a** was chosen in accordance to the calculations of § 6.

Several frame shaped baffles 2 are placed along the beam trajectory to intercept ions reflected against the walls at grazing incidence.

Other ion baffles are 3 and 4 protecting the pump connection and 5 trapping beams of low masses. They are all stainless steel plates.

The vacuum chamber is provided with a stainless steel lining 6 which is covered with thin copper sheets, thus enabling easy cleaning.

The oil baffle 7 prevents the oil vapour from the high vacuum pump from penetrating into the vacuum chamber. It consists of copper plates cooled down to $-30\ ^{o}C$ by means of a refrigerator operating on CH_3Cl.

The chlorine baffle 8, used when chlorides are applied as charge materials, serves to retain chlorine from the pumps. It is also made of copper (silver covered) and liquid air cooled. The liquid air is supplied from a stainless steel dewar which, by means of a floating system and compressed air, is automatically replenished from a 25 l container. The consumption is about 3 l/h. After a separation run, the chlorine is removed from the baffle through a bypass line avoiding the pumps.

§ 21. The collector

A sketch of the collector is given in fig. 28.
1 is a water cooled copper plate, onto which the collector chambers 2 are mounted somewhat obliquely with respect to the entering beam. The chambers are made of pure copper, silver, aluminium,

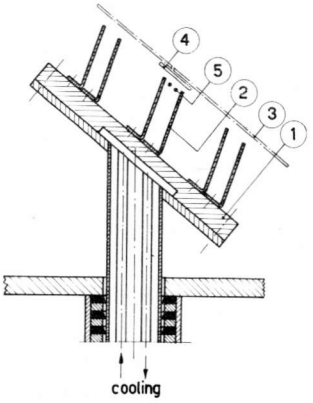

Fig. 28. Sketch of collector

graphite or another material as wanted by the nuclear physicists who are to use the separated isotopes. The thickness of their walls varies between 0.1 and 3 mm; it is also possible to cover them with foils. The chambers are placed at the correct distance to collect each of the isotopes; the foundation plate is placed at an angle of 50° as calculated in § 6.

A shutter 3 provided with a narrow (1 mm) slit and a measuring electrode 4 is situated in front of the collector.

This clap is closed during the adjustment of the separator, which is accomplished by way of the measuring electrode (§ 26); it is opened when the actual separation starts. Furthermore, it is closed automatically when, by some accident, the beams might shift too much during the separation run, due to which contamination of the collected isotopes could be feared (§ 27).

In one of the collector chambers two needle electrodes 5 are fitted which serve the automatic fixing of the ion beams (§ 27).

The base plate 1 is supported by a stainless steel tube. This tube is vacuum sealed by means of Simmerrings, so that the collector is movable.

The cooling tubes of the collector as well as the electrical connections to the needle electrodes pass through the supporting tube. The latter are not indicated in the figure, nor is the moving system of the shutter, which is accomplished by way of a separate Simmerring seal.

Chapter IV

ELECTRICAL AND VACUUM EQUIPMENT

§ 22. Generation and stabilization of the magnet current

The principal installation for the generation of the excitation current of the magnet is a 220 V, 100 Amp. D.C. generator with its exciter driven by an asynchronous 3 phase motor on a common shaft.

It was pointed out in § 5 that the magnetic field must have a stability of 1 : 5000 to separate effectivily heavy isotopes. It is possible to stabilize the magnetic field directly [P3]. To do this the magnetic field strength is measured or compared continuously and when a deviation from the tuned value occurs, the generator receives a signal and tends to correct the field strength.

However, it is much simpler to stabilize the excitation current of the magnet. This can be done if the magnetic resistance of the circuit is sufficiently constant. In our case this condition is satisfied, as long as temperature variations do not exceed 10^{o} C.

Due to the large time constant (a few seconds) of the excitation coil, only relatively slow variations of the current can occur. Therefore the stabilizer is essentially a D.C. device.

The system used by us is similar to that described by Verster [V3]. Since it was published in detail by Schutten [S15], we shall only give the principle of the stabilization circuit here (Fig. 29).

The resistor R_s (0.01 Ω) is connected in series with the excitation coil. By means of a bridge circuit, the voltage drop over R_s (which is proportional to the excitation current) is compared to a very constant, adjustable voltage (the reference voltage). Any difference between these two voltages is amplified and led to the power supply of the excitation coils of the exciter. In this way the current is controlled and the voltage drop over R_s approaches that of the reference voltage. As a result these two voltages are kept at essentially the same value.

This method places high demands on the constancy of both R_s and the reference voltage. The resistor is made from manganine and, by water cooling, its temperature is kept constant within 5^{o} C. Therefore its resistance does not change more than 3.10^{-5}.

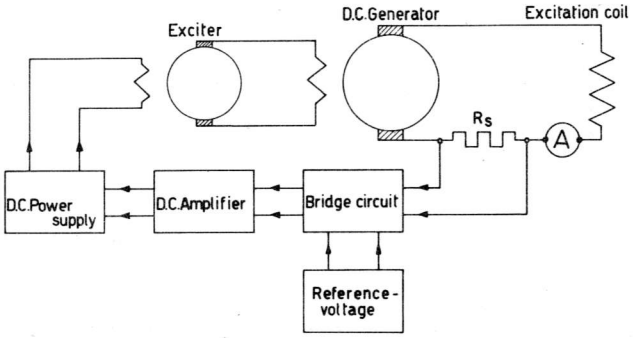

Fig. 29. Basic scheme of stabilization circuit

The reference voltage is obtained from an electronically stabilized supply (stability 1 : 30,000). The required voltage (corresponding to the value of the excitation current to be stabilized) is selected by means of a four stage decade resistor. The current through the decade can be checked in a bridge containing a Weston cell. The D.C. amplifier was taken from Liston *et al* [L6]. The d.c. signal is first converted into an a.c. voltage by means of a vibrating relay contact, then amplified in three stages push pull, and finally rectified synchronously by a four triode circuit. The output voltage can be read on a mV meter.

The excitation current for the exciter is supplied by a number of penthodes connected in parallel. The voltage on the control grids consists of two parts. One is adjustable by means of a potentiometer and this actually controls the excitation current; the other, in series with it, is the output from the D.C. amplifier and serves to stabilize the current. The number of penthodes (1, 3, 5 or 8) can be chosen by means of a switch so that they can always operate in a favourable region of their characteristic.

In order to bring the excitation current of the separator to a certain value, the input of the d.c. amplifier is first short circuited. The correct number of penthodes is chosen and then, with their grid voltage, the excitation current is regulated to approximately the required value. The decade is set at the same value and the D.C. amplifier switched in. Finally, the grid voltage of the penthodes is adjusted until the average output of the D.C. amplifier is zero. It takes about half a minute to select and stabilize a field. The current through the decade resistor is checked by means of the Weston cell several times a week.

We observed, on the creep galvanometer of the Grassot circuit (§ 23), that the fluctuations in the magnetic field due to rather quick variations in the excitation current, were of the magnitude of 1 : 20,000.

The long term drift was determined by observing the average output of the D.C. amplifier and comparing the reference voltage against the Weston cell. After a warming up period of 3½ hours, this drift was less than 1 : 15,000.

In § 12 it was pointed out that an additional power supply was necessary because the resistance of the excitation coil (3 Ω) was larger than was first expected.

Stabilization of this source is not necessary; therefore, we chose a set of Westinghouse selenium rectifying cells with a transformer. The output of this unit is 90 V, 110 Amp. Fig. 30 shows the complete circuit.

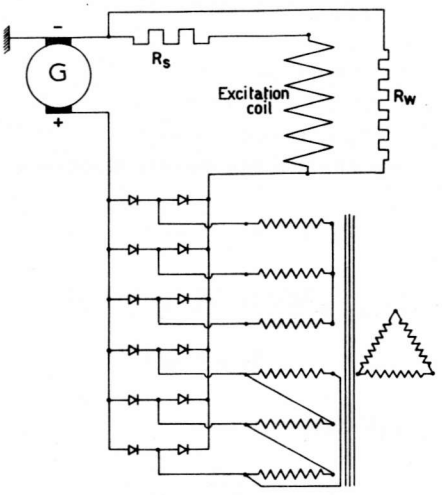

Fig. 30. Power supply of the excitation coil

The two separate secundary windings of the transformer (connected in star and delta respectively) make twelve phase rectifying possible. Due to the large time constant of the excitation coil, the ripple of the current is negligible. R_w is the potentiometer which supplies the potentials for the guard pieces that prevent leakage currents through the cooling water (§ 16). It is connected beyond the resistor R_s; consequently, fluctuation of the current through it does not influence the stabilization of the excitation current.

§ 23. Measurement and final shaping of the magnetic field

The magnitude and shape of the magnetic field of the separator were measured by Grassot's method [G5]. In this method a search coil is connected to a creep galvanometer (Fig. 31).

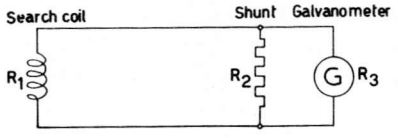

Fig. 31. Circuit for the measurement of magnetic fields according to Grassot

In order to make the galvanometer creep, it is shunted with R_2 which is small as compared to the resistance R_3 of the galvanometer.

When the coil is moved in the magnetic field to be measured, B, the deflection of the galvanometer is proportional to the variations in the flux $\Delta \Phi$ encompassed by the coil.

This follows from the galvanometer equation:

$$Q \ddot{\alpha} + D \dot{\alpha} + C \alpha = G i \qquad (23 - 1)$$

which, for very large damping, is approximated by

$$D \dot{\alpha} = G i \qquad (23 - 2)$$

We can use the relations:

$$D = \frac{(n'A'B')^2}{R_3 + R_1R_2/(R_1+R_2)} \qquad (23 - 3)$$

(neglecting air damping)

$$G = n'A'B' \qquad (23 - 4)$$

and

$$i = \frac{R_2}{R_1R_2 + R_2R_3 + R_3R_1} \frac{d\Phi}{dt} \qquad (23 - 5)$$

where A' is the area and n' the number of turns of the galvanometer coil and B' is the induction in the galvanometer gap.

Then the integration of (23 – 2) with respect to time, between t_1 and t_2, taken immediately before and immediately after the movement of the coil, yields:

$$\Delta \alpha = \frac{R_2}{(R_1 + R_2)\ n'A'B'} \Delta \Phi \qquad (23 - 6)$$

It is desirable to make the damping of the galvanometer as

large as possible since this facilitates the reading of the instrument. This damping can be obtained by making $R_2 < 0.1\ R_3$.

From (23 – 6) it can be seen that the sensitivity can be increased by using a large search coil since, for the measurement of a fixed ΔB, $\Delta \Phi$ is proportional to the area and the number of turns of the coil. However, if $R_1 > R_2$ a further increase of the number of turns is of no value because R_1 increases simultaneously and no gain in sensitivity will be obtained. Therefore, a search coil of relatively large area is more desirable in making delicate measurements.

But, a coil of large area introduces an error. We want to know the induction at a certain point (the center of the coil) and we measure the average value of the field within the coil. This error can be circumvented by shaping the coil in a special way.

Brown and Sweer [B16] constructed a spherical search coil based on the following property of harmonic functions: The average value of the function on a spherical surface is equal to its value at the center of the sphere, provided that no sources are present within the sphere. Obviously this is also valid for the value averaged over the volume of the sphere. The components of the magnetic field are harmonic functions and the coil measures the average value of the component in the direction of its axis and, consequently, the exact value of this component at its center.

Since the construction of such a spherical search coil is a rather tedious task, it is advantageous to investigate, for the particular fieldshape to be measured, whether sufficient accuracy cannot be obtained with a simpler form of coil.

Verster [V4] *e.g.* used a cylindrical coil for the measurement, along the axis, of the axially symmetrical field of his β spectrometer. The ratio of the length of this coil to its diameter was $\sqrt{3} : 2$. He showed that in this coil the second order errors canceled each other.

For our case, we can also arrive at a simplified search coil for which the error can be neglected.

We want to measure the magnetic field in the median plane, where it can be represented by the power series:

$$B_z\ (r,o) = B_o\ (1 - \tfrac{3}{4}\ \delta^2 + \tfrac{7}{8}\ \delta^3 \ldots.) \qquad (23 - 7)$$

with

$$\delta = \frac{r - r_o}{r_o} \qquad (23 - 8)$$

The field outside the median plane can be derived from (23 – 7) and Maxwell's equations which, for our reduced coordinates, δ and ζ $(= \frac{z}{r_o})$, are:

$$\frac{\partial B_r}{\partial \zeta} = \frac{\partial B_z}{\partial \delta} \qquad (23 - 9)$$

and

$$\frac{\partial B_z}{\partial \zeta} = -\frac{\partial B_r}{\partial \delta} - \frac{B_r}{1+\delta} \qquad (23 - 10)$$

Successive integration of (23 - 9) and (23 - 10) yields, to a close approximation:

$$B_z\,(r,z) = B_o\,(1 - \tfrac{3}{4}\,\delta^2 + \tfrac{3}{4}\,\zeta^2 + \tfrac{7}{8}\,\delta^3 - \tfrac{15}{8}\,\delta\zeta^2 \ldots.) \qquad (23 - 11)$$

Now suppose that a rectangular, one layer, search coil with dimensions $2\alpha r_o$, $2\beta r_o$ and $2\gamma r_o$ in the r, z and φ-directions respectively is placed with its center in the median plane.

If we neglect the curvature of the "φ-direction", the field measured by the coil will be:

$$B_{z(m)} = \frac{1}{4\alpha\beta} \int_{\delta-\alpha}^{\delta+\alpha} d\delta \int_{-\beta}^{+\beta} B_z\, d\zeta \qquad (23 - 12)$$

Substitution of (23 - 11) and integration with respect to ζ yields:

$$B_{z(m)} = \frac{B_o}{2\alpha} \int_{\delta-\alpha}^{\delta+\alpha} (1 - \tfrac{3}{4}\,\delta^2 + \tfrac{1}{4}\,\beta^2 + \tfrac{7}{8}\,\delta^3 - \tfrac{5}{8}\,\delta\beta^2 \ldots.)\, d\delta \qquad (23 - 13)$$

By integrating (23 - 13), we find:

$$B_{z(m)} = B_o\,(1 - \tfrac{3}{4}\,\delta^2 - \tfrac{1}{4}\,\alpha^2 + \tfrac{1}{4}\,\beta^2 + \tfrac{7}{8}\,\delta^3 + \tfrac{7}{8}\,\delta\alpha^2 - \tfrac{5}{8}\,\delta\beta^2 \ldots.) \qquad (23 - 14)$$

If we make $\alpha = \beta$, the error is, to a first approximation $\frac{1}{4}\,\delta\alpha^2$.

Demanding an error < 0.05% and by using $|\delta|_{max} = 0.2$ the condition to be met is: $\alpha < 0.1$.

We chose $\alpha = \beta = \gamma = 0.04$ and made a cubic coil with sides of 8 cm.

The error due to the fact that the coil is not curved in the φ-direction is still another order of magnitude smaller. Since the part of the coil covering a "wrong region" is only 0.02 of the total area and the maximum deviation from the average field there is 4.10^{-4}, this error will not exceed 10^{-5}.

Our search coil consisted of 16 layers, each of them having a cubic form. This was achieved by making use of the coil spool shown in fig. 32.

The coil was wound from 1 mm copper wire; it contained 870 turns and its resistance was 4 Ω.

The sensitivity of this coil in combination with a Kipp galvanometer (type Kc, 300 Ω) was so high that we had to reduce the

large as possible since this facilitates the reading of the instrument. This damping can be obtained by making $R_2 < 0.1\ R_3$.

From (23 - 6) it can be seen that the sensitivity can be increased by using a large search coil since, for the measurement of a fixed ΔB, $\Delta \Phi$ is proportional to the area and the number of turns of the coil. However, if $R_1 > R_2$ a further increase of the number of turns is of no value because R_1 increases simultaneously and no gain in sensitivity will be obtained. Therefore, a search coil of relatively large area is more desirable in making delicate measurements.

But, a coil of large area introduces an error. We want to know the induction at a certain point (the center of the coil) and we measure the average value of the field within the coil. This error can be circumvented by shaping the coil in a special way.

Brown and Sweer [B16] constructed a spherical search coil based on the following property of harmonic functions: The average value of the function on a spherical surface is equal to its value at the center of the sphere, provided that no sources are present within the sphere. Obviously this is also valid for the value averaged over the volume of the sphere. The components of the magnetic field are harmonic functions and the coil measures the average value of the component in the direction of its axis and, consequently, the exact value of this component at its center.

Since the construction of such a spherical search coil is a rather tedious task, it is advantageous to investigate, for the particular fieldshape to be measured, whether sufficient accuracy cannot be obtained with a simpler form of coil.

Verster [V4] *e.g.* used a cylindrical coil for the measurement, along the axis, of the axially symmetrical field of his β spectrometer. The ratio of the length of this coil to its diameter was $\sqrt{3} : 2$. He showed that in this coil the second order errors canceled each other.

For our case, we can also arrive at a simplified search coil for which the error can be neglected.

We want to measure the magnetic field in the median plane, where it can be represented by the power series:

$$B_z\ (r,o) = B_o\ (1 - \tfrac{3}{4}\ \delta^2 + \tfrac{7}{8}\ \delta^3 \ldots.) \qquad (23 - 7)$$

with

$$\delta = \frac{r - r_o}{r_o} \qquad (23 - 8)$$

The field outside the median plane can be derived from (23 - 7) and Maxwell's equations which, for our reduced coordinates, δ and ζ $(= \frac{z}{r_o})$, are:

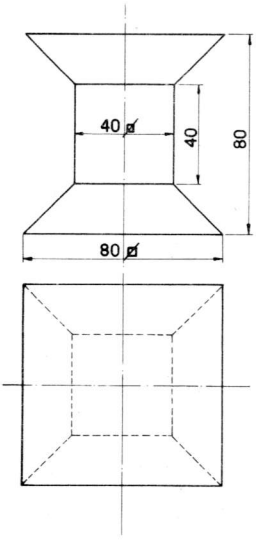

Fig. 32. Spool of search coil

value of R_2 to as low as 0.6 Ω. Even then the sensitivity was 0.133 gausz/mm.

The search coil discussed (S_1) was used only for differential measurements of Δ B for the determination of $B_z(r,o) = f(r)$.

For absolute measurements, we had another coil (S_2) at our disposal. It was a simple, one layer, cylindrical coil, 86 mm in diameter and consisted of 20 turns. An accuracy of a few percent was enough for these absolute measurements. We used a curved scale with the galvanometer and its linearity was checked in steps of 5 cm with a deflection sweep of 8 cm. A maximum deviation of 1 mm was found.

The scale was read in mm and the measurements were reproducible to this accuracy. The damping of the meter was sufficient to obviate errors due to a finite reading time; the time constant was a few minutes.

We connected a calibration coil, whose permanent magnet produced an accurately known flux ($\Delta \Phi = 23408$ maxwell), in series with S_2. By this and the (measured) area of S_2, we determined the sensitivity of the circuit. It amounted to 11.9 gausz per mm of deflection.

By reversing S_2 between the pole faces (at $\delta = 0$, $\zeta = 0$), we determined the magnetization curve $B_o = f(I_M)$ (Fig. 33).

The figure shows that the maximum field to be obtained is not as strong as we had expected: at an excitation current of 100 Amps the field is 3160 in stead of 3780 gausz, which means a re-

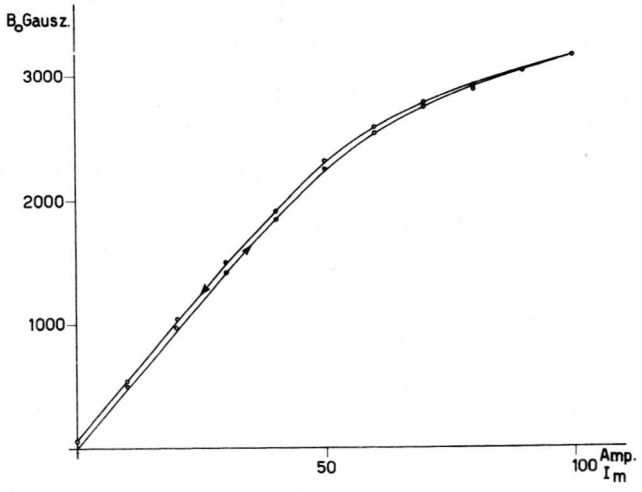

Fig. 33. Magnetic field *versus* excitation current

duction of 17%. Obviously, the back of the yoke is saturated earlier than we had expected. Two causes for this disappointment can be mentioned: The stray field may be larger than was determined or the composition of the steel it not the same as that of the sample investigated. Probably both are true: the vicinity of large steel columns of the structure of the laboratory and other steel constructions may increase the stray field and the composition of the steel was not guaranteed. Anyhow, the drawback is not too serious: it means that the separation of the heaviest isotopes must be carried out at a somewhat reduced accelerating voltage; for mass number 238 this voltage must be 21 kV.

The field shape $B_z(r,o)$ was determined with the search coil S_1. A wooden coil holder provided with a scale, was placed on the lower pole piece at such a level that the center of the coil placed in it, lay in the median plane. By shifting the coil along the holder we measured $\Delta B_z = f(r)$.

The calibration of the coil S_1 was done in the following way: The excitation current was set at a certain value I_M. The galvanometer was connected and its deflection, at a small variation ΔI_M of the current, was determined.

Then

$$\Delta B_o = \frac{\Delta B_o}{\Delta I_M} \Delta I_M \qquad (23 - 16)$$

ΔI_M was accurately known from the settings of the decade resistor of the current stabilizer; $\frac{\Delta B_o}{\Delta I_M}$ had to be determined from fig.

33. This could also be done with sufficient accuracy since we chose I_M on the straight part of the magnetization curve. The sensitivity thus determined was 0,133 gausz per mm of deflection. The field shape $B_z(r,o)$ was measured for different values of the angle coordinate φ. (According to Konopinski's notation $\varphi = 90^o$ at the ion source, -90^o at the collector), Fig. 34 shows the result for $\varphi = 67^o30'$, 45^o and 0^o respectively.

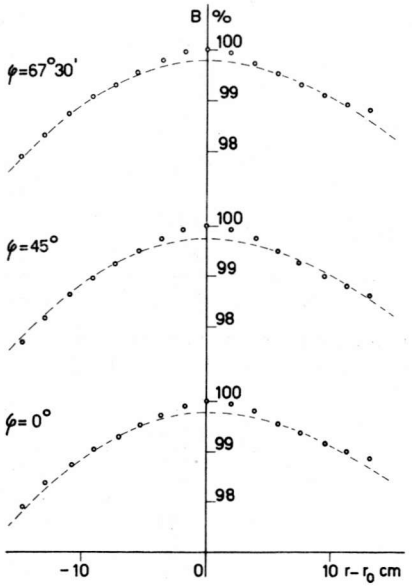

Fig. 34. Original field shape

The desired theoretical shape, according to Konopinski, is indicated as a dotted line. It is obvious that the field was about 0.25% too strong in the vicinity of r_o. By means of a small grinding machine in a movable mount, about 0.5 mm was taken away from the height of one of the ribs in the profile of the pole pieces. The result of this finishing can be seen in fig. 35.

With a view to the vacuum sealing, the boundaries of the pole pieces were not made circular but polygonal, with internal angles of $157^o30'$ (§ 17).

In order to investigate the influence of these boundaries on the fieldshape, we measured $B_z(r,o)$:

a. across the field at an angle.
b. across the field midway between two angles of the polygon (Fig. 36).

An appreciable deviation is to be observed on the outer edge of the field. On the inside, however, the agreement is satisfac-

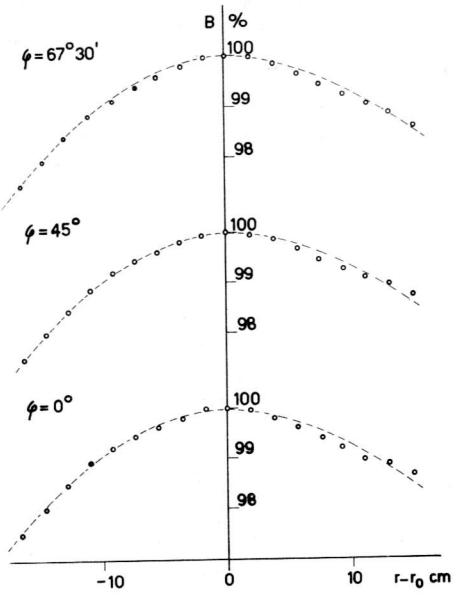

Fig. 35. Fieldshape after grinding of the pole pieces.

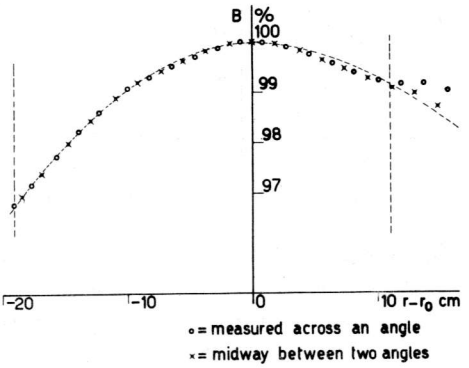

Fig. 36. Influence of the polygonal shape of the pole pieces

tory. Therefore, we decided to shape the defining baffle (§ 6, § 20) in such a way that the ion beam will be asymmetric with respect to r_o. At the baffle ($\varphi = 0$), the beam will have a maximum width of 30 cm: 11 cm to the outside and 19 cm to the inside of r_o. In this way the radial angle of entrance of the ion beam is limited between $-0.19 < \alpha < +0.11$ (§ 6). The boundaries of the baffle are indicated by the vertical dotted lines in fig. 36. Between these lines the deviation from the theoretical shape is within 0.1%.

From the measurements which we had up to this point, we learned that the maximum field was to be found at the same radius r_o for any value of φ. We then determined $B_z = f(\varphi)$ along the circle of this radius (r_o = 102 cm). To do this the search coil was placed at the correct level on a wooden block which was slid along the profile of the pole piece. From this measurement it turned out that the "basic shimming pattern" determined with the model was nearly correct. A very slight amount of additional shimming was necessary in order to compensate for the influence of the steel oil diffusion pump which is situated close to the pole gap. Fig. 37 shows that the deviations are within 1‰, with the exception of the points near $\varphi = \pm 90^{\circ}$. At these points the field begins to fall off quickly.

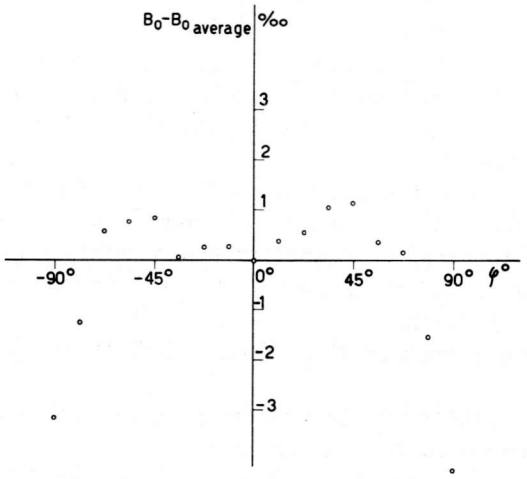

Fig. 37. Checking of the axial symmetry of the field

From measurements of $B_z = f(r)$ at $\varphi = 67^{\circ}30'$ (the location of the oil diffusion pump) and $\varphi = -67^{\circ}30'$, we found, that the field shape was not influenced by the proximity of the pump. Measurements of $B = f(r)$ at various excitation currents showed that the influence of this current on the field shape can be neglected.

During the measurements with the sensitive search coil S_1 we checked the effectiveness of the current stabilization. From the fluctuations in the galvanometer we could deduce a "short term stability" of 1 : 20,000.

§ 24. Power supply of the ion source

Since the accelerating chamber is connected to earth, the ion

source will be at a high positive potential with respect to earth.

Therefore, the electrical power required for the operation of the source must be supplied to it at that level. This is achieved by means of a 10 kVA three phase insulating transformer, insulated for 50 kV. By connecting the star point of the secundary windings of this transformer to the house of the ion source, we obtain a three phase main supply of normal voltage (127/220 V) at the required level.

From these "mains" we feed (Fig. 38):

1. A rectifying unit RU_1 for the filament current.
2. A rectifying unit RU_2 for the arc current.
3. The furnace for the inlet system of the ion source.
4. Fans and a waterpump for cooling.
5. Electronic equipment at H.T. level.

The rectifiers RU_1 and RU_2 are combinations of a three phase transformer and a set of Westinghouse selenium cells; the rectification is two way three phase and the chokes L_1 and L_2 keep the ripple below 1%.

RU_1 has a maximum output of 12 V, 200 A and it supplies the filament current. We use direct current because the life of the filament would probably be shortened appreciably by the continuous vibration that would be caused by the strong alternating current in the magnetic field.

The maximum output of RU_2, which supplies the arc current, is 400 V, 10 A.

The anode resistor R_2 is necessary to prevent instabilities in the arc discharge of the ion source.

The variacs Va_1 and Va_2, which control the filament current and the arc voltage, are operated by means of an insulating shaft driven by a servo motor. In this way the anode voltage and the anode current can be adjusted to the required values from the control panel while the separator is in operation.

The variac Va_3 controlling the heater current of the furnace can be adjusted manually by a pertinax shaft.

The resistor R_1 in the anode circuit of the ion source serves the stabilization of the arc current.

The potential drop across R_1 is lead to the bridge B_1 where it is compared with a potential taken from the potentiometer P_1. Any difference between these potentials is amplified and causes the motor M_3 to turn the potentiometer P_1 until equilibrium is reached.

By way of a pertinax shaft, a potentiometer P_2 at earth level is fixed to P_1 in such a way that the output voltage of P_2 is proportional to that of P_1 and, consequently, to the arc current.

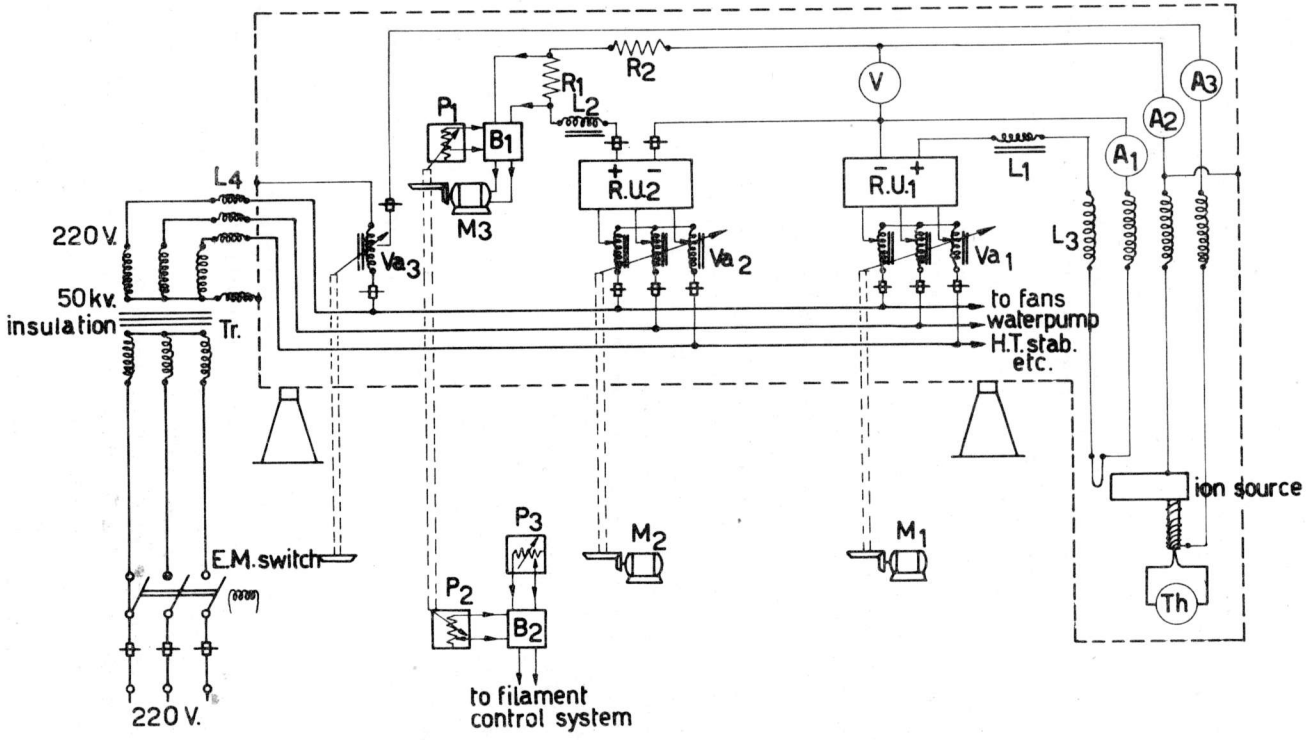

Fig. 38. Power supply of the ion source

In the bridge circuit B_2, the output voltage of P_2 is compared with that of P_3, which potentiometer, placed on the control panel, is manually adjustable and calibrated in units arc current. The potential difference is amplified and causes the motor M_1 to turn the variac of the filament current until the arc current reaches the tuned value. In order to obviate hunting due to the large thermal time constant of the filament, M_1 is turned intermittently. This system is very useful, because, the filament continuously becoming thinner, it is necessary to diminish gradually the filament current, in order to keep the arc current constant.

The accelerating voltage is applied to the house of the ion source. When breakdowns occur between this house and the extraction electrode or the vacuum chamber, the h.f. oscillations related to them are for a greater part restricted to the source by means of the h.f. chokes L_3. These chokes hamper the propagation of the oscillations into the power supply with its vulnerable selenium cells. The h.f. chokes L_4 further retain them from the transformer Tr and the main power supply.

All the electric and electronic equipment at high tension level is carried by a welded construction of channel iron, placed on four 60 cm porcelain insulators which are mounted on top of the magnet of the separator. The cooling system for the ion source is also attached to that rack.

Corona effects create an irregular load on the high tension installation and may impair the stabilization.

In order to obviate these effects the rack with all the devices at high tension level are enclosed in a smoothly rounded corona cap. This cap is constructed from a frame of 1¼" steel tubes to which 1.25 mm steel plates are welded. It consists of two sections. The lower one is shaped like a dish and attached to the bottom of the rack and the upper (larger) part, shaped like a hood, is placed on the dish. This hood can easily and rapidly be slid upward along a set of rails. By means of an electrical winch mounted above the cap and connected to the hood by an insulating plastic cable the cap can thus be opened simply and quickly. This is necessary, not only for the eventuality of repairs or making changes but also because several fuses are within the corona cap. A perspex window in one side of the cap makes it possible to read the various meters which are at the high potential level.

The compact installation of the electrical devices seriously impedes heat dissipation. To prevent the rectifying cells from becoming too hot they are cooled by means of fans. A fan of high capacity refreshes the air inside the cap at a rate of 60 m^3/min. A kind of large "trunk", provided with a door, comes down from the "dish" of the cap to the flange of the ion source. It con-

tains all electrical, vacuum and cooling connections to the source.

All installations at the high potential level which are not enclosed in the caps or the "trunk" are properly rounded or provided with rounded corona shields.

The location of the corona cap and the connection to the source can be seen on the picture Fig. 48.

§ 25. The high tensions for the acceleration system

We designed our high voltage supply for a maximum output of 50 kV, 100 mA. It was constructed by Philips, Eindhoven. Fig. 39 shows the circuit.

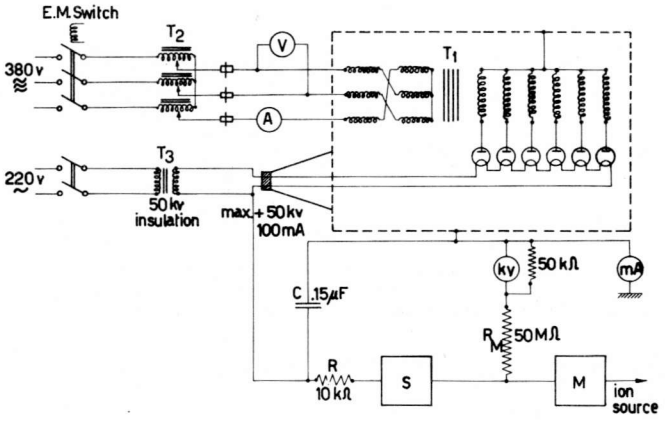

Fig. 39. H.T. supply for the accelerating voltage

The high tension transformer T_1 is fed from the variable three phase transformer T_2, by means of which the accelerating voltage is controlled. The rectification is six phase. The transformer T_3, for the filaments of the rectifying tubes, is insulated for 50 kV. The high tension transformer and the rectifying tubes are mounted in an oil tank with water cooling. Because the negative terminal of the supply is connected to the tank, this tank is insulated from earth, which enables the measurement of the load current at earth potential by an (electronic) mA meter. The ripple in the rectified voltage is smoothed out by the filter formed by the condenser C (0.15 μF) and the self inductance of the H.T. transformer. The resistor R (10 kΩ) mounted in oil is necessary to limit the current during high tension breakdowns which inevitably occur now and then between ion source and vacuum chamber.

The high tension is electronically stabilized by means of the

stabilizer S and measured by a mA meter (kV) connected in series to the measuring resistor R_M (50 MΩ) which is mounted in oil. The kV meter is at earth level in the panel box, like the mA meter which indicates the load current and like the control meters A and V.

The stabilized H.T. can be modulated with a few kV at a frequency of 50 C/sec (M). By means of this modulation a visible mass spectrum on an oscilloscope screen can be obtained, which enables a very easy and quick adjustment of optimum conditions in ion source, acceleration system and vacuum chamber with respect to focus and ion current intensity (§ 26).

It was pointed out in § 5 that the accelerating voltage must be stabilized to at least 1 : 2500. This is achieved in the following way (Fig. 40).

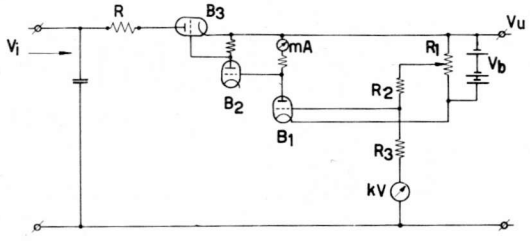

Fig. 40. Schematic diagram of high tension stabilizer

The signal for the stabilizer is obtained across R_2 and part of R_1, which are connected in series with the measuring resistor R_3 (= R_M in Fig. 39). After two stages of amplification this signal is conducted to the grid of the power triode B_3 which is the stabilizing valve. The two amplifiers B_1 and B_2 are operated by a conventional stabilized 300 V supply V_B which obtains its power from the 50 kV insulating transformer (§ 24) serving the power supply of the ion source. An additional transformer insulated for 10 kV is connected in between. This is necessary, since the modulator applies a potential between the stabilizer and the ion source. The reference voltage for the stabilizer is also obtained from the 300 V supply: The potentiometer R_1 is adjusted such, that the tubes B_1 and B_2 operate in a normal region of their characteristic. This is checked on a mA meter in the plate circuit of B_1.

The high voltage installation is placed on top of the separator except the variable transformer T_2 (fig. 39) which is in the panel box. From this panel we can also adjust potentiometer R_1 (Fig. 40) by means of a pertinax shaft and a mag slip connection.

The stabilizer for the high tension is placed inside the corona cap (§ 24); the mA meter is visible through the perspex window.

The modulator is shown in fig. 41.

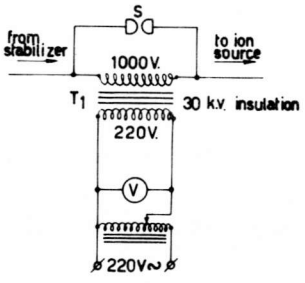

Fig. 41. Modulator for the accelerating voltage

It consists of an insulating transformer T_1 which can supply a secundary voltage of 1000 V. This transformer is provided with an air gap in its magnetic circuit in order to obviate saturation of the iron due to the D.C. (max. 100 mA) through its secundary. On the primary side, the voltage can be regulated by means of the variable transformer T_2 which, like the voltmeter V, is mounted in the operation panel. The spark gap S protects the transformer during H.T. breakdowns.

The negative high tension installation (max. 15 kV, 100 mA) for the lens electrode consists of a three phase H.T. transformer with rectifying tubes. An R-C filter reduces the ripple to 1%. No stabilizer is applied.

The negative H.T. supply is installed on a floor which is an extension to the right of the top of the magnet (Fig. 48).

The connection to the lens electrode is provided by a special high tension cable.

§ 26. Measurements at the collector

Two types of measurements can be carried out at the collector:

1. Display of part of the mass spectrum on an oscilloscope screen.
2. Measurement of the collector current.

The first can be achieved by modulation of the accelerating voltage by a 50 C/sec sinusoidal signal of maximum 1000 V (§ 25). Due to this modulation, the ion beams are swept over the collector in the same frequency. During this operation, the actual collector is closed by a cover Co (Fig. 42), which is provided with a narrow measuring slit, 1 mm wide. This slit is curved in accordance with the shape of the image (§ 6) and placed exactly in

front of one of the receiving chambers RC_1 of the collector. The ions passing through the measuring slit are collected on the electrode E and cause a fluctuating voltage across R_1.

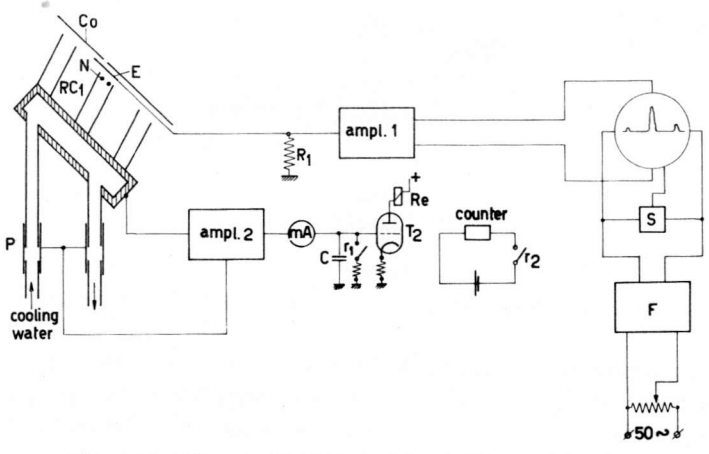

Fig. 42. Measuring circuit at the collector

The signal, after amplification, is put on the vertical deflection plates of an oscilloscope which is mounted in the panel box. A 50 C/sec. sinusoidal voltage, the phase of which can be adjusted by a filter F, provides the horizontal deflection. The fly back of the oscilloscope is suppressed by a signal on the grid of the CR tube, obtained from the suppressor S. By controlling the magnetic field the successive peaks of the whole mass spectrum of the material admitted to the ion source become visible. An example of a mass spectrum on the oscilloscope is shown in fig. 43.

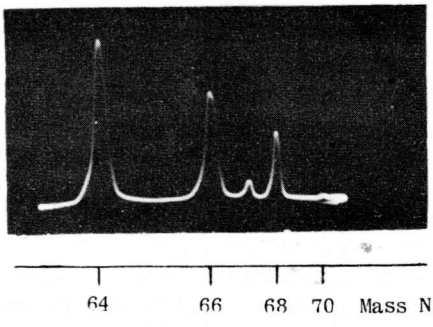

Fig. 43. Photo of oscilloscope screen showing the mass spectrum of Zn (collector current 10.5 mA)

The spectrum on the screen immediately gives all the information we want with respect to sharpness of the image on the collector and beam intensity for all types of ions. Looking on the screen we can easily adjust the electron current, the anode voltage and the gas pressure in the source, the potential of the lens electrode and the position of the collector so as to have optimum conditions of separation. Therefore, each separation run is preceded by an adjustment by means of this modulation. The cover before the collector must be closed in order to obviate contamination of the targets by the sweeping beams of other isotopes. After the adjustment, the modulation is turned off gradually, during which process the peak of the isotope to be collected in RC_1 must be kept on the screen till the very last by controlling the magnetic field. When the modulation is reduced to zero, the cover is removed and so the collection of the separated isotopes is started.

During the separation process, the collector current is measured on a mA meter (most sensitive reading 0.1 mA full scale). Moreover, the total quantity of material reaching the collector is measured by means of a current integrator. This consists of a condensor C being charged via Ampl. 2. When the voltage across this condensor has reached a certain value, the plate current of tube T will make the relay Re operate. One of the relay's contacts causes a kick of a counter, another discharges the condensor, so that the relay falls off and the cycle starts again. The sensitivity of the current integrator is changed by way of Ampl. 2 at the same time as that of the mA meter.

The collector is water-cooled. In order to obviate errors in the measurement of the collector current due to the conductivity of this water, we apply shield pipes P. These pipes are kept at the same potential as the collector and therefore, no leakage current will flow from the collector to earth. There is a current from P to earth but this current is supplied by a special cathode follower tube in Ampl. 2 which keeps the shield pipes at the correct potential.

From time to time during the separation process (*e.g.* each hour) the position of the image is controlled on the oscilloscope screen by closing the cover and giving a small modulation. A rough control is also possible by (visual) observation of the image through a perspex window of the vacuum chamber. There the focal lines of isotopic beams with an intensity of 0.2 mA or more are visible as bright images.

§ 27. Measures against contamination of the collected isotopes

In spite of the application of various stabilizers (high tension, arc current, magnetic field) it is conceivable that, during operation, a shift or broadening of the image might occur, due to which a beam or part of a beam would enter a neighbouring collector chamber.

In this way an isotope of very low concentration, collected in a run of several days or even weeks could be contaminated seriously in a short time.

In order to prevent this, we make use of an automatic control system, the principle of which is given in fig. 44.

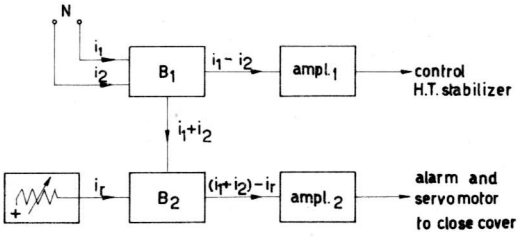

Fig. 44. Automatic control of the image

In one of the collector chambers two needle electrodes N (fig. 28, fig. 42) are fitted. The currents to these electrodes, i_1 and i_2, are applied to a bridge circuit B_1, where they are converted into two signals, *viz.* $(i_1 - i_2)$ and $(i_1 + i_2)$.

When the beam has been properly adjusted, $i_1 = i_2$. If, by any accident, the beam shifts its position a little, i_1 and i_2 will differ from each other. This difference is amplified and operates, by means of a servo motor, the H.T. stabilizer, until the correct position of the image has been restored. If this proceeding might fail (*e.g.* due to a defect in the H.T. stabilizer) an alarm is given by way of a terminal switch on the servo motor and, at the same time, the cover before the collector chambers is closed automatically.

The signal $(i_1 + i_2)$ is applied to a second bridge circuit B_2 where it is compared with the adjustable reference current i_r. $(i_1 + i_2)$ is approximately constant for small shifts of the image, but a deviation will occur at larger shifts or at a broadening of the image. The difference $(i_1 + i_2) - i_r$ is amplified and, at a certain value, it operates an alarm as well as a servo motor which closes the cover before the collector.

Contamination of the collected isotopes can also be caused by

continuous H.T. breakdowns at the ion source, due to which the beams of various isotopes will be swept over the collector.

The image control system mentioned is insensitive for such rapid fluctuations and therefore a special installation was designed to protect the isotopes from the effect of too many breakdowns. The principle is given in fig. 45.

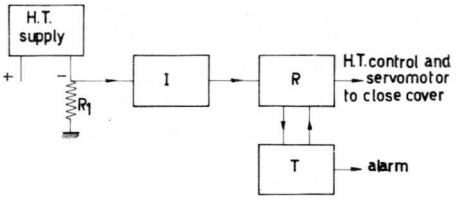

Fig. 45. Breakdown safeguard system

Breakdowns create voltage fluctuations across the resistor R_1 connected to the negative terminal of the H.T. supply for the accelerating voltage. These fluctuations are integrated in the circuit I and, at a certain value of this "integrated breakdown signal", a relay circuit R comes into action, switches off the high tension and closes the cover before the collector chambers.

Since breakdowns are often maintained due to local heating effects on the electrodes causing evaporation, it will, in many cases, be sufficient to cool down for a few seconds, after which the high tension can be switched on without starting directly a new breakdown. Therefore, after 10 seconds of rest, the H.T. is switched on again and automatically regulated up to the normal value. Then the cover is reopened.

When, however, three of such "integrated breakdowns" occur within a time interval of five minutes (which is controlled by the timing circuit T) it is supposed that something is definitely out of order. Then the high tension is not switched on again, and an alarm is given.

The two installations mentioned in this section greatly simplify the operation of the separator, doing away with the necessity of a continuous and scrupulous watch over the instruments.

§ 28. Provision of the vacuum

The basic diagram of the vacuum circuit of the separator is shown in fig. 46.

R is a rotating Kinney backing pump, H is a three stage fractionating high vacuum pump, B a one stage booster pump; both are

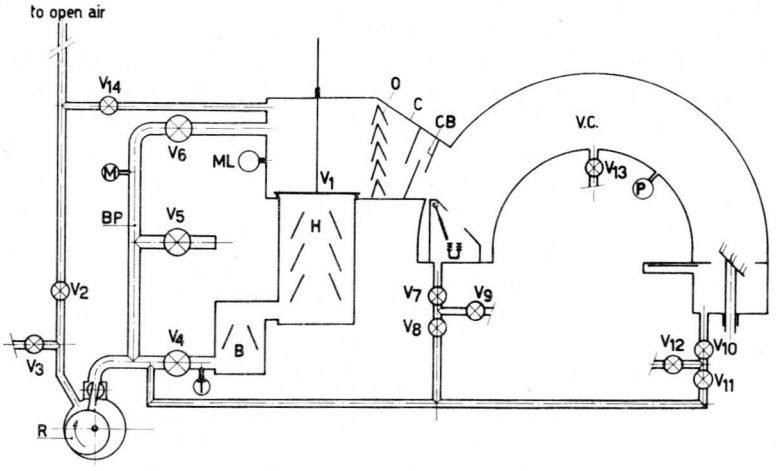

Fig. 46. Vacuum circuit of the separator

Philips' pumps, operated on silicone oil type DC 703. In the connection C to the vacuum chamber V.C., two baffles are fitted. The oil baffle O, cooled to about -30° C by means of a CH_3Cl refrigerator, prevents the oil vapour from penetrating into the vacuum chamber. The chlorine baffle C.B. retains chlorine from the pump, when chlorides are used as charge materials for the ion source.

The main valve V_1 is operated electrically by means of a servo mechanism.

The high pressure side of the Kinney pump leads, either by V_2 and a waste pipe to the open air, or by V_3 to a chemical system by way of which expensive gases can be regenerated.

The bypass B.P. and the valves V_4, V_5, V_6 enable the admission of air into the separator as well as rough pumping, while the high vacuum pumps are maintained vacuum or even in operation. This reduces loss of time for small proceedings inside the vacuum chamber. The most common manipulations (on the ion source and the collector) are further facilitated by the application of air lock systems. The ion source is placed in a chamber, the opening of which can be closed by a door; the collector can be withdrawn into a chamber which, after that, can also be closed. Both doors are operated via Simmerring seals.

The sets of valves V_7, V_8, V_9 and V_{10}, V_{11}, V_{12} enable filling and evacuation of the air locks during continuous operation of the high vacuum pumps.

The Kinney pump, type V.S.D. 8811 has a speed of 18 l/sec at a pressure of 0.02 mm Hg. It is provided with an electrically

heated oil separator, which makes it possible to strip the oil from volatile constituents when necessary.

The Philips' pumps and the refrigerator are mounted on a common wheeled frame. In this way the pumps with connection can easily be removed from the vacuum chamber. The casing of the main valve of the high vacuum pump is furnished with a perspex observation window and, on the inside, with an incandescent lamp. By looking into the pump its operation can be judged from the observed phenomena (oil drops, vapour stream, bubbles, etc.).

The connection, constructed from non magnetic, stainless steel, is funnel shaped with a maximum cross section of 80 × 50 cm^2, a minimum of 40 × 16 cm^2 and a length of 60 cm. On the side of the chamber, it is provided with a flange of the same dimensions as the normal outer plates of this chamber and mounted to it in a similar way (§ 17).

For normal operation, the high vacuum is read on a P.I.G. manometer P, mounted in the vacuum chamber. The fore pressure is indicated by a thermocouple manometer T. The membrane manometer M (0 – 76 cm) on the bypass enables the observation of the pressure during the rough evacuation of the chamber. For special measurements a Mac Leod manometer ML is available.

The pyrex Mac Leod manometer is a barometric type; the sensitivity is $0.5.10^{-6}$ mm Hg for the first millimeter.

The thermocouple manometer is simply a Th 4 tube, mounted in the fore vacuum. At a fixed filament current, the thermo potential is read on a mA meter. The instrument is very useful in the region of 10^{-3} to 1 mm Hg; it shows immediately if any appreciable leakage is in the vacuum system.

By means of the valve V_{13} very dry compressed air can be blown into the vacuum chamber in order to remove chlorine from the baffle C.B. when it is brought to room temperature. Then the valves V_1, V_2 and V_6 are closed, but V_{14} is opened so that the chlorine escapes into the open air.

We have done some measurements on the capacity of the high vacuum pump. By means of an adjustable leak, air was admitted into the vacuum chamber and the pressure inside was determined with the Mac Leod. The quantity of air admitted was measured from the displacement of a drop of mercury in a horizontal glass tube which was connected to the leak.

Under the most favourable conditions of fore pressure and heating power, the pumping speed, at a pressure of 10^{-5} mm Hg, is 5000 l/sec (air).

The temperature of the cooling water has no influence on the pumping speed within the limits 13 – 40^{o} C.

Variation of the heating power has a large effect. Although

the pump was designed for 5000 W, we observed that the capacity at 2500 W. was about twice as large. However, the operation was instable at that low power input. Looking through the observation window, we perceived that showers of oil drops "rained down" from the upper hat of the pump system now and then. And at each shower the pressure suddenly rose by a factor of 3 to 4. Obviously, the instabilities were caused by a too low temperature of the upper hat at the small heating power. Therefore, we mounted an additional heating spiral to the hat, consuming about 70 Watts. The showers disappeared and we obtained a stable operation of the pump and a large pumping speed.

The heating power is provided by an Inventum boiler plate which, by means of a switch, can be connected in two ways: when the pump is switched on, a power of 5000 Watts causes a quick heating of the oil; when the pump begins to operate, the power is switched over to 2500 W. and, at the same time, additional heating is supplied to the hat.

The pumping speed in the vacuum chamber, reduced mainly by the baffles, is 1500 to 2000 l/sec. The ultimate vacuum, obtained when no gas is admitted, is 3.10^{-6} mm Hg; the normal operating pressure is 1 to 5.10^{-5} mm.

Two devices which were originally not designed for high vacuum work, are frequently used by us in the high vacuum system.

The first is the Dikkers-Jenkins globe valve, normally used in low pressure steam tubing. A slight modification makes this valve very useful for high vacuum work. For this purpose we mount a small cylinder around the valve spindle, into which cylinder a few vacuum oil is applied. In this way leakage along the spindle is prevented. With a rubber valve disk a perfectly tight and very cheap vacuum valve is obtained. We use them in various sizes from 1/4" up to 2" bore.

In the second place, Angus oil seal rings, the so called "Simmer-rings", made from Gaco (oil resistive rubber) are used by us for movable vacuum seals.

A possible construction is shown in fig. 47.

A seal consists of two Simmer rings (1) between which a few vacuum oil is applied. The movable shaft (6) is carried by the gland (3). This gland also presses, by way of the pressing rings (2), the O-rings (4), which provide the seal between the outer side of the Simmer rings and the casing (7) of the seal. The insulated lining (5) of the gland enables to use the shaft as a support for an electrode, which may have a potential of several hundred volts with respect to the vacuum chamber.

Other constructions are also possible; the one described is used by us in a number of places to our full satisfaction. The

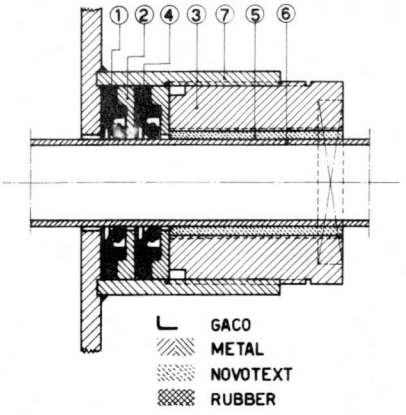

Fig. 47. Movable seal with Simmer rings

Simmer rings are very cheap and their thin "lips" make an easy movement possible. The shaft must be supported in axial direction in order to withstand the atmospheric pressure and its surface must be polished smoothly.

§ 29. Gas inlet system for the ion source

It was pointed out in § 9 that solid compounds and – if possible – solid elements are preferable as charge materials. Therefore, the principal inlet system is the furnace mounted in the ion source (fig. 26), in which the charge materials are evaporated. The volume of this furnace is 10 cc, which means that – on the average – twice a day a new charge must be brought in. Recharging is very easily accomplished: the ion source air lock system is filled with argon gas, the furnace is taken out of the source, refilled and mounted again and the air lock evacuated. This operation is accomplished within a quarter of an hour. After another 15 to 20 minutes, the furnace is again at the required temperature and the separation process can be continued.

For gaseous charge materials an adjustable leak according to Nier [N3] is applied: a copper capillary of 2 mm inner diameter is flattened and wound around a spindle. By turning the spindle by means of a worm gear the capillary is more or less tightened and, consequently, the gas flow controlled. An insulating pertinax shaft enables an adjustment of this leak during operation of the separator. The high pressure side of the leak is connected either to a tank with pressure reducing valve containing the gas (*e.g.* N_2, O_2, A) or to a small bottle containing a low boiling liquid charge material, such as BCl_3, $SiCl_4$ or CS_2.

A normal consumption rate is 200 cc gas of atmospheric pressure per hour.

§ 30. Safeguards

For an instrument like the separator, in which high vacuum, high voltages and forced coolings are applied, and which must be suitable for continuous operation so that different persons must handle it by means of over 150 operation buttons and valves, an extensive safeguard and control system is indispensable.

There is in the first place the protection of persons from touching electrical parts. Whereas for "normal" voltages (a few hundred volts) the usual carefulness is observed, particular measures are taken for the high voltages.

The ion source and the lens electrode are very dangerous objects, since they are at high tension and within easy reach (about 1.60 m from the floor). Therefore, a movable gauze protection cage surrounds the ion source, the "trunk" of the coronacap and the lens electrode. This cage can be removed by a servo mechanism and, in the closed position, it presses a contact which is connected in the operating circuit of the electromagnetic main switches of the high tension installations. Moreover, when the cage is opened, the ion source is automatically short circuited to earth so that the condensors in the system are discharged.

The high voltage supplies are placed on top of the separator and, consequently, are beyond the immediate reach. However, the magnet is furnished with a steel gallery (See Fig. 48) which can be reached by a steel stair case and it might be thinkable that someone would walk upstairs in an unguarded moment and be struck by the high voltage. Therefore, the stairs are provided with a hinge on the top and, in the horizontal position, they press a safety contact in the operating circuit of the main switches. If one wants to climb the stairs he must first let them down, due to which the high tensions are switched off.

Beside the measures mentioned for the protection of persons, numerous provisions are taken to protect the expensive instruments from imprudences and troubles of all kinds.

Of course, all electrical devices are provided with fuses and control lights. Electrical motors which are not in immediate reach are operated by electromagnetic switches with thermal relays.

The h. f. oscillations occurring during high tension breakdowns are excluded from the power supply of the ion source by means of h. f. chokes in the connections to the source (§ 24). Moreover,

gas fuses applied at "dangerous points", like the selenium rectifying cells, limit eventual peak voltages to a few hundred volts.

Fuses for the excitation coil of the magnet are applied only on the AC side of the unit. This is done because a sudden cut in the circuit of the coil would be dangerous, since this would cause a high induction voltage due to the large self inductance of the coil. This induction voltage is reduced by the copper jacket, acting as a short circuit winding and by the potentiometer for the compensation of the leakage currents through the cooling water (§ 16). From experiments at very low excitation currents we deduced that an induction voltage of 2 kV would occur when, at the maximum current of 100 Amps, the circuit would suddenly be cut. Without the potentiometer and the jacket, it was higher by a factor of 10. Special care was taken to assure the cooling of the excitation coil. The zero coil of the controller of the motor which drives the generator, and the operation circuit of the electromagnetic switch for the additional rectifying unit are connected in parallel with the motor of the force pump for the cooling water. Consequently, it is impossible to run the generator or to switch on the rectifying unit, unless the force pump is operating. Moreover, a pressure relay is connected to the force pump, which comes in action and gives an alarm by means of a siren when the water supply is interrupted.

Since the cooling system of the coil consists of a number of parallel branches, it is necessary to have an indication if one of these branches would be stopped up. This is achieved by means of thermocouples applied to the successive layers of the coil (§ 16). These thermocouples are connected to a rotating switch (1 r.p.m.) so that the temperature of all the layers can be read successively. If the temperature of one of the layers might exceed a certain limit, an alarm is given and the failing layer is known so that measures can be taken.

All important water coolings (of the vacuum pumps, ion source air lock chamber, accelerating electrodes, collector) are provided with pressure relays connected to the signal and alarm installation. The flow of cooling water through the supports of the ion source is also controlled.

When the refrigerator of the oil baffle stops while the high vacuum pumps are in operation or when the supply of liquid air to the chlorine baffle is interrupted, an alarm is given. This happens also when the pressure in the vacuum chamber exceeds a certain value. The signal for this alarm, obtained from the P.I.G. manometer, at the same time switches off the high tensions of the accelerating system in order to avoid breakdowns.

During the night, the vacuum pumps are kept in continuous operation without any surveillance. The signal installation is then switched over to "night control".

Any trouble which would cause an alarm by day then automatically closes down the entire pumping system: the pumps and refrigerator are stopped, the main valve is closed as well as the valve between backing and high vacuum pumps, the P.I.G. manometer is switched off. Since this night-system is operated by a special D.C. safety line, it even protects the instrument from the consequences of temporary breaks in the A.C. main power supply.

Safety measures against contamination of the collected isotopes by shifting or broadening of the images were mentioned in § 27.

§ 31. Operation

The electrical operation-, control- and measuring devices are concentrated mainly in three boxes situated on both sides of the separator (Fig. 48).

From the panel box on the left side, the vacuum pumps, the refrigerator of the oil baffle, the liquid air supply system for the chlorine baffle, the main valve of the high vacuum pump and the force pump for the cooling water of the excitation coil are operated. The safeguard- and signal installation is also placed in this box. Finally some panels of the "pump-box" are used for the manometers: P.I.G. and thermocouple manometer and the meter for the pressure of the force pump.

The panel box on the very right is entirely occupied by the control- and stabilization devices for the excitation current of the magnet.

The largest box consists of 24 panels. It contains control, signal and stabilizing devices for the high tensions and the supply of the ion source, meters to read the load currents of the high tension supplies, the current to the earthed electrode, and the collector current, the current integrator to indicate the quantity of collected isotopes, the control of the modulation of the accelerating voltage and an oscilloscope screen to show the mass spectrum.

An additional mA meter, connected in the P.I.G. circuit is mounted in this box. The temperature of the layers of the excitation coil is read on a mA meter, operated by the 16 thermocouples in succession.

Servo mechanisms for removing the upper part of the corona cap

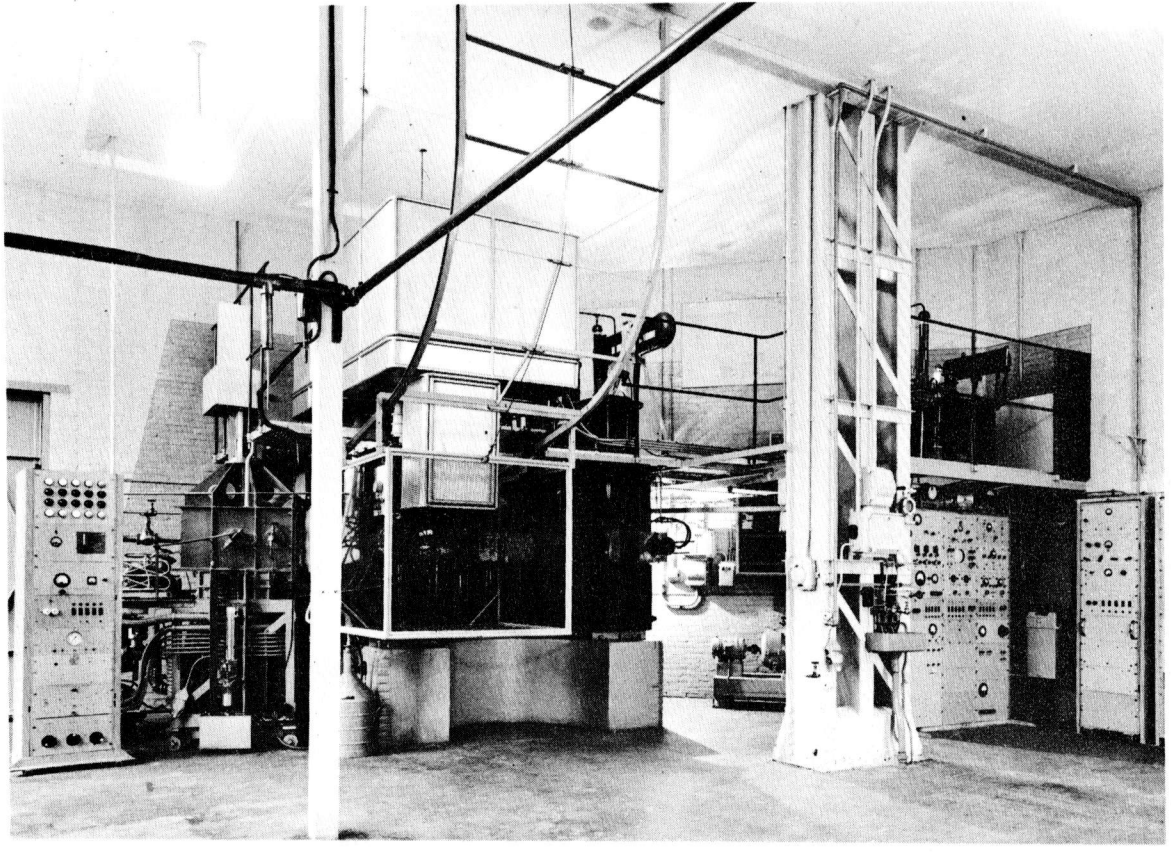

Fig. 48. Front view of the separator with panel boxes

and the protecting cage of the ion source, are operated from here.

The valves of the water coolings are combined into two groups: those of the pumps, refrigerator, air lock chamber and acceleration electrodes on the left side of the foundation of the separator; those of baffle, collector and high tension transformer against the steel pillar on the right side of fig. 48.

The silica gel drying installation for compressed air with supply valves is also mounted to this pillar.

The cooling of the excitation coil has a separate heavy supply pipe with valve behind the magnet. The water meter is also placed there.

Chapter V

EXPERIMENTAL RESULTS

§ 32. Various conditions of operation

A number of measurements were carried out in order to find optimum conditions concerning the separating power and the collector current.

These measurements were done in such a way that of the many existing parameters, only one at a time was varied, the remaining conditions being kept constant. An exception was made for the negative voltage of the lens electrode, which was always regulated so as to give optimum focusing conditions.

The separating power was determined by measuring the peak width on the oscilloscope screen at 5% of the peak height (See fig. 43) and correcting for the width of the slit before the measuring electrode. An ion exit slit of 2 mm width was applied. The most important results will now be mentioned:

a. Arc- and Heil-source

Under favourable conditions, a separating power of 150 at collector currents up to 10 mA could easily be obtained with the arc source. With the Heil source, however, the maximum separating power obtainable at a collector current as low as 0.5 mA, was only 20.

In the latter case, the ion output current from the source was high, even at very low pressures (it could be increased to 100 mA), but we observed, on the screen, that a tremendous hash was present in the beam. Obviously, the space charge compensation was ineffective due to the oscillations (§ 4) and the beam was "blown up".

Under certain conditions, the arc source too can be run in a state which gives a poor resolving power. And these situations are always characterized by a lot of hash, visible on top of the peaks on the oscilloscope. This seems to bear out our impression, that oscillations hamper the space charge compensation. Anyhow, we concluded that the arc source is more favourable to be used in the separator than the Heil source, although the latter has a lower operating pressure and consequently a higher gas efficiency. We decided to continue the experiments on the arc source exclusively.

b. Arc conditions

Both the collector current and the separating power depend strongly on the arc conditions (arc voltage and current and the pressure in the source).

Whereas the collector current increases generally with the intensity of the arc, the separating power shows strong fluctuations when the arc voltage or current is gradually varied. An example is given in fig. 49, where the influence of the arc voltage is shown, the pressure and arc current being kept constant. The figure applies to zinc, at an arc current of 1 Amp and an accelerating voltage of 16 kV. The zinc pressure in the source, as calculated from the amount of charge material consumed, was $1.5.10^{-3}$ mm Hg.

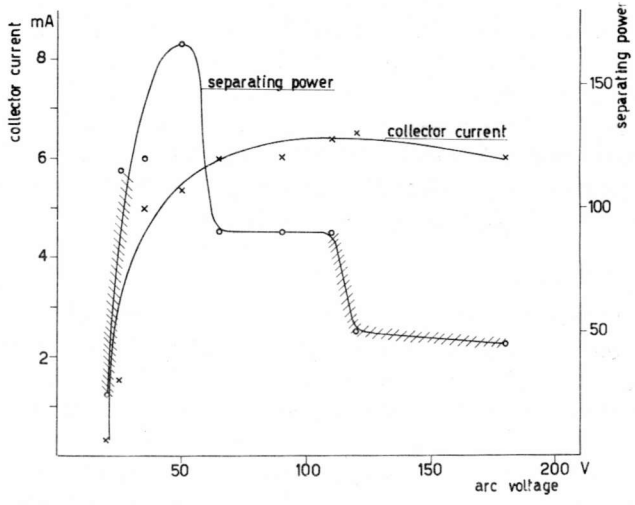

Fig. 49. Influence of arc voltage in source on collector current and separating power. (Zn, arc current 1 Amp, pressure $1.5.10^{-3}$ mm Hg, accelerating voltage 16 kV).

Regions of much hash are indicated by hatching. It is obvious that the very poor separating power (below 100) at a too low or a too high arc voltage is connected to the hash in the discharge, due to which the space charge compensation of the ion beam is hampered.

Pictures, similar to fig. 49 are obtained when the arc current or the pressure in the source are varied. The width and the number of useful hash-free regions depend on the kind of gas in the source.

When the stable region, on which the source is adjusted, is narrow, stabilization of the arc conditions is very important.

The physical origin of the hash is not yet fully understood. A special investigation of the discharge in the source is in progress.

c. Accelerating voltage

At constant source conditions, the accelerating voltage was varied and, with it, the magnetic field in order to keep the beam on the collector.

Typical curves are given in fig. 50, where, beside the separating power and the collector current, the ion current from the source is indicated.

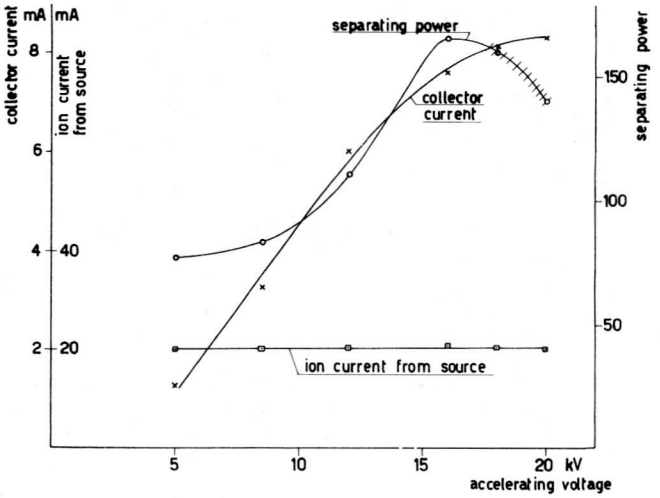

Fig. 50. Effect of accelerating voltage (Zn, arc 1 Amp, 50 V; pressure 2.10^{-3} mm Hg)

The latter current is constant throughout the region observed. This means that the current is not limited by space charge but by the supply of ions to the exit slit of the source. This was to be expected since the ion density in the D C arc applied, is much lower than in a Heil type ion source.

The collector current increases from 1.3 mA at 5 kV to a maximum of 8.3 mA at 20 kV, probably due to reduction of ion loss, caused by defocusing.

The separating power also rises rapidly up to a maximum of 166 at 16 kV and then falls down while hash is observed.

The increase is explained by a better space charge compensation at higher ion velocities (σ_i increases with v, § 4). The hash may be induced in the source either by the strong magnetic

field or by the penetration of the accelerating field. Especially when a broad ion exit slit is used we have observed that it is possible to extinguish the arc in the source by increasing the accelerating voltage and thus pushing back the plasma. Before the arc is completely extinguished, it starts producing hash due to which the separating power decreases.

d. Lens voltage

The effect of the negative lens voltage on the collector current and the separating power is different for weak and strong currents. Whereas for weak currents, both are practically independent of the negative high voltage, there is a marked influence at strong currents (fig. 51).

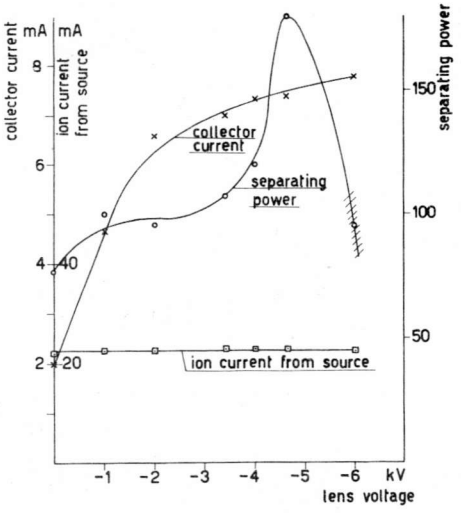

Fig. 51. Action of lens voltage at strong ion currents (Zn, arc 1 Amp, 50 V; pressure 2.10^{-3} mm Hg; accelerating voltage 16 kV)

The ion current from the source remains constant, but the collector current increases rapidly, especially at the first few kV. This is explained by the reflection of secundary electrons from the beam, thus increasing their space charge compensating action in the immediate vicinity of the acceleration system. As a result, the loss of ions due to defocusing is appreciably reduced. At the same time, the separating power rises to a maximum of 180 at - 5.7 kV, which is apparently the condition that the focal line of the beam, after 180^{o}, coincides with the collector plane.

At - 6 kV the separating power is further diminished by hash,

produced in the source by the penetration of the field of the lens electrode.

The negative voltage, necessary for optimum focusing, depends on the arc conditions as well as on the accelerating voltage. In general, it increases with the arc intensity and also with the accelerating voltage. In the latter case, however, it is limited to the value where it starts producing hash in the source.

e. Gaseous charge materials

Generally speaking there is no essential difference in the behaviour of gaseous and solid charge materials in the source. In fact, the arc is run in a gas in both cases, since the ion source is always kept at a sufficiently high temperature, so that the vapour is unsaturated. There is, however, one important exception: gaseous charge materials cause an increase of the pressure in the vacuum chamber, whereas solids condense on its cold walls and do not influence the high vacuum unfavourably (§ 9). On the contrary: many elements tend to getter when present as very fine particles and thus will improve the vacuum.

As a result the collector currents can be appreciably higher for solids than for gases. In order to check the theory of § 9, we have measured the collector current for argon as a function of the pressure in the source at constant arc current, arc voltage and accelerating voltage. The result is shown in fig. 52, where the ion current from the source is also indicated.

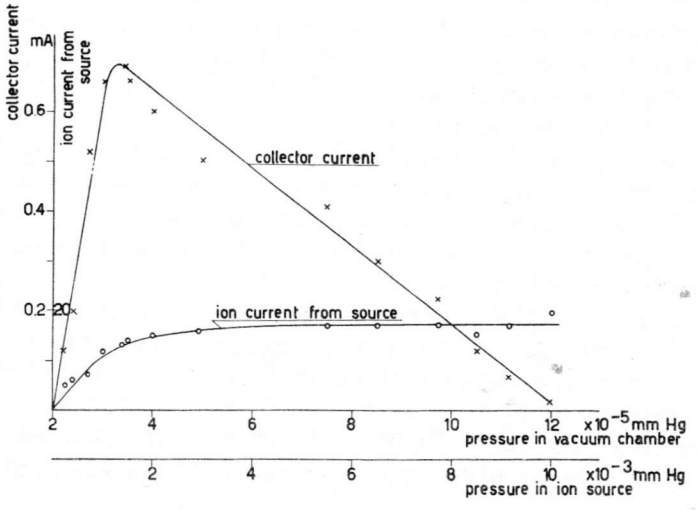

Fig. 52. Influence of pressure in the source for gaseous charge materials (Argon, arc 150 V, 1 Amp; accelerating voltage 18.7 kV)

The pressure in the source was derived from that in the vacuum chamber, supposing that the vacuum was 2.10^{-5} mm Hg when no gas was admitted. This was justified by the extrapolation of the curves for zero current. The general shape of the collector current curve is as predicted in § 9, except for a steeper decrease at higher pressures. This is caused by the fact that the ion current from the source is proportional to the source pressure only at low pressures (below $1.5.10^{-3}$ mm Hg), whereas for higher pressures it becomes constant. The transition is easily understood, since it occurs just in the region where the mean free path of the electrons in the source becomes of the order of their total available path length. As a result, the maximum in the collector current will be shifted to a somewhat lower pressure than was calculated in § 9. The conclusion still holds that the collector current obtainable with gaseous charge materials will be much lower than with solids. Indeed, we found a gain of at least a factor 3 experimentally.

Another experiment gave us some evidence that the loss of ions from the beam was not merely due to elastic scattering, but that charge exchange is also an important process.

Air was admitted to the source and all conditions, including the source pressure, were kept constant, whereas the air pressure in the vacuum chamber outside the source was varied. The intensity of the ion beams, at the collector, for mass 28 (N_2) and 30 (NO) were measured. (NO is a type of ion of which astonishingly large quantities are produced when air is admitted to the source).

At increasing chamber pressure, the collector currents of both beams decreased rapidly, but for NO the reduction was less than for N_2. Fig. 53 shows the ratio of $^{N_2}/_{NO}$ as a function of the air pressure in the vacuum chamber.

Apparently, the total collision cross section for N_2 ions is greater than for NO – ions. This can be explained when it is supposed that charge exchange plays an important part in the collisions. Indeed, the cross section for charge exchange is a maximum when ions collide on molecules of the same kind. Then the transfer of potential energy is zero and a state of resonance exists [M3]. The gas in the vacuum chamber will contain a large quantity of N_2 molecules, but no appreciable amount of NO molecules. Therefore, N_2 ions will collide easier than NO ions and, consequently, the ratio $^{N_2}/_{NO}$ will decrease at a higher chamber pressure. A similar effect has been observed for all other types of ions.

f. Types of ions

When the source is run on a molecular gas, various types of

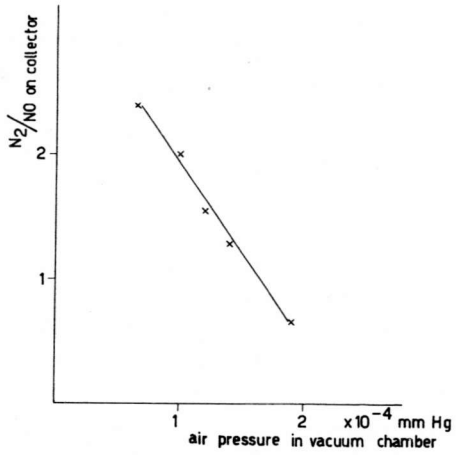

Fig. 53. Influence of charge exchange for different types of ions

ions will be produced, the abundances of which depend on the arc conditions.

We admitted air at a source pressure of 2.10^{-3} mm Hg and measured the intensity, at the collector, of the beams of N, O, N_2, NO and O_2. We observed:

1. At constant arc current (0.7 A) the ratio $^{N}/_{N_2}$ increased continuously from 0.3 to 0.8 when the arc voltage was raised from 35 V to 290 V. At the same time the ratio $^{O}/_{O_2}$ increased from 0.25 to 0.75.

2. At constant arc voltage (100 V), the ratio $^{N}/_{N_2}$ increased continuously from 0.6 to 1.1 and the ratio $^{O}/_{O_2}$ from 0.7 to 3.5 when the arc current was raised from 0.6 A to 4.4 A.

The conclusion is that a high arc voltage as well as a high current density favour the formation of atomic ions. This is in agreement with earlier experiments on hydrogen [S5].

3. As for the ratio $^{NO}/_{N_2}$, this increased also with the arc voltage (from 0.36 to 0.5) and with the arc current (from 0.4 to 1) for the variations mentioned above.

4. At constant arc conditions (140 V, 1.3 A), the source pressure was increased from 2.10^{-3} to $1.2.10^{-2}$ mm Hg. The ratio $^{N}/_{N_2}$ increased from 0.7 to 1.3.

This is also in agreement with the earlier experiments mentioned, but the result will be influenced seriously by the charge exchange process in the vacuum chamber which discriminates in favour of the atomic ions. Whereas for the gases N_2 and O_2 it is possible to obtain an ion output with an atom – molecule ratio of about 2, the situation is yet more favourable in the case of chlorides, which are frequently applied as charge materials for

metals. *E.g.* the mass spectrum of UCl_4 at normal operating conditions (arc 120 V, 1.3 A.) shows: U^+ 5.7 mA, UCl^+ 0.9 mA, UCl_2^+ 0.5 mA, UCl_3^+ 0.25 mA, UCl_4^+ 50 μA, Cl^+ 2.8 mA, Cl_2^+ 0.3 mA U^{++} 1.1 mA. In those cases the loss by compound ions is not serious.

g. Width of ion exit slit

When the exit slit of the ion source was increased from 2 to 4 mm, there was no appreciable gain in collector current when gaseous charge materials were used. This was to be expected from the considerations of § 9: For a larger exit slit area, the pressure in the source must be reduced in order to maintain a sufficient vacuum in the vacuum chamber. For solids (Zn) there was an increase of about 50% at the cost of a slight decrease of the resolving power. Moreover the arc appeared to be less stable, due to the larger penetration of the accelerating field, which tends to push back the plasma in the source. With the uranium separation (charge material UCl_4), we attempted to increase the collector current further by widening the slit to 6 mm. But then the arc was so instable that effective operation did not seem possible and we returned to a slit of 4 mm width.

h. Position of collector

The collector was made movable in order to place it always at the focusing point of the beams.

However, it turned out that this adjustment could much easier be achieved by way of the high voltage of the lens electrode, and this is the way it is now actually done.

When working with uranium, we perceived that the image of U^+ was extremely bright. So we had an excellent opportunity of doing some visual observations by way of a perspex window in the vacuum chamber. We observed:

1. The total radial opening angle of the beam is indeed of the order of 15^o.
2. The curved shape of the image is in accordance with the calculations in § 6.
3. Our calculations on the position of the focal plane for different masses (§ 6) was also confirmed.

§ 33. Separations

A few experimental separations were carried out in order to check the reliability of the instruments and to find imperfections in the separator and the working method.

a. Zinc

The operation conditions were:
Charge material: Zinc metal.
Temperature of furnace 410 – 455° C.
Accelerating voltage 14.4 kV.
Negative lens voltage 0.
Arc 85 V, 4 A.
Ion current from source 28 mA
Ion loss on negative electrode 1.5 mA } mean values
Ion loss on earthed electrode 8 mA
Collector current 5.0 – 5.9 mA
Collector material: copper foil
Air pressure in vacuum chamber 10^{-5} mm Hg.

During the separation run we experienced much trouble from small sparkings between the ion source and the electrodes. The latter were made of copper and water cooled. Fairly large amounts of zinc condensed on them and, after some time, started bladdering. For this reason, we were compelled to work at a rather low accelerating voltage.

The separating power was not good either (50 on the average), and we could not get a hash free beam.

This was strange, because some days before, during measurements, we had a "clean" beam with a separating power of over 150. The cause of this became clear later. When the source was opened after the separation, its arc chamber was covered with a very thin layer of ZnO and the electrical conductivity of the surface was poor. It is obvious that the arc was hampered by this layer and in this way the hash was explained. We concluded that the ZnO had been formed when we admitted air to the source to refill the furnace when it was still hot.

However, this conclusion was, at least partly, wrong, as turned out later.

A run of 9 hours was made. According to the current integrator, 120 mg Zn had reached the collector. About 15% of this amount had struck a diaphragm, which was situated in front of the collector and, consequently, 100 mg Zn had entered the collector chambers, which were made of copper.

Part of this zinc and a larger amount of copper were scratched off from the collector walls, chemically dissolved and, by successive electrolysis, zinc metal was recovered on platinum electrodes. In this way we obtained the following enriched samples: Zn^{64} : 16 mg, Zn^{66} : 7.9 mg, Zn^{67} : 2.6 mg, Zn^{68} : 4.9 mg and Zn^{70} : 0.3 mg.

An analysis was made with the mass spectrometer, which was constructed on the model magnet (§ 13). The result is shown below:

Sample	Relative abundance at.%				
	Zn^{64}	Zn^{66}	Zn^{67}	Zn^{68}	Zn^{70}
Natural Zn	48.9	27.8	4.1	18.6	0.63
Enriched Zn^{64}	[94]	3.0	0.4	2.1	0.0
„ Zn^{66}	10.7	[85]	1.5	2.6	0.0
„ Zn^{67}	12.3	34	[29]	25	0.0
„ Zn^{68}	5.7	8.5	6.2	[79]	0.2
„ Zn^{70}	16	15	5	39	[25]

In view of the rather bad separating power at which the separation was performed, this result is not too disappointing. In fact, it is most promising for future separations to be carried out at much more favourable conditions.

It is not believed that the recovery of the zinc was 100%, since in that case the above results would correspond to a collector efficiency of about 32%. The actual collector efficiency had been determined in a previous, shorter run, in which we collected the Zn^{64} isotope alone. Whereas the current integrator indicated that 9.0 mg of Zn had entered the collector chamber, a quantitative chemical analysis (colorimetric and polarographic) gave a result of 5.7 mg. Consequently the collector efficiency amounted up to 63%.

b. Magnesium

Immediately after the experimental Zn separation described above, we cleaned the source, charged the furnace with magnesium metal and carried out some measurements. We obtained a collector current of 5 mA and a good separating power (150).

The next day we started a separation and found to our surprise that the separating power was extremely bad (about 25), while a tremendous hash appeared in the beam. Now the source had been kept under vacuum, as we had not recharged the furnace. After the separation run, however, we found that the walls of the arc chamber were covered with a practically insulating layer of magnesium oxide and magnesium nitride. Being charged negative, this layer will hamper the arc seriously. Consequently, there was no doubt about the origin of the hash.

Our practice of running the source on a solid charge material is: first we start the arc on a gas which is admitted by an adjustable leak; when the source has run hot we heat the furnace

and, when sufficient vapour is produced, we close the gas valve. This procedure is applied in order to prevent condensation of the charge material on the walls of the source when it is still cold.

For convenience we had used air as a "starting gas". But obviously this air attacked the thin layer of magnesium metal which had condensed on the source walls when they cooled down after the measurements of the previous day. In a similar way the formation of ZnO in the separation run mentioned before, was explained.

In view of this, we decided, henceforward, to apply only argon gas as starting gas. And indeed, we did not meet troubles of this kind any more. The measurements on Zn given in the preceding section *e.g.*, were carried out with argon as starting gas.

A separation run of 7 hours was made on magnesium. The operation conditions were:

Charge material: Magnesium metal.
Temperature of furnace 440 – 480° C.
Accelerating voltage 13 kV.
Negative lens voltage 0.
Arc 2.2 A, 100 V.
Ion current from source 20 mA.
Ion loss on negative electrode 2 mA. } mean values
Ion loss on earthed electrode 3 mA.
Collector current 4.0 – 6.9 mA.
Collector material: Cu foil.
Air pressure in vacuum chamber 10^{-5} mm Hg.

Because magnesium metal condensed on the electrodes the same way as zinc did we had similar troubles with sparkings.

Assuming a collector efficiency of 65%, we collected 30 mg of Mg in total. The collector foils were forwarded to nuclear physicists for measurements on (p, γ) reactions.

From the separations of Zn and Mg we learned that the application of water cooled copper electrodes is undesirable for solid charge materials. Therefore, we applied graphite electrodes carried by stainless steel tubes, as mentioned in § 19. This turned out to be a great improvement.

c. Uranium

We used UCl_4 as a charge material for uranium. This compound requires very careful treatment since it is extremely hygroscopic. It is kept in a perfectly dry atmosphere and the charging of the furnace is carried out as quickly as possible.

A separation run of 9½ hours was carried out with the following data:

Charge material: UCl_4.
Temperature of furnace 400 – 550° C.
Accelerating voltage 19 kV.
Negative lens voltage 2.5 kV.
Arc 110 V, 1.4 A.
Ion current from source 35 mA.
Ion loss on negative electrode 7 mA. } mean values
Ion loss on earthed electrode 3 mA.
Collector current 2.0 – 4.8 mA.
Collector material: Al foil.
Air pressure in vacuum chamber 10^{-5} mm Hg.

This time we had no troubles with breakdowns. The separating power could not easily be judged from the mass spectrum on the oscilloscope screen since the U^{235} peak is practically invisible. But the image on the collector gave off such a splendid light that its width was readily determined visually. The image was sufficiently sharp for the U separation.

However, it turned out that the "stable regions of arc operation" as meant in § 32b were quite narrow and, as a result, the arc tended to switch to and fro from one state to another, one of them showing hash and a broadening of the image. Therefore it was necessary to adjust almost continuously the arc current to a certain value. This inconvenience brought us to the conclusion that the arc current should be stabilized and after the separation run, the stabilizer mentioned in § 25, was constructed.

According to the current integrator, 300 mg of U had reached the collector. In a previous, shorter run, we had determined the collector efficiency for uranium, which turned out to be 75% (current integrator: 13.8 mg, colorimetric chemical analysis : 10.3 mg).

Consequently, the collector was supposed to contain 225 mg of U^{238} and 1.6 mg of U^{235}.

A second, larger separation was characterized by the following conditions:
Charge material: UCl_4.
Temperature of furnace 400 – 690° C.
Accelerating voltage 19 kV.
Negative lens voltage 5 kV.
Arc 120 V, 1.8 A.
Ion current from source 35 mA.
Ion loss on negative electrode 14 mA. } mean values
Ion loss on earthed electrode 0.
Collector current 4 – 7 mA.
Collector material: Al foil.
Air pressure in vacuum chamber 10^{-5} mm Hg.

This separation run was really much quieter than the preceding one. Thanks to the arc current stabilizer a scrupulous manual adjustment of the arc conditions was no longer necessary.

However, one last inconvenience has remained: It turned out that about each half hour the temperature of the furnace had to be raised a little by increasing the heater current in order to obtain constant arc conditions. Especially in the beginning and at the end of a furnace charge, this inconvenience was rather serious and hash appeared now and then. We could not utilize the total amount of material of each charge: when about 15% was left, the furnace was recharged. This recharging was carried out every 7½ hours and at each second recharge we replaced the filament in order to avoid additional loss of time. Consequently, the filament life was at least 15 hours.

The necessity of increasing the furnace temperature during operation is probably caused by a temperature gradient existing in the furnace, partially due to heating from the arc chamber, partially also to radiation losses.

However, it is not fully understood why the temperature range for UCl_4 is so much higher than for Zn and Mg. Perhaps the heat conduction through the charge material is better and, consequently, the temperature gradient smaller in the cases of Zn and Mg. It is also possible that the UCl_4 contained a certain amount of UCl_6 which has a higher vapour pressure.

Assuming a collector efficiency of 75%, we collected in a run of 26 hours 880 mg of U^{238} and 6.2 mg of U^{235}.

No analysis of the separated uranium isotopes was made; the collector foils were handed over to nuclear physicists.

§ 34. Present state of affairs and plans for further development

In the present state of the separator, we are capable of carrying out separation runs of at least a few days on many elements. The collector currents obtainable, at least for solid charge materials, are sufficiently strong and, probably, a further increase is possible by improvements in source and acceleration system.

However, the ultimate object of a completely universal instrument has not yet been reached. Limitations are:

1. Separating power

With an ion exit slit of 100×2 mm^2 and the present constellation of acceleration system and ion baffle, we can have a separating power of 180 under the most favourable source conditions.

This is in astonishingly good agreement with the calculations of § 6. It means that Konopinski's field is realized almost perfectly and that the space charge compensation is practically 100%.

Up to now, we did not need more, but when elements as Hg must be separated, we shall find ourselves obliged to take measures to raise the separating power further. Undoubtedly this will be possible by shaping the ion exit slit or reducing its area. But, of course, the latter will be at the cost of the yield.

2. *Vapour pressure*

Concerning the vapour pressure of the elements, there are limitations to both sides.

In the first place, elements with a very high vapour pressure (*e.g.* gases as N_2, O_2, A, etc.) require a special collector technique, which has not yet been developed, though a general scheme was given in § 10.

On the other hand, there are some elements (*e.g.* Pt) which have, as well as their compounds, an extremely low vapour pressure.

When the isotopes of these elements must be separated, it will be necessary to increase the temperature of both the furnace and the source chamber to a very high value (*e.g.* 2000° C). This will be an enormous technical problem [B17].

3. *Efficiency*

In most cases, the efficiency is no major problem: The cost of the inlet material is, in general, negligible compared to the total cost of production.

In some special cases, however, the inlet material is very expensive. This applies to certain rare earths and especially to artificially radioactive isotopes to be separated.

A typical efficiency scheme is given in fig. 54.

It applies to a separation of Zn with the conditions we had during the measurements of § 32.

The first loss is suffered in the furnace: a residue of about 10% is not used, because of the rapidly increasing instability of the arc when the furnace is getting empty.

Though the house of the ion source is at a high temperature, there are some places (*e.g.* the filament holders and the colder parts of the carrying tubes) which are sufficiently cold to cause condensation of charge material. This loss is also estimated to be 10%.

The most serious loss is caused by neutral atoms or molecules leaving the exit slit of the ion source: whereas 22 mA is a normal value of the ion current drawn from the source, the gas loss

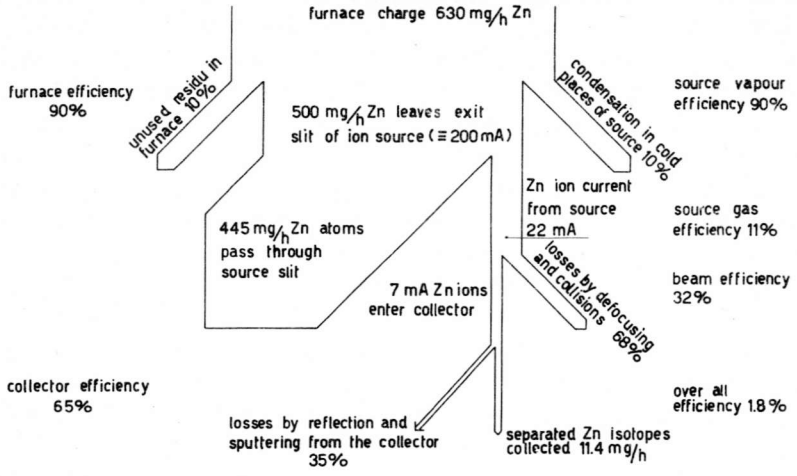

Fig. 54. Efficiency scheme for Zn separation

amounts to 445 mg per hour, corresponding to 180 mA. Consequently, the gas efficiency of the source is 11%.

Only 7 mA out of the 22 reach the collector; the rest is lost by defocusing and collisions with gas molecules.

Finally, about 35% of the entering ions leave the collector again by reflection and sputtering.

The over all efficiency of the separator for this example is 1.8%.

This efficiency is different for each element. For uranium *e.g.* there is an additional loss by the formation of molecular ions, but the collector efficiency is greater. The source gas efficiency also depends on the kind of gas.

In some cases, the collected material is left on the collector foil and in that form used as a target for nuclear physical experiments.

In other cases, however, the separated isotopes must be recovered from the foil and an additional chemical efficiency factor is introduced.

This factor mainly depends on the equipment available. For the rough recovery of Zn, mentioned in § 33a, it was about 50%, but it will be much higher when the appropriate equipment (such as a vacuum evaporation unit) comes to our disposal shortly.

Though the total efficiency factor of 1.8% does not seem too bad in comparison with the corresponding figure for a normal mass spectrometer (Zemany [23] states a value of 6.10^{-3}%), a further improvement will be possible.

From fig. 54 it is clear that the most important factor in the

scheme is the source gas efficiency. This factor may be increased to about 0.9 by making use of a Finkelstein type ion source [F2]. Since the magnetic field in this type of source is in the direction of the extracted ion beam, it will be necessary to place the source outside the main magnetic field of the separator. An electrostatic lens system must project an image at the place where our present source is situated. Probably, the ion current must be kept low in order to avoid space charge troubles. But for some special cases where the efficiency is of more importance than the yield, the experiment seems feasible.

Another possible way may be the application of a carrier gas with high excitation and ionization potentials. A much higher degree of ionization of the actual inlet material can then be obtained due to collisions of the second kind. Incidentally we got an experimental proof of the possibility of this method. One day we had carried out measurements on Zn. We emptied the furnace and cleaned all parts of the source mechanically. The next day we admitted argon gas to the source, but we did not get more than 0.3 mA of A^+ on the collector. In stead we had a strong Zn^+ beam and during 6 hours, we had a Zn^+ collector current of 3 mA on the average. Obviously the small amounts of Zn left in some parts of the source, were separated with a very high efficiency. The effect mentioned is a well known phenomenon in gaseous discharges. It may be applied for the separation of expensive elements, in which case the choice of the "carrier inlet material" will be of great importance.

An increase of the beam efficiency might be possible if the accelerating voltage could be increased sufficiently. Unfortunately, this voltage is limited by high tension breakdowns up to now. Probably an improvement of the construction of the screening caps around the source and of the acceleration system will enable a further increase. But the principal difficulty is the presence of the strong magnetic field, being at right angles to the electric field (§ 18). This problem does not exist in a sector type spectrometer, where the ion source is placed in a separate weak magnetic field.

We could now ask whether our choice of a 180^o field was indeed the most favourable. Our principal argument was the fact that for this type the ion trajectories lie completely within the magnetic field and, consequently, the space charge compensating electrons are hampered seriously in their motion (§ 5).

However, Bernas [B3] has shown that a sector type spectrometer can also be used with strong ion currents if the electrons are kept in the ion beam by an appropriate system of electrodes.

His instrument is smaller than ours and, consequently, both his separating power and his yield are smaller.

It still remains to be seen, if a sector type with the same main radius will give results comparable with a 180^{o} type. If this turns out to be true, the main advantage (beside a cheaper magnet) will be the more favourable location of the ion source outside the main magnetic field. A drawback is the increase of the length of the ion paths by a factor 1.4, causing a corresponding rise of ion loss by collisions on gas molecules.

In order to increase the beam efficiency, a thorough investigation of the lens properties of the acceleration system will also be necessary. An improvement of this system will probably reduce the losses caused by defocusing.

An extensive investigation on scattering and capture cross sections may give useful indications with respect to the inlet material to be used for minimum collision losses.

The furnace efficiency can be increased by an enlargement of the furnace. This, however, will mean a completely new source construction. Accepting this, the problem of condensation in the remaining "cold" places can also be tackled.

Finally, a higher collector efficiency can be obtained by reducing the sputtering and reflection effects. It seems feasible to bring the collector at high tension level, in such a way that the ions strike the collector with only a few hundred eV energy. This is, however, a much embracing task, in which many new problems may arise.

Summarizing we may say: Many elements can now be separated, but much work is still ahead.

SAMENVATTING

Het onderwerp van dit proefschrift is de electromagnetische isotopenseparator, die, als een onderdeel van het research programma van de Stichting voor Fundamenteel Onderzoek der Materie, te Amsterdam werd gebouwd. Deze bouw was mogelijk door de financiële steun van de Nederlandse Organisatie voor Zuiver Wetenschappelijk Onderzoek.

Hoofdstuk I. Algemene beschouwingen

In de eerste paragraaf worden een aantal toepassingen van gescheiden isotopen genoemd.

§ 2 beschrijft de historische ontwikkeling van de isotopenscheiding vanaf het pionierswerk van Aston tot de spectaculaire uraanscheiding ten behoeve van de atoombom.

In § 3 worden de verschillende scheidingsmethodes met elkaar vergeleken en de keuze van de electromagnetische methode voor separaties ten behoeve van kernphysische experimenten wordt gemotiveerd.

§ 4 behandelt de moeilijkheden, die de positieve ruimtelading van de ionenbundel bij de afbeelding veroorzaakt. Het is noodzakelijk deze ruimtelading te compenseren m.b.v. electronen, die ontstaan door ionisatie van het restgas in de vacuumkamer. Dit probleem stelt bepaalde eisen aan de vorm van het magneetveld en aan de ionenbron.

In § 5 worden de verschillende oorzaken van afbeeldingsfouten en de maatregelen hiertegen behandeld. De energiespreiding van de versnelde ionen moet zo klein mogelijk gehouden worden door de juiste keuze van het type ionenbron. Door een geschikte veldvorm moeten de ionen, die onder een vrij grote hoek uittreden, op de collector gefocusseerd worden. De eindige breedte van de uittreespleet van de ionenbron wordt als verbreding van het beeld op de collector geaccepteerd. Een berekening van de invloed van botsingen van ionen met gasmoleculen toont aan, dat een goed vacuum (enkele malen 10^{-5} mm) noodzakelijk is. Reflectie van ionen kan door baffles worden tegengegaan. De gebruikte electrische en magnetische velden moeten zeer constant zijn.

Tenslotte wordt een keuze gemaakt uit de mogelijke vormen van analyserende velden. De keuze van het veld van Konopinski en Beiduk (180^{o}, radiaal inhomogeen) wordt toegelicht.

Uitgaande van de berekeningen van Beiduk en Konopinski worden in § 6 de afbeelding van een rechthoekige uittreespleet en de

stand van het focusseringsvlak bij de collector bepaald alsmede de gewenste vorm van de begrenzende baffle op 90^{o} voorbij de bron.

In § 7 wordt de configuratie van het gebruikte versnellingssysteem aangegeven. Het bestaat uit: de ionenbron op de positieve versnellingspotentiaal, de extractie electrode of lenselectrode op een regelbare negatieve potentiaal en een derde, geaarde electrode. De ionenbron en de extractie electrode zijn zodanig ontworpen, dat ze tezamen een Pierce lens vormen. De voordelen van dit systeem boven een enkelvoudige versnellingselectrode worden genoemd.

Het onderwerp van § 8 is het te gebruiken type ionenbron. Na een overzicht van de eigenschappen van verschillende ionenbronnen en van onze te stellen eisen, volgt de keuze van het type. Mede in verband met de te verwachten h.f. oscillaties in de ionenbundel, die de ruimteladingscompensatie zouden kunnen verhinderen, werd de h.f. bron niet gekozen. Dezelfde vrees bestond voor de magnetische oscillatiebron, maar omdat deze op zeer eenvoudige wijze in een magnetische boogbron kan worden omgeschakeld, werd besloten in eerste instantie een Heilbron te construeren.

In § 9 worden de voordelen van vaste en gasvormige inlaatmaterialen voor de ionenbron tegen elkaar afgewogen. Het blijkt dat vaste materialen (in het bijzonder: vaste elementen), die in een oventje verdampt worden, een hogere collectorstroom leveren t.g.v. de vermindering van ionenverlies door botsingen in het restgas.

De problemen, samenhangende met het verzamelen van de gescheiden isotopen, worden in de laatste paragraaf van het eerste hoofdstuk besproken. Maatregelen moeten genomen worden tegen het verlies van materiaal door reflectie en „sputtering" en door verdamping. Het eerste wordt bereikt door het gebruik van opvangkamers van een speciale vorm, het tweede door de isotopen eventueel chemisch te binden.

Hoofdstuk II. Ontwerp van de separator en voorbereidend werk

In § 11 worden de vorm en hoofdafmetingen van de magneet vastgesteld. Een ongewone vorm werd gekozen, waarbij weliswaar een sterk lekveld aanwezig is, maar die het grote voordeel heeft van een zeer goede toegankelijkheid van de vacuumkamer aan alle kanten. De hoofdafmetingen van de magneet zijn: straal r_o = 102 cm, breedte van de ringvormige poolschoenen 50 cm, nuttige hoogte van het interferricum 17 cm. De gebruikte versnellingsspanning is 20 à 30 kV. Voor massa 238 is bij 30 kV een magneetveld van 3780 gausz nodig.

§ 12 geeft het ontwerp van de bekrachtigingsspoel. Hij bestaat

uit 785 windingen koperbuis 9 × 5 mm Ø, waardoor leidingwater onder een druk van 17 atmosfeer geperst wordt. Het benodigde vermogen is maximaal 30 kW, de temperatuurstijging van het koelwater blijft beneden 20° C.

§ 13 beschrijft de metingen aan een modelmagneet (schaal 1 : 5) met behulp van een roterende fluxmeter. Het shimprofiel en de radiale vorm van de poolschoenen werden hiermede bepaald.

Het weerstandnetwerk, dat o.a. gebruikt wordt voor modelmetingen aan electrostatische lenzen, is het onderwerp van § 14.

Hoofdstuk III. Constructie van de separator

De constructie van de belangrijkste onderdelen van de separator wordt achtereenvolgens in de §§ 15 – 21 behandeld.

Het juk werd uit stalen platen samengesteld, welke platen door bouten worden samengehouden.

Het werk aan de bekrachtigingsspoel bestond o.a. uit het isoleren en aaneenlassen van de stukken koperbuis en het wikkelen van de spoel. Speciale aandacht moest besteed worden aan de aansluitingen van de verschillende lagen van de spoel, die electrisch in serie, maar voor het koelsysteem parallel geschakeld zijn.

De poolschoenen, welke een speciaal profiel bezitten ter verkrijging van de juiste veldvorm, vormen de boven- en onderzijde van de vacuumkamer. De zijwanden van deze kamer bestaan uit messingplaten. De afdichting geschiedt met rubber op analoge wijze als bij het Amsterdamse cyclotron.

Het huis van de ionenbron is geheel van grafiet vervaardigd, waarbij de voorplaat met uittreespleet afneembaar is. De gloeidraad is van 2 mm dik wolframdraad. De bron wordt gedragen door een tweetal dubbelwandige roestvrij stalen buizen, die met water gekoeld worden. Door een dezer buizen steekt de gloeidraadhouder, die bestaat uit een coaxiaal stelsel watergekoelde koperbuizen. Door de andere buis steekt de drager van een oventje voor het inlaten van vaste stoffen. De hoogspanningsisolatie wordt gevormd door twee 40 cm lange porceleinen buizen.

De beide electroden van het versnellingssysteem zijn van grafiet en worden gedragen door roestvrij stalen buizen.

Bijzondere zorg moest worden besteed aan het voorkomen van hoogspanningsdoorslagen en -ontladingen, die bij de gebruikte configuratie in het magneetveld zeer gemakkelijk kunnen optreden. Het was daarom nodig, een stelsel afschermkappen op geringe onderlinge afstand aan te brengen.

Een uitgebreid systeem van baffles is gemonteerd in een roestvrij stalen voering, die in de vacuumkamer is geplaatst. Deze baffles dienen om de afmetingen van de ionenbundel te begrenzen,

om ongewenste reflecties van ionen tegen de wanden van de vacuumkamer tegen te gaan en om verontreiniging van deze wanden door het neerslaan van de ingelaten materialen te voorkomen. Om moeilijk condenseerbare dampen (vooral chloor) neer te slaan is in de pompleiding een baffle aangebracht, die met behulp van vloeibare lucht tot - 180° C wordt gekoeld.

De collector bestaat uit een stevige watergekoelde koperen plaat, waarop kamers met parallelogram-vormige doorsnede geschroefd worden, enigszins schuin t.o.v. de binnenkomende ionenbundel. Het materiaal van de kamers (bv. Al, Cu, C, Ag) wordt vastgesteld in overleg met de kernphysici, die de gescheiden isotopen gaan gebruiken. Tijdens het instellen van de separator worden de opvangkamers door middel van een van buiten af bedienbare klep afgesloten, om verontreiniging van de targets door andere isotopen te voorkomen. De metingen tijdens het instellen worden uitgevoerd met behulp van een meetelectrode met smalle spleet, die zich, bij gesloten klep, voor een der opvangkamers bevindt.

Hoofdstuk IV. Electrische installatie en vacuum systeem

De opwekking en electronische stabilisatie van de bekrachtigingsstroom van de magneet is het onderwerp van § 22. De gelijkstroom (max. 100 Amp) wordt opgewekt door middel van een gelijkstroomgenerator en een aanvullend aggregaat bestaande uit een 6 phase transformator met selenium gelijkrichtcellen. Het maximale vermogen is 30 kW. De constantheid van de stroom is 1 : 10^4.

In § 23 worden de laatste afwerking van de poolschoenen en de metingen van het magneetveld (volgens de methode van Grassot) beschreven. De overeenkomst van de veldvorm met de theoretische vorm is binnen 1‰.

De electrische voeding van de ionenbron wordt in § 24 behandeld. Deze voedingsinstallatie, die zijn energie krijgt uit een 10 kW driephase scheidingstransformator, bevindt zich geheel op hoogspanningsniveau en is opgesteld binnen in een coronakap. De benodigde gelijkstromen en spanningen worden geleverd door twee sets, elk bestaande uit een driephase transformator met gelijkrichtcellen. Deze transformatoren krijgen hun spanningen van driephase variacs, die m.b.v. servomechanismen tijdens het bedrijf geregeld kunnen worden. De boogstroom in de ionenbron is gestabiliseerd. In de coronakap bevinden zich voorts de electronische stabilisator voor de versnellingsspanning, het waterkoelsysteem van de ionenbron, bestaande uit een autoradiator met ventilator en perspomp, en een variac voor de voeding van de oven van het inlaatsysteem.

De hoogspanningen voor het versnellingssysteem (§ 25) worden verkregen met behulp van transformatoren en gelijkrichtbuizen. De

versnellingsspanning is 1 : 2500 gestabiliseerd en wordt verkregen van een installatie, die maximaal 50 kV, 100 mA kan afgeven. Om het massaspectrum op een oscillograafscherm zichtbaar te maken kan deze spanning bovendien gemoduleerd worden met maximaal 1000 V, 50 perioden.

De negatieve hoogspanning voor de lens kan tot 15 kV worden opgevoerd. Beide hoogspanningen zijn continu regelbaar met behulp van 3 phase variacs.

§ 26 behandelt de metingen aan de collectorzijde. Het instellen van de separator geschiedt aan de hand van het massaspectrum, dat op een oscillograafscherm bekeken kan worden. Tijdens het separeren kan de totale collectorstroom worden afgelezen, terwijl de opgevangen hoeveelheid materiaal door een stroomintegrator wordt aangegeven.

In § 27 worden maatregelen genoemd tegen verontreiniging van de opgevangen isotopen door verschuivingen en verbredingen van de afbeeldingen. Verschuivingen worden gecompenseerd door regeling van de versnellingsspanning. Als de afbeelding zich verbreedt wordt de klep voor de collectorkamers automatisch gesloten, terwijl alarm wordt gegeven. Hetzelfde gebeurt als er teveel hoogspanningsdoorslagen bij de ionenbron optreden.

In § 28 wordt het vacuumsysteem beschreven. Het voorvacuum wordt geleverd door een roterende Kinneypomp (18 l/sec bij 0.02 mm Hg). Verder zijn aanwezig een Philips booster pomp en een Philips 3 traps fractionnerende hoogvacuum pomp (5000 l/sec bij 10^{-5} mm Hg). Beide werken met silicone olie. De olie baffle wordt tot -30^{o} gekoeld door middel van een koelmachine. De druk wordt afgelezen op een thermokoppel manometer (voorvacuum), een Penning manometer en een MacLeod manometer. Een omloopleiding maakt het mogelijk lucht in de separator toe te laten en deze later tot voorvacuum te verwijderen, terwijl de hoogvacuumpompen blijven doorwerken. Luchtsluizen bij de ionenbron en de collector maken handelingen aan deze installaties (b.v. verwisselen van een gloeidraad) mogelijk zonder lucht in de vacuumkamer te laten.

Het gebruik van Dikkers Jenkins balafsluiters en van Simmerringen in het hoogvacuumsysteem worden genoemd.

In § 29 wordt het toevoeren van de te scheiden materialen naar de ionenbron behandeld. Gassen en dampen van laag kokende vloeistoffen worden via een regelbaar lek ingelaten. Vaste stoffen worden in een oventje gebracht, dat zich in één der dragers van de ionenbron in het vacuum bevindt.

In § 30 wordt een overzicht gegeven van de talrijke beveiligingen, waarvan de separator voorzien is. Behalve de bescherming van personen tegen het aanraken van onder spanning en onder hoogspanning staande onderdelen, is een uitgebreid systeem aanwezig

om de verschillende apparaten te beveiligen tegen eventueel optredende storingen in de electrische circuits, in de koelingen en in het vacuum.

§ 31 beschrijft hoe de separator, in hoofdzaak vanaf een drietal centrale kasten, bediend wordt.

Hoofdstuk V. Experimentele resultaten

In § 32 worden de resultaten weergegeven van een aantal metingen, die tot doel hadden de invloed van verschillende grootheden op de collectorstroom en het scheidend vermogen te onderzoeken.

Het was niet mogelijk een goed oplossend vermogen met de Heilbron te verkrijgen. Dit wordt geweten aan de sterke ruis in de ontlading tengevolge waarvan de ruimteladingscompensatie in de beam onvoldoende is. Daarom is uitsluitend verder gewerkt met de boogbron.

Het oplossend vermogen blijkt sterk af te hangen van de ontladingstoestand (boogstroom en -spanning, gasdruk) in de bron, verder van de versnellingsspanning en de negatieve lensspanning.

Bij gasvormige inlaatstoffen bestaat er een optimale werkdruk in de bron met betrekking tot de collectorstroom. Er zijn aanwijzingen, dat een belangrijk deel van het verlies van ionen in de vacuumkamer door omlading veroorzaakt wordt.

Voor enkele inlaatstoffen is de atoom-molecule verhouding in de ionen output bepaald als functie van de ontladingstoestand in de bron.

Tenslotte werden de invloed van de breedte van de ionen uittreespleet en van de plaats van de collector nagegaan.

In § 33 wordt een beschrijving gegeven van enkele uitgevoerde proefseparaties. In totaal werden opgevangen: ca. 50 mg Zn, 30 mg Mg en 1100 mg U.

Alleen van de Zn isotopen werd een massaspectrometrische analyse gemaakt. Enkele onvolkomenheden in het apparaat, die tijdens de proefseparaties naar voren kwamen, werden verbeterd.

In de laatste paragraaf wordt een overzicht van de huidige stand van zaken gegeven. Vele separaties zijn mogelijk maar algehele universaliteit is nog niet bereikt. Begrenzingen zijn: het oplossend vermogen (max. 180), de dampspanning van de te scheiden stoffen (zowel gassen als stoffen met zeer lage dampspanning leveren moeilijkheden op) en de efficiency. Deze laatste is van de orde van enkele %, hetgeen voor zeer kostbaar inlaatmateriaal te laag is.

Mogelijkheden van verdere ontwikkeling worden genoemd.

REFERENCES

A 1. Aston F.W., Mass Spectra and Isotopes, E. Arnold & Co. London 1942.
A 2. Aston F.W., Isotopes, E. Arnold & Co. London 1922.
A 3. Allen W.D., Nature, Lond. **168** (1951) 451.
A 4. Alfven H.A. and Cohn-Peters H.J., Ark. Mat. Astr. Fys. **31 A** (1944) 18.
A 5. Ardenne M.v., Phys. Z. **43** (1942) 91.

B 1. Barwich H., Z. Phys. **100** (1936) 166.
B 2. Bernas R.H. and Nier A.O.C., Rev. sci. Instrum. **19** (1948) 895.
B 3. Bernas R.H., Rapport C.E.A. N. 158, Fontenau aux Roses 1952.
B 4. Bernas R.H. and Sarrouy J.L., C.R. Acad. Sci., Paris **19** (1951) 1092.
B 5. Brewer A.K. and Madorsky S.L., J. Res.Nat.Bur.Stand., Wash. **38** (1947) 129.
B 6. Bergström I., Thulin S., Svartholm N. and Siegbahn K., An Electromagnetic Isotope Separator, Ark. Fys. I Nr. 11.
B 7. Bainbridge K.T., Phys. Rev. **40** (1932) 130.
B 8. Bainbridge K.T. and Jordan E.B., Phys. Rev. **50** (1936) 282.
B 9. Bondy H., Johannsen G. and Popper K., Z. Phys. **95** (1935) 46.
B10. Bleakney W. and Hipple J.A. Jr., Phys. Rev. **53** (1938) 521.
B11. Brown H., Mitchell J.J. and Fowler R.D., Rev. sci. Instrum. **12** (1941) 435.
B12. Barber N.F., Proc. Leeds Phil. Soc. **2** (1933) 427.
B13. Bock C.D., Rev. sci. Instrum. **4** (1933) 575.
B14. Beiduk F.M. and Konopinski E.J., Rev. sci. Instrum. **19** (1948) 594.
B15. Bohm D., Burhop E.H.S., Massey H.S.W. and Williams R.M., The Characteristics of Electrical Discharges in Magnetic Fields. National Nuclear Energy Series **1** – **5** Mc Graw Hill New York 1949.
B16. Brown W.F. and Sweer J.H., Rev. sci. Instrum. **16** (1945) 276.
B17. Bell W.A. Jr., Love L.O., Normand C.E. and Prater W.K., Lecture at meeting A.P.S. Albuquerque New Mexico Sept. 2 – 5, 1953.

C 1. Chapman S. and Dootson F.W., Phil. Mag. **33** (1917) 248.
C 2. Chapman S., Phil. Mag. **34** (1917) 146.
C 3. Clusius K. and Dickel G., Naturwissenschaften **26** (1938) 546.
C 4. Clusius K. and Dickel G., Naturwissenschaften **27** (1939) 148.
C 5. Clusius K. and Becker E.W., Z. Naturforsch. **2a** (1947) 154.
C 6. Classen J., Phys. Z. **9** (1908) 762.
C 7. Coggeshall N.D. and Jordan E.B., Rev. sci. Instrum. **14** (1943) 125.

D 1. Daunt J.G., Probst R.E., Johnston H.L., Aldrich L.T. and Nier A.O.C., Phys. Rev. **72** (1947) 502.
D 2. Dempster A.J., Proc. Amer. Phil. Soc. **75** (1935) 755.
D 3. Dempster A.J., Phys. Rev. **11** (1918) 316.
D 4. Dushman S., Scientific Foundations of Vacuum Technique, J. Wiley & Sons, New York 1949.

E 1. Euchen A. and Bratzler K., Z. phys. Chem. (A) **174** (1935) 273.
E 2. Enskog D., Phys. Z. **12** (1911) 533.
E 3. Engel A.v. and Steenbeck M., Elektrische Gasentladungen I, J. Springer, Berlin 1932.

F 1. Fowler R.D. and Gibson G.E., Phys. Rev. **46** (1934) 1075.
F 2. Finkelstein A.T., Rev. sci. Instrum. **11** (1940) 94.

G 1. Gurney R.W., Proc. Roy. Soc. A. **134** (1931) 137.
G 2. Goldfinger P. and Scheepers L., J. chem. Phys. **31** (1934) 628.
G 3. Greene C.H. and Voskuyl R.J., J. Amer. Chem. Soc. **56** (1934) 1649.
G 4. Glasstone S., Sourcebook on Atomic Energy, D. v. Nostrand, New York 1950.
G 5. Grassot M.E., J. Phys. **4** (1904) 696.

H 1. Hertz G., Z. Phys. **79** (1932) 108.
H 2. Hertz G., Z. Phys. **91** (1934) 810.
H 3. Harkins W.D. and Hayes A., J. Amer. Chem. Soc. **43** (1921) 1803.
H 4. Harmsen H., Hertz G. and Schütze W., Z. Phys. **90** (1934) 703.
H 5. Harteck P., Proc. Phys. Soc., Lond. **46** (1934) 277.
H 6. Holleck L., Z. Elektrochem. **44** (1938) 111.
H 7. Hemptinne M. de and Capron P., J. Phys. Radium **10** (1939) 171.
H 8. Huffmann J.R. and Urey H.C., Ind. Eng. Chem. **29** (1937) 531.
H 9. Hutchison C.A., Stewart D.W. and Urey H.C., J. Chem. Phys. **8** (1940) 532.
H10. Hintenberger H., Z. Naturforsch. **3a** (1948) 125.
H11. Heil H., Z. Phys. **120** (1943) 212.

J 1. Jones R.C. and Furry W.H., Rev. mod. Phys. **18** (1946) 151.
J 2. Jordan E.B., Phys. Rev. **57** (1940) 1072.

K 1. Keesom W.H. and Dijk H. van, Proc. Roy. Acad. Amsterd. **34** (1931) 42.
K 2. Keesom W.H., Dijk H. van and Haantjes J., Physica **1** (1934) 1109.
K 3. Keesom W.H., Dijk H. van and Haantjes J., Proc. Roy. Acad. Amsterd. **36** (1933) 248.
K 4. Kendall J. and Crittenden E.D., Proc. Nat. Acad. Sci., Wash. **9** (1923) 75.
K 5. Krüger H., Z. Phys. **111**(1939) 467.
K 6. Korsching H. and Wirtz K., Naturwissenschaften **27** (1939) 367.
K 7. Kunsmann C.H., Phys. Rev. **25** (1925) 892.
K 8. Kuhn W. and Martin H., Z. phys. Chem. (B) **21** (1933) 93.
K 9. Klemm A., Hintenberger H. and Hoernes P., Z. Naturforsch. **2a** (1947) 245.
K10. Kerwin L., Rev. sci. Instrum. **20** (1949) 36.
K11. Koch J., Thesis Copenhague 1942.
K12. Koch J., Z. Phys. **100** (1936) 669.
K13. Koch J., Nature, Lond. **161** (1948) 566.
K14. Kistemaker J., Appl. sci. Res. **B1** (1948) 268.
K15. Kistemaker J. and Douwes Dekker H.L., Physica **16** (1950) 209.
K16. Keene J.P., Phil. Mag. **40** (1949) 369.

L 1. Lewis G.N. and Cornish R.E., J. Amer. Chem. Soc. **55** (1933) 2616.
L 2. Lewis G.N., J. Amer. Chem. Soc. **55** (1933) 1297.
L 3. Langer L.M. and Cook C.S., Rev. sci. Instrum. **19** (1948) 257.
L 4. Langmuir I. and Compton K.T., Rev. mod. Phys. **3** (1931) 237.
L 5. Liebmann G., Brit. J. appl. Phys. **1** (1950) 92.
L 6. Liston M.D., Quinn C.E., Sargeant W.E. and Scott G.G., Rev. sci. Instrum. **17** (1946) 194.
L 7. Linder E.G. and Hernqvist K.G., J. appl. Phys. **21** (1950) 1088.

M 1. Morand M., Ann. Phys. Paris (10) **7** (1927) 164.
M 2. Mattauch J., Phys. Rev. **50** (1936) 617.
M 3. Massey H.S.W. and Burhop E.H.S., Electronic and Ionic Impact Phenomena, Clarendon Press, Oxford 1952.

N 1. Nier A.O.C., Rev. sci. Instrum. **18** (1947) 398.
N 2. Nier A.O.C., Rev. sci. Instrum. **11** (1940) 212.
N 3. Nier A.O.C., Ney E.P. and Inghram M.G., Rev. sci. Instrum. **18** (1947) 191.
N 4. Newhall H.F., Phys. Rev. **61** (1942) 737; **62** (1942) 11.

O 1. Oliphant M.L., Shire E.S. and Crowther B.M., Proc. Roy. Soc. A **146** (1934) 922.

P 1. Pierce J.R., J. appl. Phys. **11** (1940) 548.
P 2. Packh D.C. de, Rev. sci. Instrum. **18** (1947) 789.
P 3. Packard M.E., Rev. sci. Instrum. **19** (1948) 435.

R 1. Rumbaugh L.H. and Hafstad L.R., Phys. Rev. **50** (1936) 681.
R 2. Robinson C.F., Rev. sci. Instrum. **20** (1949) 745.
R 3. Rosenblum E.S., Phys. Rev. **72** (1947) 731.

R 4. Reinders M.E., Zilverschoon C.J. and Kistemaker J., Appl. sci. Res. **B 2** (1951) 264.
R 5. Rauch S.E., J. appl. Phys. **22** (1951) 1128.

S 1. Soddy F., Am. Rep. Chem. Soc. (1910) 285.
S 2. Smythe W.R., Rumbaugh L.H. and West S.S., Phys. Rev. **45** (1934) 724.
S 3. Smythe W.R. and Hemmendinger A., Phys. Rev. **51** (1937) 178 and 1052.
S 4. Smyth H.D., Atomic Energy for Military Purposes. Princeton University Press 1945.
S 5. Smyth H.D., Phys. Rev. **25** (1925) 452.
S 6. Smith L.P., Parkins W.E. and Forrester A.T., Phys. Rev. **72** (1947) 989.
S 7. Stephens W.E., Phys. Rev. **45** (1934) 513.
S 8. Spighel M., J. Phys. Radium **10** (1949) 207.
S 9. Svartholm N. and Siegbahn K., Ark. Mat. Astr. Fys. **33a** (1946) N 21.
S10. Svartholm N., Ark. Mat. Astr. Fys. **33a** (1946) N 24.
S11. Shull F.B. and Dennison D.M., Phys. Rev. **71** (1947) 681.
S12. Shull F.B. and Dennison D.M., Phys. Rev. **72** (1947) 256.
S13. Skartstrøm C., Carr H.E. and Beans J.W., Phys. Rev. **55** (1939) 591.
S14. Setlow R.B., Rev. sci. Instrum. **20** (1949) 558.
S15. Schutten J., Appl. sci. Res. **B2** (1950) 249.

T 1. Thomson J.J., Rays of positive Electricity, Longmans, Green & Co,, London 1913.
T 2. Thode H.G. and Urey H.C., J. chem. Phys. **7** (1939) 34.
T 3. Thode H.G., Gorham J.E. and Urey H.C., J. chem. Phys. **6** (1938) 296.
T 4. Thode H.G., Graham R.L. and Ziegler J.A., Canad. J. Res. B **23** (1945) 40.
T 5. Taylor H.S., Nature, Lond. **144** (1939) 8.
T 6. Tate J.T. and Smith P.T., Phys. Rev. **46** (1934) 773.
T 7. Taylor J.E., Rev. sci. Instrum. **15** (1944) 1.
T 8. Thomas E., Thesis, Brussels 1952.
T 9. Thonemann P.C., Moffatt J., Roaf D. and Sanders J.H., Proc. Phys. Soc., Lond. **61** (1948) 483.

U 1. Urey H.C., Brickwedde F.G. and Murphy G.M., Phys. Rev. **40** (1932) 1.
U 2. Urey H.C. and Greiff L., J. Amer. Chem. Soc. **57** (1935) 321.
U 3. Urey H.C., Huffmann J.R., Thode H.G. and Fox M., J. chem. Phys. **5** (1937) 856.
U 4. Urey H.C., Aten A.H.W. and Keston A.S., J. chem. Phys. **4** (1936) 622.

V 1. Veenstra P.C. and Milatz J.M.W., Physica **16** (1950) 528.
V 2. Verster N.F., Physica **16** (1950) 815.
V 3. Verster N.F., Appl. sci. Res. **B1** (1949) 358.
V 4. Verster N.F., Appl. sci. Res. **B1** (1949) 363.

W 1. Wahl M.H., Huffmann J.F. and Hipple J.A. J. chem. Phys. **3** (1935) 434.
W 2. Washburn E.W. and Urey H.C., Proc. Nat. Acad. Amer. **18** (1932) 496.
W 3. Washburn E.W., Smith E.R. and Smith F.A., J. Res. Nat. Bur. Stand., Wash. **13** (1934) 599.
W 4. Walcher W., Z. Phys. **108** (1938) 376.
W 5. Walcher W., Z. Phys. **122** (1944) 401.

Y 1. Yates E.L., Proc. Roy. Soc. A. **168** (1938) 148.

Z 1. Zworykin V.K., Morton G.A., Ramberg E,G., Hillier J. and Vance A.W. Electron Optics and the Electron Microscope. J. Wiley & Sons Inc., New York 1948.
Z 2. Zilverschoon C.J., Ned. T. Natuurk. **16** (1950) 323.
Z 3. Zemany P.D., J. appl. Phys. **23** (1952) 924.

STELLINGEN

1. Vermeulens beschouwingen over dimensies en eenheden zijn aanvechtbaar.

   R. Vermeulen. Phil.Res.Rep. **7** (1952) 432.

2. De theorie van Schwartz over de „electronenpomp" is onjuist.

   H. Schwartz. Rev.Sci.Instr. **24** (1953) 371.

3. Bij de calorimetrische bepaling van ionenstromen met energieën van enkele keV kan een aanzienlijke systematische fout ontstaan door sputteringseffecten.

   H. Alfvén en H.J. Cohn-Peters. Ark.Mat.Astr.Fys. **31A** (1944) 18.

4. Looptijdmethodes toegepast in de massaspectrometrie zijn onbruikbaar voor isotopenscheiding op grote schaal.

5. Bij de metingen van de rotortemperatuur van ultracentrifuges met een thermistor dient men de weerstandsverandering van de thermistor bij mechanische belasting in aanmerking te nemen.

   D.F. Waugh en D.A. Yphantis. Rev.Sci.Instr. **23** (1952) 609.
   C.W. Hiatt. Rev.Sci.Instr. **24** (1953) 182.

6. Demonstratieproeven voor thermodiffusie, uitgevoerd met een He-luchtmengsel zijn overtuigender dan die, waarbij gebruik wordt gemaakt van een Br_2-luchtmengsel.

7. De vraag, of een primair electron in een oscillerende magnetische gasontlading na één oscillatie weer in de kathode terugkeert, is van geen betekenis voor het ioniserend vermogen van dat electron.

   P.C. Veenstra en J.M.W. Milatz. Physica **16** (1950) 528.

8. Drukmetingen, uitgevoerd met een MacLeod-manometer geven, ook bij gassen, systematisch een te lage uitkomst.

9. De opgave van Setlow over de opbrengst van zijn ionenbron is misleidend.

   R.B. Setlow. Rev.Sci.Instr. **20** (1949) 558.

10. De regel, dat het oplossend vermogen van een electronenmicroscoop maximaal een tiende van de objectdikte bedraagt, is slechts op bepaalde gevallen toepasbaar.

V.E. Cosslett, Practical Electron Microscopy 1951, p 168.

11. De door Wilkinson gegeven vergelijking voor het „opbouwen" van teller stoten kan in eenvoudiger vorm gegeven worden. Zijn resultaten volgen dan uit de Laplace transformatie.

D.H. Wilkinson. Ionization Chambers and Counters. 1950, p 251.

12. Bij de constructie van een electromagneet met staalkern is het voordelig de bekrachtigingsspoel zodanig te ontwerpen, dat de afschrijvingskosten hiervan ongeveer gelijk zijn aan de som van verbruiks- en afschrijvingskosten van de voedingsinstallatie.

13. Ten behoeve van de verkeersveiligheid dienen de voorrangsregels bij T-kruisingen van gelijkwaardige wegen gewijzigd te worden.